ALESSANDRA DE SOUZA FONSECA

OBTENÇÃO E MODIFICAÇÃO DE NANOFIBRAS CELULÓSICAS PARA PRODUÇÃO DE NANOCOMPÓSITO HÍBRIDO

LAVRAS – MG

2016

ALESSANDRA DE SOUZA FONSECA

OBTENÇÃO E MODIFICAÇÃO DE NANOFIBRAS CELULÓSICAS PARA PRODUÇÃO DE NANOCOMPÓSITO HÍBRIDO

Tese apresentada à Universidade Federal de Lavras, como parte das exigências do Programa de Pós-Graduação em Ciência e Tecnologia da Madeira, área de concentração em Madeira como Matéria-Prima, para a obtenção do título de Doutora.

Orientador

Dr. Gustavo Henrique Denzin Tonoli

Coorientadores

Dr. José Manoel Marconcini

Dr. Caue Ribeiro

Dr. Fabio Akira Mori

LAVRAS - MG

2015

Ficha catalográfica elaborada pelo Sistema de Geração de Ficha Catalográfica da Biblioteca Universitária da UFLA, com dados informados pelo(a) próprio(a) autor(a).

Fonseca, Alessandra de Souza.
Obtenção e modificação de nanofibras celulósicas para produção de nanocompósito híbrido / Alessandra de Souza Fonseca. – Lavras : UFLA, 2016.
166 p. : il.

Tese (doutorado) – Universidade Federal de Lavras, 2015.
Orientador: Gustavo Henrique Denzin Tonoli.
Bibliografia.

1. Nanofibrilas de celulose. 2. Composição química residual. 3. Método sol-gel. 4. TEOS. 5. Aerogel celulose-sílica. I. Universidade Federal de Lavras. II. Título.

ALESSANDRA DE SOUZA FONSECA

OBTENÇÃO E MODIFICAÇÃO DE NANOFIBRAS CELULÓSICAS PARA PRODUÇÃO DE NANOCOMPÓSITO HÍBRIDO

Tese apresentada à Universidade Federal de Lavras, como parte das exigências do Programa de Pós-Graduação em Ciência e Tecnologia da Madeira, área de concentração em Madeira como Matéria-Prima, para a obtenção do título de Doutora.

APROVADA em 17 de dezembro de 2015.

Dr. Juliano Elvis de Oliveira	UFLA
Dra. Maria Alice Martins	EMBRAPA
Dra. Lívia Elisabeth Vasconcellos de Siqueira Brandão	UFLA
Dr. Lourival Marin Mendes	UFLA

Dr. Gustavo Henrique Denzin Tonoli
Orientador

LAVRAS - MG

2015

AGRADECIMENTOS

Agradeço a Deus por tudo e por todos os que tive o prazer de conhecer, conviver e construir laços fraternos de uma amizade verdadeira no período que estive em Lavras e nos lugares por onde passei durante a pós-graduação.

Aos meus pais, Mario Antonio Peixoto da Fonseca e Ercimor de Souza Fonseca, e ao meu irmão, Marco Antonio de Souza Fonseca, pela amorosidade, paciência e apoio em todos os momentos, mesmo a vida nos convidando a viver duras experiências separados geograficamente. O amor supera qualquer distância e a confiança nos desígnios de Deus sempre confortou nossos corações!

Ao homem, amigo, confidente e companheiro de jornada, Newton Coelho Monteiro, por construir junto ao meu coração um laço eterno de amor, confiança e fidelidade. Foi companheiro presente e ativo na minha vida pessoal e profissional, acompanhando-me desde a monografia. Contando com seu apoio incondicional, foram geradas, monografia, dissertação e, agora, a tese. Queira Deus que de nossa relação pessoal, saudáveis e prósperos frutos também possam ser contabilizados, futuramente!

Aos amigos que me esperam em Manaus, pelos ótimos momentos dos reencontros e pela descontração sempre garantida, reanimando-me sempre o espírito ao bom regresso às atividades da Pós-Graduação, em Lavras.

À Universidade Federal de Lavras por me acolher durante toda a Pós-Graduação, garantindo-me a oportunidade de crescer profissionalmente. Ao Programa de Pós-Graduação em Ciência e Tecnologia da Madeira, em nome de todos os docentes, discentes e servidores por toda amizade, por todo conhecimento e aprendizado construídos durante nossos cinco anos de convivência.

Ao meu orientador, Gustavo Henrique Denzin Tonoli, pelo exemplo de postura do ser humano, professor e orientador dentro da academia. Obrigada por ter acreditado no meu potencial quando, eu mesma, cega pelo desalento, não acreditei. Obrigada pelos "empurrões" profissionais, pelas breves conversas que sempre me faziam refletir. Obrigada por todo apoio que você proporcionou mesmo antes de se tornar meu orientador. Obrigada pelas oportunidades que você ajudou a construir, fazendo-me crescer pessoal e profissionalmente. Enfim, muito obrigada por ter sido o meu orientador!

À toda equipe do Centre of Biocomposite and Biomaterials Processing, da Universidade de Toronto, Canadá, pela excelente acolhida e por garantir que os experimentos da tese fossem desenvolvidos com êxito. Para minha alegria, deixei por lá mais que contatos profissionais, deixei amigos queridos que levo e levarei sempre junto ao meu coração, sob as mais belas e felizes lembranças.

Agradeço também ao apoio e amizade da Dra. Ires Paula de Andrade Miranda, do laboratório de Palmeiras do Instituto Nacional de Pesquisas da Amazônia – INPA, cuja parceria iniciou-se durante a realização de meu Mestrado, sob sua coorientação.

Agradeço à empresa Brasjuta da Amazônia S.A. pela doação das fibras de juta, o que permitiu o desenvolvimento do primeiro artigo da tese.

Agradeço à CAPES pela concessão das bolsas de doutorado e doutorado-sanduíche, garantindo que a pós-graduação fosse desenvolvida plenamente.

Agradeço a todos os pesquisadores, servidores e estudantes da Embrapa Instrumentação Agropecuária, em São Carlos-SP, que direta ou indiretamente contribuíram para o desenvolvimento deste trabalho que começou a ser construído em 2012.

Agradeço a todos os amigos que conheci durante os anos de 2010-2015, dos espalhados pelo mundo aos que ficarão em Lavras, por todos os momentos

alegres, consoladores e amorosos que dividiram comigo. A existência de vocês em minha vida tornou a distância de meus familiares, meu lar, meu namorado e de minha Paris dos Trópicos, o Porto de Lenha ou a calorosa e receptiva Manaus menos dolorosa.

Agradeço ainda à doutrina espírita que me fez reconhecer nos anos que estive em Lavras, o chamado da vida ao amadurecimento, ao serviço no bem, ao meu autoconhecimento, auxiliando-me a passar por momentos de solidão e dor confiando na amorosidade divina e na sua providência, agindo para o meu progresso moral e intelectual.

RESUMO

O objetivo central deste trabalho foi obter e depositar sílica em nanofibrilas de celulose pelo método sol-gel, utilizando o precursor de sílica Tetraetil ortosilicato – TEOS em diferentes concentrações, produzindo ao final aerogéis híbridos celulose-sílica. Ao se obter as nanofibrilas de celulose em grinder a partir de fibras de juta pré-tratadas, observou-se que a composição química da matéria-prima inicial associada ao seu grau de desfibrilamento exerceu influência positiva nas propriedades mecânicas dos filmes produzidos constituídos de diferentes concentrações de lignina e hemiceluloses residuais (artigo 1). Ao se avaliar seis concentrações de TEOS (0.00%, 0.25%, 0.50%, 1.00%, 2.00% e 3.00%) na deposição de sílica em nanofibrilas de celulose, a partir de polpa comercial branqueada mista de coníferas e folhosas, verificou-se que a presença do precursor de sílica, mesmo em menores concentrações (0.25%), influenciou a morfologia celulósica, favorecendo a produção dos nanocompósitos híbridos celulose-sílica. O aumento da concentração de TEOS promoveu a formação de aerogéis híbridos mais estáveis termicamente. Foi observada reduzida capacidade adsorvente dos aerogéis híbridos, estrutura porosa e não compactada, principalmente, para as concentrações 0.50 e 1.00% (artigo 2). Baseados nos resultados obtidos para as seis concentrações testadas, produziu-se aerogéis a partir de nanofibrilas de celulose de Eucalyptus, testando-se quatro concentrações de TEOS (0.00%, 0.25%; 0.50% e 1.00%) e verificou-se que 0.25% de TEOS favoreceu a formação de aerogéis híbridos de estrutura porosa, homogênea e macia. A concentração 0.50% de TEOS foi a que influenciou na formação de aerogéis híbridos porosos mais estáveis termicamente. A reduzida capacidade adsorvente foi observada para as concentrações de 0.25% de TEOS. Mecanicamente, todos os aerogéis híbridos exibiram um comportamento elástico, sendo capazes de recuperar parcialmente suas dimensões originais depois de submetidos às forças de compressão (artigo 3).

Palavras-chave: Nanofibrilas de celulose. Fibras celulósicas. Método sol-gel. TEOS. Aerogel celulose-sílica.

ABSTRACT

The main objective of this study was to obtain and deposit silica in cellulose nanofibrils by means of the sol-gel method using the silica tetraethyl orthosilicate - TEOS precursor at different concentrations, producing hybrid cellulose-silica aerogels. After obtaining cellulose nanofibrils by mechanical defibrillation from pretreated jute fibers, the chemical composition of the raw materials, related to the defibrillation degree had a positive influence over the mechanical properties of the produced films, consisting of different lignin and hemicelluloses residual concentrations (Article 1). When evaluating six concentrations of TEOS (0.00%, 0.25%, 0.50%, 1.00%, 2.00% and 3.00%) on the silica deposition in cellulose nanofibrils from mixed commercial and bleached pulp of hardwood and softwood, the presence of the silica precursor, even at lower concentrations (0.25%) influenced the cellulosic morphology, favoring the production of cellulose-silica hybrid nanocomposites. The increase in the concentrations of TEOS promoted the formation of hybrid aerogels more thermally stable. The reduced capacity for moisture adsorption of the hybrid aerogels was obtained mainly using the concentrations of 0.50% and 1.00%, presenting a porous and uncompressed structure (Article 2). Based on the results obtained for the six concentrations tested (Article 2), aerogels were produced from Eucalyptus cellulose nanofibrils, by testing four concentrations of TEOS (0.00%, 0:25%; to 0.50% and 1.00%), verifying that 0.25% of TEOS favored the formation of porous, homogeneous and smooth structured hybrid aerogels. The concentration of 0.50% TEOS influences the formation of porous and more thermally stable hybrid aerogels. The reduced adsorption capacity was observed for the concentration of 0.25% TEOS. Mechanically, all hybrid aerogels exhibited an elastic behavior, and are capable of partially recovering their original dimensions after subjected to compressive forces (Article 3).

Keywords: Microfibrillated cellulose. Cellulosic fibers. Sol-gel method. TEOS. Cellulose-silica aerogel.

LISTA DE FIGURAS

PRIMEIRA PARTE

SEGUNDA PARTE – ARTIGOS

ARTIGO 1

ARTIGO 2

ARTIGO 3

LISTA DE TABELAS

SEGUNDA PARTE – ARTIGOS

ARTIGO 1

ARTIGO 2

ARTIGO 3

SUMÁRIO

PRIMEIRA PARTE

1 INTRODUÇÃO

Pesquisas relacionadas à produção, caracterização e aplicação de fibras e nanofibras celulósicas vem ganhando destaque em todos os países e em diferentes linhas de pesquisa. O desenvolvimento de compósitos e nanocompósitos com inclusão de fibras e nanofibras assume papel de destaque frente à demanda por materiais amigáveis ao meio ambiente, exigidos pela nova economia de mercado adotada em todo mundo, que anseia por materiais originados de fontes renováveis de natureza biodegradável.

Neste contexto, fibras e nanofibras, de diferentes morfologias e estruturas, são o objeto de estudo de diferentes instituições de pesquisa, que buscam ofertar ao mercado novos materiais que substituam os produtos convencionais, originados de fontes não renováveis, como petróleo e minério.

Dentre os tipos de nanofibras, os whiskers ou nanocristais de celulose configuravam como um dos produtos de celulose mais estudados, quanto à sua obtenção, caracterização e aplicação. Muitos trabalhos já solucionaram diversos gargalos envolvidos em sua aplicação como reforço em compósitos de diferentes naturezas, devido as suas características físico-químicas.

As nanofibrilas de celulose (NFC), obtidas desde a década de 80 do século XX, apresentam-se como um tipo de nanofibra celulósica com potencial aplicação industrial, cujas principais vantagens são facilidade, praticidade e baixo custo de obtenção, em comparação aos whiskers de celulose.

O número de pesquisas realizadas para se entender e aplicar melhor as nanofibrilas de celulose é cada vez maior. Já é possível encontrar relatos na literatura sobre otimização de seu uso como reforço em compósitos poliméricos (BHATNAGAR; SAIN, 2005; DUFRESNE, 2013; HASSAN et al., 2015).

Neste trabalho, buscaremos contribuir para a comunidade científica ao descrever o processo de obtenção, caracterização e modificação superficial das nanofibras produzidas, bem como, ao aplicar estas nanofibrilas de celulose na produção de nanocompósitos hibridos.

O uso do alcoxóide precursor de sílica, Tetraetil ortosilicato (TEOS), vem sendo muito empregado em diversas pesquisas que visam produzir partículas, nanopartículas e produtos derivados de sílica (FRICKE; TILLOTSON, 1997; OKAZAKI, 1998; XIE; PINTO et al., 2008; YU; SHI, 2009; TAMON; KITAMURA; XIE et al., 2010; YAN, 2011; ASHORI et al., 2012; CAI et al., 2012; LIU et al., 2013;) devido a sua aplicação prática e econômica na produção de nanocompósito híbridos a partir do método sol-gel, comparando-se aos métodos tradicionais.

1.1 Objetivos

O objetivo central deste trabalho foi obter nanofibrilas de celulose e produzir nanocompósitos híbridos de micro/nanofibras-sílica, a partir do precursor de sílica tetraetil ortosilicato (TEOS) em diferentes concentrações.

Os objetivos específicos foram:

a) entender como a composição química residual da matéria-prima está relacionada com as propriedades da micro/nanofibra obtida;
b) verificar se houve influência da concentração de precursor inorgânico na modificação superficial da micro/nanofibra;
c) compreender os mecanismos do precursor TEOS nas propriedades dos nanocompósitos híbridos;
d) avaliar o efeito da modificação nas propriedades morfológicas, físicas e mecânicas do nanocompósito híbrido obtido.

1.2 Conteúdo da Tese

A tese está subdividida em duas partes. A primeira parte é composta de 3 seções, contemplando (1) introdução, (2) revisão de literatura, contendo os principais tópicos abordados neste trabalho, visando embasar o leitor para o melhor entendimento dos artigos que serão apresentados na segunda parte do corpo da tese e (3) conclusão e considerações finais, onde serão expostos os principais resultados apresentados nos três artigos presentes na segunda parte da tese.

O artigo 1 contempla a obtenção das micro/nanofibras celulósicas utilizando o processo mecânico a partir de fibras de juta pré-tratadas, polpa branqueada de *Eucalyptus* e *Pinus*, avaliando-se as propriedades morfológicas, estruturais e mecânicas do filme celulósico obtidas para cada material estudado.

O artigo 2 trata especificamente da modificação química das nanofibrilas de celulose de polpa comercial branqueada mista de coníferas e folhosas a partir do método sol-gel, testando-se o precursor TEOS sob diferentes concentrações, para síntese de sílica no material celulósico, avaliando-se a sinergia entre celulose e sílica bem como a influência da sílica nas propriedades morfológicas e físicas do nanocompósito híbrido formado.

O artigo 3 apresenta as propriedades morfológicas, físicas e mecânicas do aerogel híbrido celulose-sílica obtido a partir da matriz orgânica de nanofibrilas de celulose de *Eucalyptus* e do componente inorgânico sílica, obtido a partir de concentrações do precursor TEOS, selecionadas de acordo com os resultados obtidos no artigo 2.

O presente trabalho contribui para o entendimento da produção de micro/nanofibras a partir de material lignocelulósico bem como de híbridos sílica-micro/nanofibras de celulose e de sua influência nas propriedades de um nanocompósito híbrido celulose-sílica.

2 REFERENCIAL TEÓRICO

Os tópicos seguintes constituem os principais temas abordados para execução e entendimento do trabalho.

2.1 Fibras vegetais no uso tecnológico

Em sentido geral, fibra refere-se a qualquer estrutura filamentosa e delgada, encontrada nos tecidos animais e vegetais ou em algumas substâncias minerais (HOUAISS; VILLAR; FRANCO, 2009). Em morfologia vegetal, fibra é definida como células de sustentação, responsáveis pela rigidez ou flexibilidade da madeira. Possuem forma alongada e extremidades afiladas, com maior dimensão no sentido do eixo longitudinal do tronco da árvore (Figura, 1), dividindo-se em fibras libriformes e fibrotraqueídes (APPEZZATO-DA-GLORIA; CARMELLO-GUERREIRO, 2006).

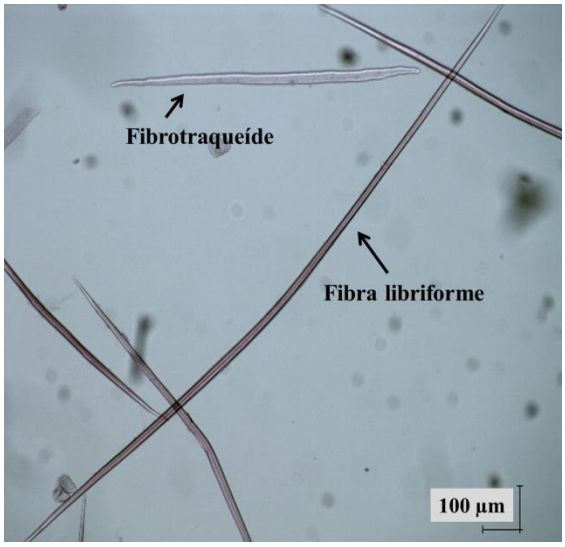

Figura 1 Tipos anatômicos de fibras vegetais

Na ciência e engenharia de materiais, fibra pode ser entendida como todo material polimérico, sintético ou natural, com características especializadas, de estrutura filamentosa alongada, apresentando uma proporção de 100:1 na relação entre seu comprimento e seu diâmetro, apresentando alta resistência à tração, sob um intervalo relativamente grande de variação de temperatura, alto módulo de elasticidade e resistência à abrasão, estabilidade química em diversos meios, solventes e às intempéries naturais, principalmente, à luz solar, relativa inflamabilidade e capacidade de perda de água – secagem (CALLISTER JUNIOR, 2008).

Já no sentido comercial, pode significar agregados de feixes fibrovasculares, contendo fibras anatomicamente puras, como ocorre em monocotiledôneas (ILVESSALO-PFÄFFLI, 1994): bambu, sisal, curauá, por exemplo, ou agregados de fibras floemáticas, como é o caso das espécies produtoras de fibras liberianas: juta, malva, cânhamo, etc. Portanto, diz respeito a todo material fibroso não obtido de madeira, ou seja, não produzido no xilema secundário de árvores, cipós e arbustos (Figura, 2). Esse entendimento do conceito de fibra lignocelulósica também é compartilhado pela maioria das publicações envolvendo a aplicação desta matéria-prima para fins tecnológicos, tais como: na indústria têxtil (SATYANARAYANA; GUIMARÃES; WYPYCH, 2007; ALVES et al., 2010), reforço de compósitos poliméricos (SANTOS; DIAS; MEIRELES, 2006; SILVA et al., 2009; ALVES et al., 2010; FARUK et al., 2012; FONSECA et al., 2013; PANTHAPULAKKAL; SAIN, 2013; GUIMARÃES JUNIOR et al., 2015a; SANTOS et al., 2015; SENA NETO, et al., 2015) produção de compósitos poliméricos biodegradáveis (SATYANARAYANA; ARIZAGA; WYPYCH, 2009; GUIMARÃES et al., 2015b), reforço de compósitos cimentícios (MACVICAR; MATUANA; BALATINECZ, 1999; SAVASTANO JÚNIOR, 2000; SANTOS et al., 2015), materiais biocompatíveis (CHEUNG et al., 2009; FERNANDES et al., 2013;

RAHMAN; AFRIN; HAQUE, 2014), produção de nanofibras celulósicas (WANG; SAIN; OKSMAN, 2007; ZULUAGA et al., 2009; HASSAN et al., 2012; ALILA et al., 2013; NGUYEN et al., 2013; HASSAN et al., 2015; GUIMARÃES JUNIOR et al., 2015b) dentre outras (SATYANARAYANA; GUIMARÃES; WYPYCH, 2007; LIN; RENNECKAR; HINDMAN, 2008; MARQUES et al., 2010; MAJEED et al., 2013; VIANA et al., 2014; OLIVEIRA et al., 2015; BERTHET et al., 2015; HASSAN et al., 2015).

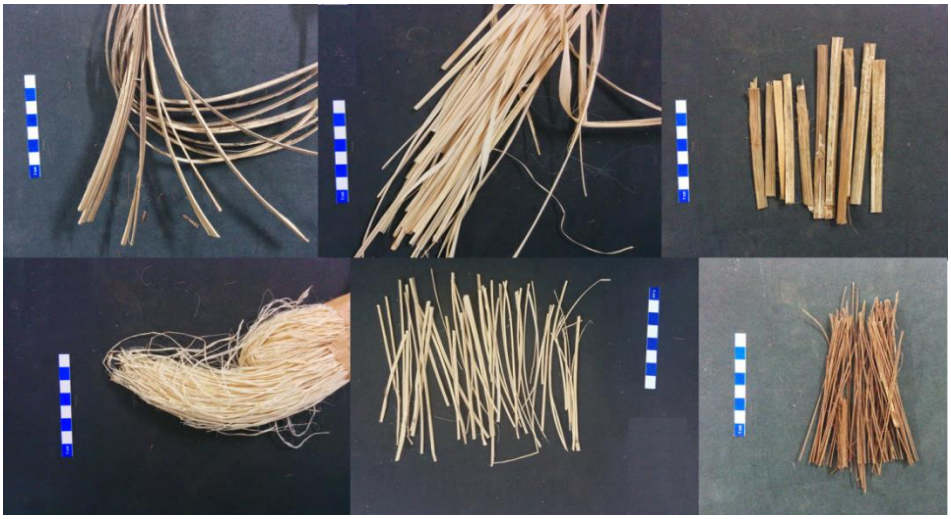

Figura 2 Diferentes tipos de fibras de origem lignocelulósica. Barra de escala equivale a 8 cm

Além disso, a biomassa lignocelulósica, outra denominação comumente referida aos resíduos agrícolas e/ou florestais, vem sendo empregada pela biorrefinaria para produção de polímeros, copolímeros, combustíveis, resinas e polióis, produtos derivados tradicionalmente da indústria petrolífera (SILVA et al., 2009; SCHUCHARDT; RIBEIRO, 2001; ARORA; BEHERA; KUMAR, 2015; BADGUJAR; BHANAGE, 2015; PATEL et al., 2015; KIM; LEE; KIM, 2016;; ZHUANG et al., 2016; ZHANG; PEI; WANG, 2016).

A biomassa vegetal é composta, principalmente, de celulose e está disponível em grande escala e representa uma majoritária fonte renovável de matéria-prima para processos biotecnológicos bem como para produção de combustíveis orgânicos, químicos e materiais (LYND; WYMAN; GERNGROSS, 1999).

Com o advento da ciência, tecnologia e inovação, ampliou-se a demanda por celulose bem como por seus produtos e subprodutos devido às suas propriedades físicas, químicas, mecânicas, estruturais além de características como atoxicidade, grande disponibilidade, biodegradabilidade, sua origem renovável e relativo baixo custo (SCHURZ, 1999; SATYANARAYANA; ARIZAGA; WYPYCH, 2009; FARUK et al., 2012).

A crescente demanda por materiais lignocelulósicos como fonte de matéria-prima para diversos segmentos industriais que tradicionalmente utilizam subprodutos derivados do petróleo se dá, principalmente, pela possibilidade de obtenção de subprodutos poliméricos, fenólicos, combustíveis, dentre outros, semelhantes em composição e qualidade aos obtidos pela indústria petroquímica e, amplamente, utilizados em nosso dia-a-dia. Contudo, permanece não competitivo em termos de custos (SCHURZ, 1999), mas apresenta-se sob competitivo custo com o petróleo de menor valor de mercado (LYND; WYMAN; GERNGROSS, 1999).

2.2 Nanofibrilas de celulose - NFC

As nanofibrilas de celulose, obtidas por tratamento mecânico, e os nanocristais de celulose, obtidos por tratamento químico, dizem respeito a uma nova matéria-prima obtida a partir de fibras de celulose, em que uma de suas dimensões encontre-se em nanoescala, cujas características e propriedades sejam

distintas do material original (INTERNATIONAL ORGANIZATION FOR STANDARDIZATION, ISO, 2015).

De maneira geral, estas nanoceluloses reúnem importantes propriedades da celulose como hidrofilicidade, ampla capacidade de modificação química e formação de morfologias fibrosas semicristalinas versáteis aliadas a características específicas de materiais em nanoescala, características essas causadas principalmente pela grande área superficial destes materiais. As nanoceluloses são classificadas de acordo com suas características e propriedades, com base em suas dimensões, funções e os métodos de preparação da fonte celulósica e de sua condição de processamento, já que o grau de polimerização da celulose, sua morfologia e razão de aspecto podem variar muito (KLEMM et al., 2011).

Em trabalhos de revisão (SIRÓ; PLACKETT, 2010; SIQUEIRA; BRAS; DUFRESNE, 2010; CHINGA-CARRASCO; 2011; KLEMM et al., 2011; MOON et al., 2011; LAVOINE et al., 2012; DUFRESNE, 2013), conceitos e classificações referentes às nanofibras de celulose já estão se consolidando no meio científico. Dentre os diferentes tipos relatados, as nanofibrilas de celulose vêm ganhando destaque pela relativa facilidade e praticidade de obtenção.

Nanofibrilas de celulose (NFC) diferem de microfibrilas de celulose. Microfibrilas de celulose são fibrilas de 3–10 nm de espessura formadas durante a biosíntese da celulose nos vegetais superiores (BRETT, 2000) enquanto nanofibrilas de celulose (NFC) consistem em agregados de microfibrilas (SVAGAN; HEDENQVIST; BERGLUND, 2009). Em revisão realizada por Siró e Placket (2010), as nanofibrilas de celulose são entendidas como um agregado de microfibrilas de celulose com diâmetro oscilando entre 10 - 40 nm, comprimento maior que 1000 nm, apresentando valores de razão de aspecto entre 100 e 150.

As nanofibrilas de celulose são obtidas por intensivo tratamento mecânico de polpa celulósica, branqueada ou não. A desintegração da parede celular vegetal produz fibrilas de celulose longas (largura de 5-50 nm e comprimento de alguns micrômetros) e fragmentos de fibras, devido à clivagem transversal ao longo do eixo longitudinal da estrutura microfibrilar da celulose, com alta razão de aspecto (MOON et al., 2011), e sua morfologia favorece a aplicação como reforço em compósitos devido a sua estrutura em forma de trama, semelhante a uma rede (LU; WANG; DRZAL, 2008; SIRÓ; PLACKETT, 2010; CHINGA-CARRASCO, 2011).

Esforços para melhor entender esta matéria-prima vieram nos esclarecer que as nanofibrilas de celulose, apesar de sua aplicação em produtos e processos modernos de alta tecnologia, caracterizam-se como material heterogêneo composto por nanofibras, fibrilas finas, fragmentos de fibras e fibras, sendo predominante o componente nanofibrilas quando obtido por homogeneização (CHINGA-CARRASCO, 2011).

Os primeiros métodos mecânicos descritos para obtenção de nanofibrilas de celulose, relatados por Herrick et al. (1983) e Turbak et al. (1983) apud Siqueira, Bras e Dufresne (2010) utilizaram polpa branqueada em suspensão aquosa processada em homogeneizador mecânico com adição de alta pressão, para facilitar a fibrilação do material (SIQUEIRA; BRAS; DUFRESNE, 2010). O material desfibrilado apresentava microfibrilas livres, com alta razão de aspecto, exibindo aspecto de gel com propriedades pseudoplásticas e tixotrópicas.

Com o avanço da tecnologia, novos métodos e equipamentos para processamento mecânico foram desenvolvidos e, atualmente, tem-se difundido o processamento mecânico à pressão atmosférica, utilizando-se equipamentos específicos para esse fim, com um tratamento mecânico muito simples, cujo princípio de funcionamento se baseia na deposição das microfibrilas de celulose,

formando a parede celular vegetal (KLEMM et al., 2011) e empregando-se polpas lignocelulósicas, contendo lignina e hemiceluloses residuais (IWAMOTO; ABE; YANO, 2008; WANG; CUI; ZHANG, 2012).

Alguns trabalhos melhoraram o processo de desfibrilação e a homogeneidade das nanofibrilas de celulose utilizando-se de pré-tratamentos da polpa lignocelulósica inicial (SPENCE et al., 2010; CHINGA-CARRASCO, 2011; ISOGAI; SAITO; FUKUZUMI, 2011; JANARDHANAN; SAIN, 2011; KLEMM et al., 2011; HASSAN et al., 2012; ALILA et al., 2013).

A proveniente de fibras lignocelulósicas vem sendo estudada para uma gama de aplicações, variando desde o uso como reforço para melhoria das propriedades mecânicas e de barreira de biocompósitos (SVAGAN, 2008; KLEMM et al., 2011; LAVOINE et al., 2012;), até como aditivos na produção de papel (LAVOINE et al., 2012; HASSAN et al., 2015), tintas e recobrimentos (LI et al. 2013), na indústria de embalagens (SPENCE et al., 2010; LAVOINE et al., 2012; MAJEED et al., 2013; LAVOINE; DESLOGES; BRAS, 2014), na produção e/ou reforço de filmes finos e *nanopapers* (CHENG et al., 2014; SEHAQUI; ZIMMERMANN; TINGAUT, 2014; URRUZOLA et al., 2014) em aplicações biomédicas e farmacêuticas (SVENSSON et al., 2005; NIKOLAJASKI et al., 2012;), bem como substratos eletrônicos (IWAMOTO et al., 2005; LIN; RENNECKAR; HINDMAN, 2008; OKAHISA et al., 2009; UMMARTYOTIN et al., 2012).

2.3 Pré-tratamentos na produção de nanofibrilas de celulose

A produção de nanofibras celulósicas, seja pela rota química, seja pela rota mecânica, exige do material lignocelulósico a maior proporção celulósica possível (Figura, 3). Como o material lignocelulósico é composto de celulose, hemiceluloses, lignina, pectina e compostos secundários, tais como ceras,

extrativos, flavonoides e terpenos o uso de espécies vegetais que, naturalmente, possuem uma proporção majoritária de celulose já é o primeiro pré-requisito a ser atendido no momento da escolha da fibra a utilizar (GHAREHKHANI et al., 2015).

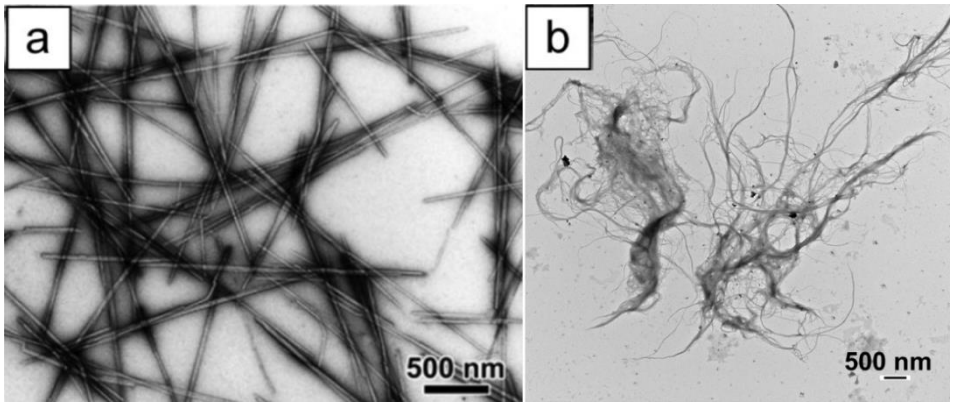

Figura 3 Morfologia representativa dos nanocristais (a) e nanofibrilas de celulose (b) Fonte imagem (a), Habibi, Lucia e Rojas (2010)

Contudo, muitos estudos utilizam-se de pré-tratamentos químicos para o isolamento da celulose de fibras vegetais, com consequente remoção ou redução de compostos químicos indesejáveis à produção de celulose em nanoescala (NGUYEN et al., 2013; SIRÓ; PLACKETT, 2010), visto que a maioria das espécies vegetais não é composta de valores acima de 60% de celulose *in natura*, exceção destacada para o algodão, que possui cerca de 99% de celulose em sua composição química natural.

Na produção de nanofibras de celulose, os pré-tratamentos mais difundidos são hidrólise ácida (ZIMMERMAN; PÖHLER; GEIGER, 2004; HUBBE et al., 2008; URRUZOLA et al., 2014), alcalino (SIQUEIRA; BRAS; DUFRESNE, 2010; SIRÓ ; PLACKETT, 2010; BUFALINO et al., 2014; 2015; URRUZOLA et al., 2014), oxidação (SAITO et al., 2006; SIRÓ; PLACKETT, 2010; ISOGAI; SAITO; FUKUZUMI, 2011; JIANG; HAN; HSIEH, 2013;

LAVOINE et al., 2012; JIANG; HSIEH, 2013) e enzimático (PÄÄKKÖ et al., 2007; HUBBE et al., 2008; SVAGAN, 2008; SVAGAN; HEDENQVIST; BERGLUND, 2009; SIRÓ; PLACKETT, 2010; JANARDHANAN; SAIN, 2011; LAVOINE et al., 2012). Neste trabalho, deter-nos-emos em abordar o pré-tratamento alcalino visando à obtenção de nanofibrilas de celulose, temática abordada no artigo 1.

O pré-tratamento alcalino destaca-se por sua praticidade, facilidade e efetividade. Sua aplicação é reportada por diferentes autores ora para remoção de pectinas e hemiceluloses (NGUYEN et al., 2013; PELISSARI; SOBRAL; MENEGALLI, 2014), ora para solubilização de lignina, mantendo-se as pectinas e hemiceluloses (SIRÓ; PLACKETT, 2010) ou remoção de lignina e hemiceluloses (JÄHN et al., 2002; KIM; NETRAVALI, 2010). É um dos tratamentos químicos menos onerosos e mais ambientalmente amigáveis, que pode melhorar as propriedades mecânicas e interfaciais de fibras vegetais tratadas sem a necessidade de utilizar produtos químicos orgânicos tóxicos (PIMENTA et al., 2008) além de melhorar a força de adesão interfacial de fibra vegetal com a matriz polimérica (GEETHAMMA et al., 1998) e copolimérica (ROSA et al., 2009) assim como as propriedades mecânicas e térmicas das fibras tratadas (PIMENTA et al., 2008).

Na produção de nanocristais de celulose, o tratamento alcalino pode ser executado a partir de soluções de hidróxido de sódio - NaOH (ZULUAGA et al., 2009; BUFALINO et al., 2014; 2015) e hidróxido de potássio - KOH (ZULUAGA et al., 2009; PELISSARI; SOBRAL; MENEGALLI, 2014;) em diferentes concentrações, geralmente seguido de uma etapa de branqueamento (SIQUEIRA; BRAS; DUFRESNE, 2010), nas soluções de hipoclorito de sódio – NaClO (NGUYEN et al., 2013), clorito de sódio – $NaClO_2$ (ZULUAGA et al., 2009; OKAHISA et al., 2011; PELISSARI; SOBRAL; MENEGALLI, 2014; URRUZOLA et al., 2014) e peróxido de hidrogênio – H_2O_2 (SUN et al., 2001;

URRUZOLA et al., 2014; BUFALINO et al., 2014; 2015) em diferentes concentrações, visando remover os grupos fenólicos e moléculas cromóforas da lignina (NGUYEN et al., 2013; PELISSARI; SOBRAL; MENEGALLI, 2014).

O tratamento alcalino composto de solução alcalina de NaOH é denominado mercerização (SARKAR, 2001; KIM; NETRAVALI, 2010; RAY; TEODORO et al., 2011; KALIA et al., 2013), auxilia no entumescimento das fibras celulósicas (GURGEL, 2007), aumenta a concentração de celulose reduzindo a composição química de lignina e hemiceluloses nas fibras lignocelulósicas e, em certos casos, altera a orientação molecular dos cristalitos de celulose e diminui seu grau de polimerização (GURGEL, 2007; KIM; NETRAVALI, 2010; SILVA et al., 2013; MIRANDA et al., 2015). A mercerização caracteriza-se por ser um dos métodos mais comuns para melhorar a estrutura e propriedades mecânicas das fibras tratadas (RAY; SARKAR, 2001). Age separando os feixes de fibras e expondo as microfibrilas de celulose (entumescimento). Em condições específicas relativas à concentração de NaOH, temperatura e velocidade de agitação mecânica, aumenta a flexibilidade da fibra celulósica (MIRANDA et al., 2015) e seu grau de cristalinidade (SILVA et al., 2013), diminui o diâmetro da fibra e a rugosidade da superfície da fibra, influenciando, positivamente, na adesão interfacial fibra-matriz e, consequentemente, nas propriedades mecânicas do compósito reforçado com as fibras tratadas (KIM; NETRAVALI, 2010; BELTRAMI; SCIENZA; ZATERRA, 2014) pois atua na redução da hidrofilicidade da fibra celulósica (GURGEL, 2007).

O branqueamento da fibra vegetal realizado com solução contendo NaOH e H_2O_2, é chamado de peróxido alcalino, sendo reportado na literatura para deslignificação efetiva de materiais lignocelulósicos (GOULD, 1984; SUN et al., 2001; TEODORO et al., 2011). Assim como o método clorito de sódio/

ácido acético (WISE; MARPHY; D'ADIECO, 1946) ou o método ácido peracético (JIMENÉZ et al., 2008; ZHAO et al., 2010; ZHAO; WU; LIU, 2011).

O peróxido alcalino é uma solução branqueadora não clorada e menos poluente ao ambiente que facilita o acesso à celulose (HENDRIKS; ZEEMAN, 2009) e melhora a adesão e dispersão das fibras vegetais à matriz polimérica com consequente melhoria das propriedades mecânicas dos compósitos reforçados com as fibras tratadas (CAMPOS et al., 2011). Atua removendo lignina pela ação de fortes radicais hidroxil, formados em pH alcalino, aumentando a concentração de carboidrato estrutural (GRAY, 2013) e apresenta excelente eficiência no tratamento de fibras provenientes de monocotiledôneas, especialmente da família Gramineae (GOULD, 1985a). Um detalhamento da ação do peróxido alcalino no branqueamento de fibras vegetais pode ser encontrado em Cabrera et al. (2014), Gould (1985b), Selig et al. (2009) e Sun et al. (2000).

A opção de se tratar o material lignocelulósico, bem como madeira, utilizando-se solução alcalina de NaOH, alta temperatura e pressão, denominada de cozimento alcalino, seguido do branqueamento peróxido alcalino é outra alternativa que vem sendo utilizada para remoção de compostos não celulósicos (BUFALINO et al., 2014; 2015).

Adotando-se o cozimento alcalino seguido do branqueamento peróxido alcalino como pré-tratamento para produção de nanofibrilas de celulose, Bufalino et al. (2015) observaram que a fibra vegetal tratada, contendo alto teor de celulose purificada, gerou nanoestruturas de celulose com menores diâmetros, menor quantidade de passagens pelo desfibrilador mecânico, comparada com os materiais com maior teor de compostos não celulósicos além de gerar filmes menos opacos e mais coloridos. Portanto, a natureza química da fonte vegetal influencia o resultado a ser obtido pelo pré-tratamento e, consequentemente, a

morfologia da nanofibra celulósica (BUFALINO et al., 2015) e seu rendimento (URRUZOLA et al., 2014).

Quando se opta pela rota química, o ataque ácido do material lignocelulósico para produção de nanocristais de celulose, exige-se da matéria-prima maior grau de isolamento da celulose, já que a presença de lignina em meio ácido interfere no processo de obtenção das nanoestruturas. Consequentemente, reagentes químicos mais fortes são utilizados para seu isolamento. Entretanto, conhecendo-se a natureza da lignina presente no material lignocelulósico em estudo, é possível reduzir gastos e planejar-se de maneira mais eficiente, o tipo e a concentração adequada de solução branqueadora, já que baixos valores obtidos na relação siringil/guaiacil (S/G) da lignina são relacionados à resistência dos grupos aromáticos e à reduzida oxidação (BUFALINO et al., 2015).

Alguns trabalhos realizados na produção de nanofibrilas de celulose relatam a necessidade de material celulósico puro ou com baixa fração de componentes não celulósicos, proveniente de fonte vegetal madeireira (BHATNAGAR; SAIN, 2005; IWAMOTO et al., 2005; IWAMOTO; NAKAGAITO; YANO, 2007; SVAGAN; HEDENQVIST; BERGLUND, 2009; BESBES; VILAR; BOUFI, 2011; CHINGA-CARRASCO, 2011; SVAGAN, 2008; KLEMM et al., 2011, PANTHAPULAKKAL; SAIN, 2012; DUFRESNE, 2013), bem como de recursos não madeireiros (DINAND; CHANZY; VIGNON, 1996; DINAND; CHANZY; VIGNON, 1999; BHATNAGAR; SAIN, 2005; ZULUAGA et al., 2009; SIRÓ; PLACKETT, 2010; CHINGA-CARRASCO, 2011; DUFRESNE, 2013; PANTHAPULAKKAL; SAIN, 2013; CHENG et al., 2014).

A produção de microfibrilas de celulose a partir de fibras vegetais foi reportada por Dufresne, Cavaillé e Vignon (1997), ao adotar o pré-tratamento químico para isolamento da celulose seguido de posterior tratamento mecânico.

O processamento mecânico pode ser pressurizado ou não e visa facilitar o processo de desfibrilamento e a redução de custos de obtenção de nanocelulose pela redução de energia de consumo a partir de pré-tratamentos enzimáticos bem como pela combinação de pré-tratamentos, sejam químicos e/ou enzimáticos (DUFRESNE; CAVAILLÉ; VIGNON, 1997; NAKAGAITO; YANO, 2004; ANKERFORS et al., 2007; HENRIKSSON et al., 2007; PÄÄKKÖ et al., 2007; SIRÓ; PLACKETT, 2010; SIQUEIRA; BRAS; DUFRESNE, 2010; BUFALINO et al., 2014; 2015).

Muitos pesquisadores acreditam que os componentes não celulósicos são indesejados no processo de produção da nanofibrilas de celulose, entretanto, resultados têm demonstrado que, dependendo do uso final deste produto, as nanofibrilas de celulose contendo lignina podem ser promissoras matérias-primas na produção de embalagens, apresentando propriedades físicas desejadas, suspensão mais homogênea contendo fibrilas com diâmetros inferiores à 100 nm (CHINGA-CARRASCO, 2011), além de possibilitar a redução de custos de produção pela redução de químicos e energia necessária à sua obtenção (SPENCE et al., 2010)

Outro aspecto a ser levado em consideração é a relativa agressividade de certos pré-tratamentos químicos à estrutura celulósica das fibras vegetais, como é o caso do branqueamento usando clorito de sódio ($NaClO_2$) que pode degradar a fibra vegetal e, consequentemente, as nanofibras celulósicas resultantes (OKAHISA et al., 2011) ou altas concentrações de NaOH que podem transformar a estrutura cristalina da celulose tipo I para tipo polimórfico II, termodinamicamente mais estável (KOLPAK; WEIH; BLACKWELL, 1978; LANGAN; NISHIYAMA; CHANZY, 1999; SCHENZEL et al., 2007). O pré-tratamento químico exige cuidado em sua execução, para que a celulose proveniente do material lignocelulósico mantenha-se íntegra, garantindo a

qualidade das nanofibras a serem obtidas (BHATNAGAR; SAIN, 2005; WANG; SAIN; OKSMAN, 2007; ZULUAGA et al., 2009).

A presença de hemiceluloses melhorou as propriedades mecânicas e reduziu a expansão térmica de compósitos reforçados com nanofibrilas de celulose, indicando que as hemiceluloses atuam como inibidores de ligações de hidrogênio entre as microfibrilas durante o processo de secagem, além de facilitar o processo de fibrilação da parede celular e promover adesão entre as nanofibras (CARLSSON; KOLSETH; LINDSTRÖM, 1983; IWAMOTO; ABE; YANO, 2008).

Em celulose nanofibrilada, a presença de lignina pode resultar em nanocelulose contendo maior hidrofobicidade comparada com nanocelulose pura, o que pode proporcionar boa compatibilidade com matrizes poliméricas na produção de compósitos (WANG; CUI; ZHANG, 2012).

2.4 Modificação química de nanofibrilas de celulose

A celulose em nanoescala possui boa compatibilidade com matrizes poliméricas, melhorando as propriedades mecânicas de compósitos reforçados com a mesma (WANG; CUI; ZHANG, 2012), mas a modificação química superficial das nanofibras de celulose pode melhorar a compatibilidade entre a celulose e as matrizes poliméricas, na produção de compósitos, nanocompósitos e bionanocompósitos (WANG; SAIN; OKSMAN, 2007; LÖNNBERG et al., 2008; LU; WANG; DRZAL, 2008; XIE; YU; SHI, 2009; LIU et al., 2013; MISSOUM; BELGACEM; BRAS, 2013; MISSOUM et al., 2013; SEHAQUI; ZIMMERMANN; TINGAUT, 2014; KHALIL et al., 2014; LAVOINE; DESLOGES; BRAS, 2014; ASHORI et al., 2014).

Em termos científicos, são três as razões principais que explicam a necessidade de se modificar a superfície da celulose e seus derivados utilizados

em compósitos poliméricos: reduzir sua hidrofilicidade bem como favorecer sua compatibilidade com polímeros hidrofóbicos e dispersividade em solventes apolares (ASHORI et al., 2014). A capacidade da celulose de formar suspensões aquosas estáveis é conhecida e tem sido usada como aliada na produção de compósitos de matrizes hidrofílicas. Entretanto, o reforço em polímeros hidrofóbicos é limitado por sua natureza hidrofílica (BULOTA et al., 2012).

Celuloses nano e microfibrilada podem ser utilizadas em várias aplicações, com suas propriedades substancialmente melhoradas. No entanto, alguns inconvenientes limitam a sua utilização, tais como agregação, baixa concentração da suspensão e incompatibilidade com matrizes poliméricas hidrofóbicas. Uma solução para superar estes problemas é a modificação química destes materiais, estudo que vem ganhando destaque na busca pela melhoria de sua compatibilidade em matrizes apolares pela hidrofobização da sua superfície (SIRÓ; PLACKETT, 2010).

Além disso, tal operação permite obter novas funcionalidades (HEINZE; LIEBERT, 2001; ANDRESEN et al., 2007; ANDRESEN; STENIUS, 2007; RODIONOVA et al., 2010; LAVOINE; DESLOGES; BRAS, 2014; MISSOUM et al., 2014; HOKKANEN et al., 2015; SAINI et al., 2015; ZHU et al., 2015; ZHANG; PEI; WANG, 2016).

Isto é possível devido à reatividade hidroxílica da celulose (HUBBE et al., 2008). Os grupos hidroxílicos podem reagir com agentes de adição, substituição e oxidação. Seus grupos acetais podem sofrer hidrólise em meio ácido ou alcalino. Os grupos aldeídicos terminais podem ser reduzidos em grupos alcoóis, oxidados em grupos carboxilas e, quando há álcali, podem ser rearranjados, formando grupos finais alcoólicos ou carboxílicos. Contudo, a conformação molecular estrutural da celulose determina a desuniformidade das reações (BROWNING, 1963).

Os grupos hidroxílicos mais reativos na superfície da celulose são O2 e O6 enquanto que O3 mantém-se praticamente não reativo devido à força de ligação "intra" cadeia dos grupos O3 e O5 (ROWLAND; HOWLEY, 1988; HABIBI; LUCIA; ROJAS, 2010) como observado na Figura 4. Informações relacionadas à estrutura, características e propriedades da celulose podem ser encontradas em diversos trabalhos citados por Kontturi (2005).

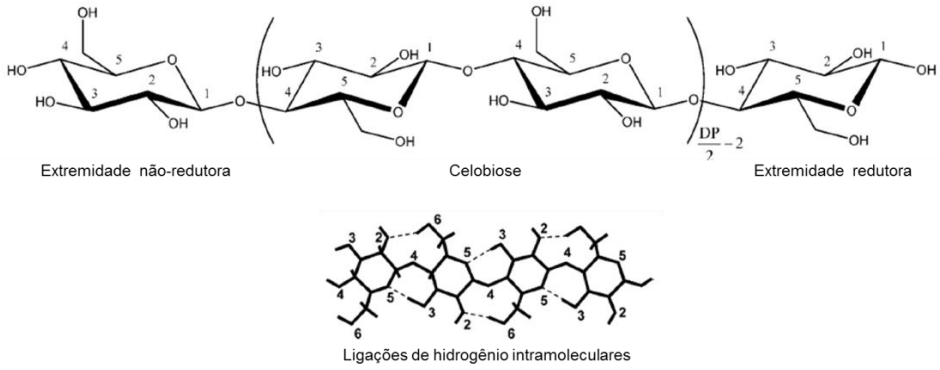

Figura 4 Esquema representativo da estrutura química da celulose e de suas ligações de hidrogênio intramoleculares

Fonte: Adaptado de Habibi, Lucia e Rojas (2010).

São muitos os métodos empregados para modificação superficial de fibras de celulose (LOVE et al., 2008; PINTO et al., 2008; XIE; YU; SHI, 2009; XIE et al., 2010; CORDEIRO; GOUVEIA; JOHNB, 2011; KABIR et al., 2012; KALIA et al., 2013).

A modificação química da celulose para fins tecnológicos é de suma importância para viabilizar sua compatibilidade química com substâncias ou produtos de natureza apolar tais como diversos polímeros sintéticos, reduzir sua hidrofilicidade bem como melhorar suas propriedades físico-mecânicas, além de possibilitar a produção de derivados de celulose para múltiplas aplicações industriais (acetato de celulose, viscose, celofane, etc) assim como novos

materiais, dentre eles: nanocompósitos e compósitos poliméricos e nanomateriais híbridos.

Estudos mais recentes tratam da modificação de nanofibras de celulose (ASHORI et al., 2014; KHALIL et al., 2014; MISSOUM et al., 2014; SEHAQUI; ZIMMERMANN; TINGAUT, 2014; HOKKANEN et al., 2015; SAINI et al., 2015; ZHU et al., 2015; ZHANG; PEI; WANG, 2016).

A modificação superficial das nanofibrilas de celulose é muito recente (SIRÓ; PLACKETT, 2010), com menos de 100 publicações vinculadas às renomadas bases de pesquisa científica.

No que diz respeito à modificação da celulose em nanoescala, temos os mecanismos físicos, por interações físicas pela adsorção de moléculas ou macromoléculas sobre a sua superfície, e os químicos, utilizando uma abordagem química para atingir ligações covalentes entre substratos celulósicos e agentes de acoplamento, como principais estratégias empregadas (MISSOUM et al., 2013).

Dentre os principais métodos de modificação química da celulose, temos a formação de grupos iônicos por carboximetilação, oxidação e sulfonação bem como a geração de superfícies hidrofóbicas por acetilação, isocianatos e sililação (KHALIL et al., 2014). Para melhor compreensão do artigo 2, iremos nos deter aos processos de deposição de partículas de sílica sobre a superfície das nanofibrilas de celulose.

2.4.1 Deposição de sílica em nanofibras de celulose

A deposição de sílica pode ser considerada um processo natural, visto que é realizada nas plantas, pela deposição de corpos silicosos em tecidos, especializados ou não, dentro do corpo de diferentes espécies vegetais, principalmente nas espécies de famílias denominadas acumuladoras (REIS et al.,

2007), tais como Gramineae, Arecaceae, Poaceae, Cyperaceae e Equisitaceae (TOMLINSON, 1990; REIS et al., 2007).

O silício (Si) é o segundo elemento químico mais abundante na crosta terrestre e naturalmente acumula-se em tecidos vegetais, representando cerca de 1 a 10% de sua massa seca (REIS et al., 2007).

A deposição de sílica em fibras e nanofibras de celulose (GOUSSÉ et al., 2004; HUBBE et al., 2008; KHALIL et al., 2014; RAABE et al., 2014; SIRÓ; PLACKETT, 2010) bem como no desenvolvimento de compósitos e nanocompósitos híbridos (PINTO et al., 2008; XIE; YU; SHI, 2009; XIE et al., 2010; ASHORI et al., 2012; CAI et al., 2012; RAABE et al., 2015) sintetiza as partículas de sílica em sua forma química mais estável, o quartzo (SiO_2), o mineral inerte das areias (REIS et al., 2007).

Maleki, Durães e Portugal (2014) afirmam que, a partir do método sol-gel, diferentes fontes de alcóxidos silicosos, sendo os mais comuns, tetrametil ortosilicato (TMOS) e tetraetil ortosilicato (TEOS) são utilizados para sintetização de sílica por reações de hidrólise, a partir de catalizador ácido, ou por condensação, utilizando catalizador básico.

Trabalhos vêm utilizando o método sol-gel para sintetizar sílica (SiO_2) nanoestruturada sob a superfície de fibras de celulose, a partir de alcóxidos silicosos, precursores de sílica, tais como o tetraetilortosilicato – TEOS para produzir nanomateriais híbridos (PINTO et al., 2008; XIE et al., 2010; XIE; YU; SHI, 2009; ASHORI et al., 2012; CAI et al., 2012). *Water glass* ou, traduzindo literalmente, água de sílica, também foi reportada como fonte precursora de sílica para sintetização *in situ* de sílica na produção de nanocompósitos híbridos celulose-sílica (LIU et al., 2013).

Já a síntese de sílica pelo método sol-gel sobre a superfície de nanofibras de celulose foi utilizada para formar nanocompósitos híbridos aerogéis de

celulose regenerada com baixos coeficientes de expansão térmica, alta compatibilidade e resistência e dureza melhoradas (CAI et al., 2012).

Xie, Yu e Shi (2009) produziram um compósito híbrido celulose-sílica a partir de três fontes de sílica, por meio de reações sol-gel: (i) a partir do precursor TEOS; (ii) a partir do agente de acoplamento APS e (iii) a partir do agente de cruzamento Tri-EBAC. As nanofibrilas de celulose modificadas apresentaram partículas inorgânicas em nanoescala, que estavam dispersas na matriz celulósica, ligadas à celulose por ligações covalentes do tipo *crosslink* A sílica proveniente destas ligações covalentes formou filme flexível e homogêneo sobre a celulose. Todos os compósitos híbridos apresentaram propriedades térmicas melhoradas. O método de impregnação de solução com vistas à formação de nanocompósitos híbridos celulose-sílica a partir de hidrogéis de celulose bacteriana também já foi relatado (ASHORI et al., 2012).

Para o desenvolvimento da tese, a deposição de sílica sobre a superfície de nanofibrilas de celulose para produção dos aerogéis híbridos celulose-sílica foi realizada adaptando-se a metodologia descrita por Ashori et al. (2012).

2.5 Nanocompósitos híbridos celulose-sílica

Nanocompósitos híbridos surgem como um material para múltiplas aplicações, categorizado muitas vezes como nanocompósitos funcionais de estrutura hierárquica, de funcionalidade melhorada, como resultado da junção da matriz polimérica, recebendo a funcionalidade das nanopartículas inorgânicas, o agente de reforço do nanocompósito híbrido polímero-partícula inorgânica (YAN, 2011).

A sílica (SiO_2) em nanoescala vem sendo reportada por diferentes autores como agente de reforço que melhora as propriedades mecânicas e de barreira de diversas matrizes poliméricas tais como o polipropileno, propileno

isostático, as propriedades mecânicas e de barreira, reduzindo a adsorção de umidade do amido, melhorando as propriedades térmicas e mecânicas do álcool polivinílico bem como a resistência à tração e à umidade de filmes biodegradáveis de amido/ álcool polivinílico/ sílica. Publicação utilizando nanopartículas de sílica para imobilização de sistemas enzimáticos com potencial uso para biosensibilidade também foi relatada por Azeredo (2009).

Em trabalho realizado por Xie, Yu e Shi (2009) diversos autores são citados por produzirem materiais híbridos polímero/sílica a partir da deposição de sílica nanoestruturada pelo método sol-gel, utilizando diferentes precursores inorgânicos em que diferentes polímeros são indicados para inúmeras aplicações, especialmente para fins biomédicos.

Nanocompósitos híbridos celulose-sílica podem ser produzidos por diversos métodos, dentre os mais utilizados temos: *electrospinning*, mineralização modelada, rede de ligações de hidrogênio, método sol-gel, método solução-casting e método layer-by-layer (YAN, 2011). Contudo, o método sol-gel apresenta-se como o mais frequentemente utilizado, associado ao mecanismo de imersão para formação das partículas e nanopartículas de sílica sobre a superfície celulósica.

Nanocompósitos híbridos de celulose bacteriana/sílica foram formados pela imersão do hidrogel de celulose bacteriana em solução aquosa de TEOS. Todos os nanocompósitos mostraram uma boa dispersão das fibras e uma forte adesão entre reforço-matriz. A sílica em nano-escala foi incorporada entre os vazios e microfibrilas da matriz de celulose bacteriana. As propriedades mecânicas foram melhoradas com a presença da nanopartícula de sílica. Espectros obtidos a partir de Espectroscopia na região do Infravermelho com Transformada de Fourier (FTIR) ilustraram as fortes interações químicas geradas entre as fases de sílica e celulose (ASHORI et al., 2012).

Guzun et al. (2014) também produziram nanocompósitos híbridos celulose bacteriana/sílica e nanocompósitos híbridos funcionais de celulose bacteriana/sílica/ácido úsnico. Os nanocompósitos híbridos de celulose bacteriana/sílica foram formados pela condensação/hidrólise *in situ* de sílica utilizando o precursor TEOS sobre as membranas umedecidas da celulose bacteriana.

As propriedades dos nanocompósitos foram influenciadas pela presença da sílica. Os nanocompósitos híbridos apresentaram superfície hidrofóbica e interações fortes entre sílica e celulose, tal como encontrado por Ashori et al. (2012). Os nanocompósitos híbridos funcionais, de ação antimicrobiológica, foram recomendados pelos autores para aplicações biomédicas visto apresentarem superfícies antiaderentes, de atividade anti-biofilme. Contudo, o tamanho das partículas de sílica em nanoescala, pelo método sol-gel, depende da concentração do catalisador, tempo e temperatura de reação e sua quantidade depende da temperatura de reação e da proporção água: TEOS (GUZUN et al., 2014).

Além destes, aerogéis celulose-sílica, novos compósitos híbridos, vêm ganhando destaque em pesquisas recentes por suas características e propriedades potenciais para diversas aplicações.

No artigo 3 apresentado na segunda parte desta tese, serão apresentadas as características e propriedades obtidas para o nanocompósito híbrido celulose-sílica desenvolvido.

2.5.1 Aerogéis celulose-sílica

A partir de 1930 (FRICKE; TILLOTSON, 1997), uma nova classe de materiais sólidos, chamados aerogéis, foram desenvolvidos. Aerogéis são materiais aerados, leves, formados por espumas de baixa densidade, alta

superfície específica, devido a sua natureza porosa, resultantes da secagem do gel proveniente de uma solução sol-gel; Possuem, ainda, características de baixa condutividade térmica, baixa velocidade de propagação sonora, baixa constante dielétrica e baixa taxa de refração (BRINKER; SCHERER, 1990; FRICKE; TILLOTSON, 1997; HÜSING; SCHUBERT, 1998; KOCON; DESPETIS; PHALIPPOU, 1998; WAGH et al., 1997; YAMAUCHI, 2001; JOB et al., 2005; AEGERTER; LEVENTIS; KOEBEL, 2011; SEHAQUI; ZHOU; BERGLUND, 2011; CAI et al., 2012; LIN et al., 2014) com boas propriedades para aplicações elétricas, ópticas, acústicas e térmicas (BAETENS; JELLE; GUSTAVSEN, 2011) além de potencial para estudos em catálise (HÜSING; SCHUBERT, 1998).

Os primeiros aerogéis comerciais desenvolvidos pelo método sol-gel foram aerogéis de sílica, formados a partir de extrações supercríticas, na década de 1950. Na década de 1960, organosilanos foram utilizados como precursores de sílica, para desenvolvimento de aerogéis de sílica, como método alternativo ao "water glass", por ser menos oneroso e mais prático, consumindo menor tempo e reagentes. Este método vem sendo empregado até os dias atuais (TAMON; KITAMURA; OKAZAKI, 1998). A partir de progressos adquiridos, pesquisas em aerogéis ganharam impulso na década de 1980 (FRICKE; TILLOTSON, 1997).

Aerogéis de sílica são sólidos frágeis compostos por partículas interconectadas que formam uma nanoestrutura aberta, podendo exibir propriedades mecânicas dependendo da densidade produzida (PARMENTER; MILSTEIN, 1998; WONG et al., 2014). Além de se apresentarem como materiais de insulamento inertes, atóxicos e ambientalmente amigáveis (FRICKE; TILLOTSON, 1997).

A partir dos anos 2000, uma nova classe de aerogéis baseada em biomassa foi desenvolvida: os bio-aerogéis, preparados pela dissolução

polimérica, gelatinização e coagulação de polissacarídeos em um solvente, seguido de uma etapa de secagem que pode ser supercrítica, usando CO_2 (DEMILECAMPS et al., 2015), sob pressão ambiente (FRICKE; TILLOTSON, 1997), liofilização, descompressão rápida, entre outros (MOON et al., 2011).

A partir destes processos de secagem, aerogéis de celulose podem ser obtidos a partir de soluções e suspensões celulósicas, evitando-se a aglomeração da celulose (MOON et al., 2011). Aerogéis de celulose são produzidos a partir de espumas aquosas pela estabilização de nanofibras celulósicas (CERVIN et al., 2013) com diversificada utilização tais como: produção de supercapacitores (ZHANG et al., 2014), como material adsorvente (OSHIMA et al., 2014), absorvente (CHIN; ROMAINOR; PANG, 2014; JIN et al., 2015), insulante térmico (SHI et al., 2013; NGUYEN et al., 2014;), na liberação controlada de fármacos (VALO et al., 2013) e na produção de materiais funcionais (CAI et al., 2015; HE et al., 2014). Podem atuar como potencial nova classe de produtos ou subprodutos celulósicos (SEHAQUI; ZHOU; BERGLUND, 2011; THAPLIYAL; SINGH, 2014) atendendo à demanda por bio-aerogéis flexíveis (DEMILECAMPS et al., 2015). Foram desenvolvidos a partir da década de 1950, mas só ganharam proporções maiores a partir dos anos 2000 (MOON et al., 2011), contudo pesquisas relacionadas a esses materiais ainda são escassas.

Aerogéis celulose-sílica caracterizam-se como uma nova geração de bio-aerogéis desenvolvida para fornecerem aerogéis híbridos leves e fortemente reforçados unindo a característica de alta ductilidade do aerogel de celulose e a baixa condutividade térmica relatada para o aerogel de sílica (DEMILECAMPS et al., 2015).

Aerogéis de celulose-sílica foram desenvolvidos usando diferentes métodos tais como síntese pelo método sol–gel utilizando TEOS como precursor de sílica nanoestruturada seguido de secagem crítica com CO_2 (CAI et al., 2012); gelatinização de solução de sílica sobre nanofibrilas de celulose seguida

de secagem supercrítica com CO_2 (HE et al., 2014); síntese de sílica sobre filmes hidrogéis de celulose a partir de "water glass" seguida de secagem supercrítica com CO_2 (LIU et al., 2013) e impregnação de sílica em celulose úmida coagulada utilizando polietoxidisiloxano por difusão molecular e fluxo de força induzida por gradiente de pressão (DEMILECAMPS et al., 2015) ou por imersão em solução aquosa de TEOS seguido por pressão aquecida (ASHORI et al., 2012).

Os aerogéis celulose-sílica formados pela síntese *in situ* de sílica em aerogéis de celulose via precursor TEOS apresentaram melhores propriedades de resistência mecânica e flexibilidade, grande área superficial, semi-translucidez e baixa condutividade térmica comparados aos aerogéis de celulose ou de sílica (CAI et al., 2012). Segundo os autores, com a facilidade de preparação e ampla possibilidade de composição/propriedades deste método, espera-se que seja possível embasar o desenvolvimento de diversos materiais nanoporosos avançados.

Demilecamps et al. (2015) produziram aerogéis celulose-sílica impregnando *alcogels* de celulose em solução de sílica, utilizando-se de dois mecanismos: difusão molecular e fluxo forçado. A solução de sílica foi preparada a partir do precursor de sílica TEOS, contudo, os autores utilizaram o polietoxidisiloxano (PEDS) como pré-polimerizador em etapa posterior à sintetização das partículas de sílica. Os aerogéis híbridos apresentaram acréscimo em suas propriedades mecânicas e flexibilidade, comparados aos aerogéis de celulose pura ou aos aerogéis de sílica, atingindo-se grandes taxas de deformação sem que ocorresse fratura ou significativas deformações permanentes, diferentemente do que é observado para aerogéis de sílica. Além disso, houve aumento da área superficial e redução da condutividade térmica.

Liu et al. (2013) desenvolveram aerogéis celulose-sílica a partir da síntese *in situ* de partículas de sílica sobre membranas de celulose regenerada

pela imersão em “water glass”. Contudo, as imagens apresentadas no trabalho demonstram estruturas diferentes das esperadas para aerogéis, conforme afirmam Demilecamps et al. (2015). Os nanocompósitos apresentaram partículas de sílica confinadas nos poros da trama celulósica preservando a integridade química da celulose e mantendo sua estrutura de porosidade aberta.

Aerogéis hidrofóbicos sílica-celulose foram produzidos por He et al. (2014) pela síntese de partículas de sílica sobre a superfície das nanofibrilas de celulose, utilizando-se o método sol-gel, tendo o dimetil sulfóxido como solvente e metiltrimetoxisilano (MTMS) como precursor de sílica, seguido de secagem supercrítica com CO_2. As estruturas e propriedades hidrofóbicas obtidas assemelharam-se aos resultados de aerogéis de sílica.

A flexibilidade encontrada por He et al. (2014) também foi obtida nestes nanocompósitos híbridos. Entretanto, os autores observaram ausência de interação química entre a celulose e as partículas de sílica, apesar da sinergia entre tais componentes influenciar positivamente as propriedades mecânicas finais dos aerogéis híbridos. O tempo de impregnação foi a principal diferença encontrada pelos autores para os métodos de impregnação testados, sendo necessários apenas 30 minutos de impregnação para a celulose apresentar partículas de sílica com mesmas geometrias obtidas pelo mecanismo de difusão molecular após 7 horas (DEMILECAMPS et al., 2015).

3 CONSIDERAÇÕES FINAIS

Nanofibras de celulose foram obtidas por processamento mecânico e a superfície da celulose em nanoescala foi recoberta por estruturas silicosas através do método sol-gel. Menores concentrações do precursor de sílica produziram aerogéis híbridos celulose-sílica com melhores resultados morfológicos. As propriedades físicas e mecânicas dos aerogéis híbridos mostraram-se variáveis e sem diferença estatística entre si.

Observou-se que a composição química residual das fibras de juta pré-tratadas associada ao seu grau de desfibrilamento após o processamento mecânico exerce influência sobre as propriedades mecânicas dos filmes produzidos, visto que, as porcentagens relativamente altas de lignina e hemiceluloses e a alta porcentagem de fibras e fragmentos de fibras em desfibrilação geraram filmes celulósicos com maiores propriedades mecânicas no ensaio de tração, descrito no Artigo 1.

O Artigo 2 relata como foi possível verificar que a presença do precursor de sílica mesmo em menores concentrações alterou a morfologia final da nanofibrila de celulose obtida a partir do desfibrilamento mecânico da polpa comercial mista de coníferas e folhosas, favorecendo assim, a produção dos aerogéis celulose-sílica. TEOS na concentração 0,25% influenciou na formação de rede celulósica porosa com estrutura similar às espumas poliméricas, obtendo-se o aerogel híbrido com estrutura homogênea e macia (Figura 2a e Figura 4d). O aumento das concentrações de TEOS favoreceu a formação de aerogéis híbridos termicamente estáveis (Figura 6). Em geral, a presença de TEOS reduz a capacidade adsorvente dos aerogéis, principalmente as concentrações 0.50 e 1.00% (Figura 7); estes apresentando, ao mesmo tempo, uma estrutura porosa e não compactada (Figura 2c-d). O método sol-gel pelo mecanismo adotado depositou partículas de sílica nas nanofibrilas de celulose

(Figura 3). O mecanismo do processo de sintetização de sílica por reações de hidrólise, a partir de catalizador ácido, permanece sem elucidação.

A partir dos resultados obtidos no Artigo 2, utilizou-se o TEOS em quatro diferentes concentrações (0,00%; 0,25%; 0,50% e 1,00%) e nanofibrilas de *Eucalyptus* na produção de aerogéis híbridos e verificou-se que TEOS 0,25% também influenciou na formação de trama celulósica porosa com estrutura similar às espumas poliméricas, obtendo-se o aerogel híbrido com estrutura homogênea e macia (Figura 2a, Figura 3b) . Entretanto, a concentração 0,50% favoreceu a formação de aerogéis híbridos porosos e com boa morfologia e melhor estabilidade térmica (Figura 5). Em termos de adsorção de umidade, a concentração 0.25% de TEOS apresentou os menores valores (Figura 6). Mecanicamente, no ensaio de compressão, todos os aerogéis exibiram comportamento elástico com interessante capacidade de recuperar parcialmente suas dimensões originais (Figura 7).

O presente trabalho reúne informações sobre a produção de materiais híbridos nanoestruturados buscando contribuir para o desenvolvimento de novos materiais à base de celulose visando a diversas aplicações.

REFERÊNCIAS

AEGERTER, M. A.; LEVENTIS, N.; KOEBEL, M. **Aerogels handbook**. New York: Springer 2011, 932 p.

ALILA, S. et al. Non-woody plants as raw materials for production of microfibrillated cellulose (MFC): a comparative study. **Industrial Crops and Products**, St Martin d'Heres, v. 41, p. 250– 259, Jan. 2013.

ALVES, C. et al. Ecodesign of automotive components making use of natural jute fiber composites. **Journal of Cleaner Production**, Utrecht, v. 18, n. 4, p. 313–327, Mar. 2010.

ANKERFORS, M. P. et al. Enzymatic hydrolisis combined with mechanical shearing and high-pressure homogenization for nanoscale cellulose fibrils and strong gels. **Biomacromolecules**, Washington, v. 8, n. 6, p. 1934-1941, May 2007.

ANDRESEN, M. et al. Nonleaching antimicrobial films prepared from surface-odified microfibrillated cellulose. **Biomacromolecules**, Washington, v. 8, n. 7, p. 2149-2155, June 2007.

ANDRESEN, M.; STENIUS, P. Water-in-oil emulsions stabilized by hydrophobized microfibrillated cellulose. **Journal of Dispersion Science and Technology**, Trondheim, v. 28, n. 6, p. 837-844, Aug. 2007.

APPEZZATO-DA-GLÓRIA, B.; MARIA CARMELLO-GUERREIRO, S. **Anatomia vegetal**. 2. ed. atual. Viçosa, MG: UFV, 2006. 438 p.

ARORA, R.; BEHERA, S.; KUMAR, S. Bioprospecting thermophilic/thermotolerant microbes for production of lignocellulosic ethanol: a future perspective. **Renewable and Sustainable Energy Reviews**, Colorado, v. 51, p. 699-717, June 2015.

ASHORI, A. et al. Bacterial cellulose/silica nanocomposites: preparation and characterization. **Carbohydrate Polymers**, Barking, v. 90, n. 1, p. 413–418, Sept. 2012.

ASHORI, A. et al. Solvent-free acetylation of cellulose nanofibers for improving compatibility and dispersion. **Carbohydrate Polymers**, Barking, v. 102, p. 369-375, Feb. 2014.

AZEREDO, H. M. C. Nanocomposites for food packaging applications. **Food Research International**, São Paulo, v. 42, n. 9, p. 1240–1253, Nov. 2009.

BADGUJAR, K.C.; BHANAGE, B.M. Factors governing dissolution process of lignocellulosic biomass in ionic liquid: current status, overview and challenges. **Bioresource Technology**, Essex, v. 178, p. 2-18, Feb. 2015.

BAETENS, R.; JELLE, B.P.; GUSTAVSEN, A. Aerogel insulation for building applications: a state-of-the-art review. **Energy and Buildings**, Kowloon, v. 43, n. 4, p. 761–769, Apr. 2011.

BELTRAMI, L. V. R.; SCIENZA, L. C.; ZATERRA, A. J. Efeito do tratamento alcalino de fibras de curauá sobre as propriedades de compósitos de matriz biodegradável. **Polímeros Ciência e Tecnologia**, São Carlos, v. 24, n. 3, p. 388-394, maio/jun. 2014.

BERTHET, M. A. et al. Exploring the potentialities of using lignocellulosic fibres derived from three food by-products as constituents of biocomposites for food packaging. **Industrial Crops and Products**, St Martin d'Heres, v. 69, p. 110–122, July 2015.

BESBES, I.; VILAR, M. R.; BOUFI, S. Nanofibrillated cellulose from TEMPO-oxidized Eucalyptus fibres: effect of the carboxyl content. **Carbohydrate Polymers**, Barking, v. 84, n. 3, p. 975-983, Mar. 2011.

BHATNAGAR, A.; SAIN, M. Processing of cellulose nanofiber-reinforced composites. **Journal of Reinforced Plastics and Composites**, Stanford, v. 24, n. 12, p.1-10, Aug. 2005.

BRETT, C. T. Cellulose microfibrils in plants: Biosynthesis, deposition, and integration into the cell wall. **International Review of Cytology**, Knoxville, v. 199, p. 161–199, Nov. 2000.

BRINKER, C. J.; SCHERER, G. W. **Sol–gel science**: the physics and chemistry of sol–gel processing. San Diego: Academic,1990. 881 p.

BROWNING, B. L. **The chemistry of wood**. New York: Warrenville/ London: Interscience, 1963. 689 p.

BUFALINO, L. et al. How the chemical nature of Brazilian hardwoods affects nanofibrillation of cellulose fibers and film optical quality. **Cellulose**, Bucharest, v. 22, n. 6, p. 3657-3672, Dec. 2015.

BUFALINO, L. et al. New products made with lignocellulosic nanofibers from Brazilian amazon forest. **IOP Conference Series**: materials science and engineering, Bristol, v. 64, n. 012012, p. 1-6, Aug. 2014.

BULOTA, M. et al. An investigation into the mechanical behavior of surface-modified fibrillated cellulose reinforced composites. In: CAI, Z.; OKSMAN NISKA, K. 2012. Nanocelluloses: potential materials for advanced forest products. Proceedings of Nanotechnology in Wood Composites Symposium. **General Technical Report FLP-GTR-218**. Madison, WI: U.S. Department of Agriculture, Forest Service, Forest Products Laboratory, 2012. p. 50-53. Disponível em: <https://ntrl.ntis.gov/NTRL/dashboard/searchResults.xhtml?searchQuery=PB2013102726>. Acesso em: 10 dez. 2015.

CABRERA, E. et al. Alkaline and alkaline peroxide pretreatments at mild temperature to enhance enzymatic hydrolysis of rice hulls and straw. **Bioresource Technology**, Essex, v. 167, p. 1-7, Sept. 2014.

CAI, J. et al. Cellulose–silica nanocomposite aerogels by in situ formation of silica in cellulose gel. **Angewandte Chemie International Edition**, New Jersey, v. 51, n. 9, p. 2076-2079, Feb. 2012.

CAI, H. et al. Sol–gel synthesis highly porous titanium dioxide microspheres with cellulose nanofibrils-based aerogel templates. **Inorganic Chemistry Communications**, Guangdong, v. 51, p. 71-74, Jan. 2015.

CALLISTER JUNIOR, W. D. **Materials science and engineering**: an introduction. New York: Wiley, 2008. 721 p.

CAMPOS, A. et al. Efeito do tratamento das fibras nas propriedades do biocompósito de amido termoplástico/policaprolactona/sisal. **Polímeros Ciência e Tecnologia**, São Carlos, v. 21, n. 3, p. 217-222, jun. 2011.

CARLSSON, G.; KOLSETH, P.; LINDSTRÖM, T. Polyelectrolyte swelling behavior of chlorite delignified spruce wood fibers. **Wood Science and Technology**, New York, v. 17, n. 1, p. 69-73, Mar. 1983.

CERVIN, N. T. et al. Lightweight and strong cellulose materials made from aqueous foams stabilized by nanofibrillated cellulose. **Biomacromolecules**, Washington, v. 14, n. 2, p. 503−511, Feb. 2013.

CHENG, S. et al. Aloe vera rind cellulose nanofibers-reinforced films. **Journal of Applied Polymer Science**, New York, n. 40592, p. 1-9, Mar. 2014.

CHEUNG, H.Y. et al. Natural fibre-reinforced composites for bioengineering and environmental engineering applications. **Composites Part B**: engineering, New Orleans, v. 40, n. 7, p. 655–663, Oct. 2009.

CHIN, S. F.; ROMAINOR, A. N.B.; PANG, S. C. Fabrication of hydrophobicand magnetic cellulose aerogel with high oil absorption capacity. **Materials Letters**, Erlangen, v. 115, p. 241–243, Jan. 2014.

CHINGA-CARRASCO, G. Cellulose fibres, nanofibrils and microfibrils: the morphological sequence of MFC components from a plant physiology and fibre technology point of view. **Nanoscale Research Letters**, Cheng, v. 6, n. 417, p. 1-7, June 2011.

CORDEIRO, N.; GOUVEIA, C.; JOHNB, M.J. Investigation of surface properties of physico-chemically modified natural fibres using inverse gas chromatography. **Industrial Crops and Products**, St Martin d'Heres, v. 33, n. 1, p. 108-115, Jan. 2011.

DEMILECAMPS, A. et al. Cellulose–silica aerogels. **Carbohydrate Polymers**, Barking, v. 122, p. 293-300, May 2015.

DINAND, E.; CHANZY, H.; VIGNON, M. R. Parenchymal cell cellulose from sugar beet pulp: preparation and properties. **Cellulose**, Bucharest, v. 3, n. 1, p. 183-188, Dec. 1996.

DINAND, E.; CHANZY, H.; VIGNON, M. R. Suspensions of cellulose microfibrils from sugar beet pulp. **Food Hydrocolloids**, Wrexham, v. 13, n. 3, p. 275-283, May 1999.

DUFRESNE, A.; CAVAILLÉ, J. Y.; VIGNON, M. R. Mechanical behavior of sheets prepared from sugar beet cellulose microfibrils. **Journal of Applied Polymer Science**, New York, v. 64, n. 6, p. 1185–1194, May 1997.

DUFRESNE, A. Nanocellulose: a new ageless bionanomaterial. **Materials Today**, Kidlington, v. 16, n. 6, p. 220-227, June 2013.

FARUK, O. et al. Biocomposites reinforced with natural fibers: 2000–2010. **Progress in Polymer Science**, Pittsburgh, v. 37, n. 11, p. 1552–1596, Nov. 2012.

FERNANDES, E. M. et al. Bionanocomposites from lignocellulosic resources: properties, applications and future trends for their use in the biomedical field. **Progress in Polymer Science**, Pittsburgh, v. 38, n. 10-11, p. 1415-1441, Oct./Nov. 2013.

FONSECA, A. S. et al. Properties of an Amazonian vegetable fiber as a potential reinforcing material. **Industrial Crops and Products**, St Martin d'Heres, v. 47, p. 43– 50, May 2013.

FRICKE, J.; TILLOTSON, T. Aerogels: production, characterization, and applications. **Thin Solid Films**, Urbana, v. 297, n. 1-2, p. 212–223, Apr. 1997.

GEETHAMMA, V. G. et al. Composite of short coir fibres and natural rubber: effect of chemical modification, loading and orientation of fibre. **Polymer**, Akron, v. 39, n. 6-7, p. 1483-1491, June 1998.

GHAREHKHANI, S. et al. Basic effects of pulp refining on fiber properties - a review. **Carbohydrate Polymers**, Barking, v. 115, p. 785–803, Jan. 2015.

GOULD, J. M. Alkaline peroxide delignification of agricultural residues to enhance enzymatic saccharification. **Biotechnology and Bioengineering**, Berkeley, v. 26, n. 1, p. 46-52, Jan. 1984.

GOULD, J. M. Enhanced polysaccharide recovery from agricultural residues and perennial grasses treated with alkaline hydrogen peroxide. **Biotechnology and Bioengineering**, Berkeley, v. 27, n. 6, p. 893-896, June 1985a.

GOULD, J. M. Studies on the mechanism of alkaline peroxide delignification of agricultural residues. **Biotechnology and Bioengineering**, Berkeley, v. 27, n. 3, p. 225-231, Mar. 1985b.

GOUSSÉ, C. et al. Surface silylation of cellulose microfibrils: preparation and rheological properties. **Polymer**, Akron, v. 45, n. 5, p. 1569–1575, Mar. 2004.

GRAY, M. K. **Alkaline hydrogen peroxide pretreatment for its use in an on farm bioprocessing facility**. 2013. 178 p. Thesis (Master of Science in Biosystems and Agricultural Engineering) - University of Kentucky, Lexington, Kentucky. (Theses and Dissertations--Biosystems and Agricultural Engineering. Paper 18, 2013).

GUIMARÃES JUNIOR, M. et al. Starch/PVA-based nanocomposites reinforced with bamboo nanofibrils. **Industrial Crops and Products**, St Martin d'Heres, v. 70, p. 72-83, Aug. 2015a.

GUIMARÃES JUNIOR, M. et al. Preparation of Cellulose Nanofibrils from Bamboo Pulp by Mechanical Defibrillation for Their Applications in Biodegradable Composites. **Journal of Nanoscience and Nanotechnology**, Valencia, v. 15, n. 9, p. 1-18, Sept. 2015b.

GURGEL, L. V. A. **Mercerização e modificação química de celulose e bagaço de cana-de-açúcar com anidrido succínico e trietilenotetramina**: preparação de novos materiais quelantes para adsorção de Pb (II) e Cd (II), Cr (VI) e Cu (II). 2007. 180 p. Dissertação (Mestrado em Engenharia Ambiental) – Universidade Federal de Ouro Preto, Ouro Preto, 2007.

GUZUN, A.S. et al. Plackett–Burman experimental design for bacterial cellulose–silica composites synthesis. **Materials Science and Engineering C**: materials for biological applications, Raleigh, v. 42, p. 280–288, Sept. 2014.

HABIBI, Y.; LUCIA, L. A.; ROJAS, O. J. Cellulose Nanocrystals: Chemistry, Self-Assembly, and Applications. **Chemical Reviews**, Urbana-Champaign, v. 110, n. 6, p. 3479–3500, Mar. 2010.

HASSAN, M. L. et al. Nanofibers from bagasse and rice straw: process optimization and properties. **Wood Science and Technology**, New York, v. 46, n. 1, p. 193–205, Jan. 2012.

HASSAN, M. L. et al. Palm rachis microfibrillated cellulose and oxidized-microfibrillatedcellulose for improving paper sheets properties of unbeaten softwoodand bagasse pulps. **Industrial Crops and Products**, St Martin d'Heres, v. 64, p. 9–15, Feb. 2015.

HE, X. et al. Aerogels from quaternary ammonium-functionalized cellulose nanofibers for rapid removal of Cr (VI) from water. **Carbohydrate Polymers**, Barking, v. 111, p. 683-687, Oct. 2014.

HEINZE, T.; LIEBERT, T. Unconventional methods in cellulose functionalization. **Progress in Polymer Science**, Pittsburgh, v. 26, n. 9, p. 1689-1762, Nov. 2001.

HENDRIKS, A. T. W. M.; ZEEMAN, G. Pretreatments to enhance the digestibility of lignocellulosic biomass. **Bioresource Technology**, Essex, v. 100, n. 1, p. 10-18, Jan. 2009.

HENRIKSSON, M. et al. An environmentally friendly method for enzyme-assisted preparation of microfibrillated cellulose (MFC) nanofibers. **European Polymer Journal**, New York, v. 43, n. 8, p. 3434-3441, Aug. 2007.

HOKKANEN, S. et al. Removal of arsenic (V) by magnetic nanoparticle activated microfibrillated cellulose. **Chemical Engineering Journal**, Belfast, v. 260, n. 1385-8947, p. 886–894, Jan. 2015.

HOUAISS, A.; VILLAR, M. S.; FRANCO, F. M. de M. **Dicionário Houaiss da língua portuguesa**. Rio de Janeiro: Objetiva, 2009. 1986 p.

HUBBE, M. A. et al. Cellulosic nanocomposites: a review. **BioResources**, Kurashiki, v. 3, n. 3, p. 929-980, Aug. 2008.

HÜSING, N.; SCHUBERT, U. Aerogels-airy materials: chemistry, structure, and properties. **Angewandte Chemie International Edition**, New Jersey, v. 37, n. 1-2, p. 22-45, Feb. 1998.

ILVESSALO-PFÄFFLI, M. S. **Fiber atlas**: identification of papermaking fibers. Springer series in Wood sciences. Espoo: [s. n.], 1994. 399 p.

INTERNATIONAL ORGANIZATION FOR STANDARDIZATION. **ISO Technical Specification**. ISO/AWI TS 20477. Nanotechnologies - standard terms and their definition for cellulose nanomaterial. Geneva, 2015.

ISOGAI, A.; SAITO, T.; FUKUZUMI, H. Tempo-oxidized cellulose nanofibers. **Nanoscale**, Beijing, v. 3, n. 1, p. 71-85, Oct. 2011.

IWAMOTO, S.; ABE, K.; YANO, H. The Effect of hemicelluloses on wood pulp nanofibrillation and nanofiber network characteristics. **Biomacromolecules**, Washington, v. 9, n. 3, p. 1022-1026, Feb. 2008.

IWAMOTO, S. et al. Optically transparent composites reinforced with plant fiber-based nanofibers. **Applied Physics A**, Berlin, v. 81, n. 6, p. 1109-1112, Nov. 2005.

IWAMOTO, S.; NAKAGAITO, A.N.; YANO, H. Nano-fibrillation of pulp fibers for the processing of transparent nanocomposites. **Applied Physics A**, Berlin, v. 89, n. 2, p. 461-466, Nov. 2007.

JÄHN, A. et al. Characterization of alkali treated flax fibres by means of FT Raman spectroscopy and environmental scanning electron microscopy. **Spectrochimica Acta Part A**: molecular and biomolecular spectroscopy, Krakow, v. 58, n. 10, p. 2271–2279, Aug. 2002.

JANARDHANAN, S.; SAIN, M. Isolation of cellulose nanofibers: effect of biotreatment on hydrogen bonding network in wood fibers. **International Journal of Polymer Science**, Napoli, v. 2011, Article ID 279610, p. 1-6, 2011.

JIANG, F.; HAN, S.; HSIEH, Y. L. Controlled defibrillation of rice straw cellulose and self assembly of cellulose nanofibrils into highly crystalline fibrous materials. **RSC Advances**, Sheffield, v. 3, n. 30, p. 12366-12375, May 2013.

JIANG, F.; HSIEH, Y. L. Chemically and mechanically isolated nanocellulose and their self-assembled structures. **Carbohydrate Polymers**, Barking, v. 95, n. 1, p. 32-40, Feb. 2013.

JIMENÉZ, L. et al. Bleaching of soda pulp of fibres of Musa textilis nee (abaca) with peracetic acid. **Bioresource Technology**, Essex, v. 99, n. 5, p. 1474–1480, Mar. 2008.

JIN, C. et al. Fabrication of cellulose-based aerogels from waste newspaperwithout any pretreatment and their use for absorbents. **Carbohydrate Polymers**, Barking, v. 123, p. 150-156, June 2015.

JOB, N. et al. Carbon aerogels, cryogels and xerogels: Influence of the drying method on the textural properties of porous carbon materials. **Carbon**, Providence, v. 43, n. 12, p. 2481-2494, Oct. 2005.

KABIR, M. M. et al. Chemical treatments on plant-based natural fibre reinforced polymer composites: An overview. **Composites Part B**: engineering, New Orleans, v. 43, n. 7, p. 2883–2892, Oct. 2012.

KALIA, S. et al. Surface modification of plant fibers using environmentfriendly methods for their application in polymer composites, textile industry and antimicrobial activities: a review. **Journal of Environmental Chemical Engineering**, Nicosia, v. 1, n. 3, p. 97-112, Sept. 2013.

KHALIL, H. P. S. A. et al. Production and modification of nanofibrillated cellulose using various mechanical processes: a review. **Carbohydrate Polymers**, Barking, v. 99, p. 649–665, Jan. 2014.

KIM, J. S.; LEE, Y. Y.; KIM, T. H. A review on alkaline pretreatment technology for bioconversion of lignocellulosic biomass. **Bioresource Technology**, Essex, v. 199, p. 42-48, Jan. 2016.

KIM, J. T.; NETRAVALI, A. N. Mercerization of sisal fibers: effect of tension on mechanical properties of sisal fiber and fiber-reinforced composites. **Composites Part A**: applied science and manufacturing, Bristol, v. 41, n. 9, p. 1245-1252, Sept. 2010.

KLEMM, D. et al. Nanocelluloses: a new family of nature-based materials. **Angewandte Chemie International Edition**, New Jersey, v. 50, n. 24, p. 5438-5466, May 2011.

KOCON, L.; DESPETIS, F.; PHALIPPOU, J. Ultralow density silica aerogels byalcohol supercritical drying. **Journal of Non-Crystalline Solids**, Tucson, v. 225, p. 96-100, Apr. 1998.

KOLPAK, F.; WEIH, M.; BLACKWELL, J. Mercerization of cellulose: 1. determination of the structure of mercerized cotton. **Polymer**, Akron, v. 19, n. 2, p. 123-131, Feb. 1978.

KONTTURI, E. J. **Surface chemistry of cellulose from natural fibres to model surfaces**. Eindhoven: Technische Universiteit Eindhoven, 2005. 145 p.

LANGAN, P.; NISHIYAMA, Y.; CHANZY, H. A revised structure and hydrogen-bonding system in cellulose II from a neutron fiber diffraction analysis. **Journal of the American Chemical Society**, Salt Lake City, v. 121, n. 43, p. 9940-9946, Oct. 1999.

LAVOINE, N. et al. Microfibrillated cellulose – Its barrier properties and applications in cellulosic materials: a review. **Carbohydrate Polymers**, Barking, v. 90, n. 2, p. 735-764, Oct. 2012.

LAVOINE, N.; DESLOGES, I.; BRAS, J. Microfibrillated cellulose coatings as new release systems foractive packaging. **Carbohydrate Polymers**, Barking, v. 103, p. 528-537, Mar. 2014.

LI, F. et al. Multi-functional coating of cellulose nanocrystals for flexible packaging applications. **Cellulose**, Bucharest, v. 20, n. 5, p. 2491–504, Oct. 2013.

LIN, J. et al. Cellulose nanofibrils aerogels generated from jute fibers. **Carbohydrate Polymers**, Barking, v. 109, p. 35–43, Aug. 2014.

LIN, Z.; RENNECKAR, S.; HINDMAN, D.P. Nanocomposite-based lignocellulosic fibers 1. Thermal stability of modified fibers with clay-polyelectrolyte multilayers. **Cellulose**, Bucharest, v. 15, p. 333-346, Apr. 2008.

LIU, S. et al. High strength cellulose aerogels prepared by spatially confined synthesis of silica in bioscaffolds. **Colloids and Surfaces A**: physicochemical and engineering aspects, Paris, v. 439, p. 159-166, Dec. 2013.

LÖNNBERG, H. et al. Surface grafting of microfibrillated cellulose with poly(e-caprolactone)-Synthesis and characterization. **European Polymer Journal**, New York, v. 44, n. 9, p. 2991-2997, Sept. 2008.

LOVE, K. T. et al. Modification of Kraft wood pulp fibre with silica for surface functionalisation. **Composites Part A**: applied science and manufacturing, Bristol, v. 39, n. 12, p. 1815–1821, Dec. 2008.

LU, J.; WANG, T.; DRZAL, L. T. Preparation and properties of microfibrillated cellulose polyvinyl alcohol composite materials. **Composites Part A**: applied science and manufacturing, Bristol, v. 39, n. 5, p. 738-746, May 2008.

LYND, L. R.; WYMAN, C. E.; GERNGROSS, T. U. Biocommodity engineering. **Biotechnology Progress**, Pittsburgh, v. 15, n. 5, p. 777-793, Oct. 1999.

MACVICAR, R.; MATUANA, L. M.; BALATINECZ, J. J. Aging mechanisms in cellulose fiber reinforced cement composites. **Cement and Concrete Composites**, Barking, v. 21, n. 3, p. 189-196, July 1999.

MAJEED, K. et al. Potential materials for food packaging from nanoclay/natural fibres filled hybrid composites. **Materials and Design**, Amsterdam, v. 46, p. 391-410, Apr. 2013.

MALEKI, H.; DURÃES, L.; PORTUGAL, A. An overview on silica aerogels synthesis and different mechanical reinforcing strategies. **Journal of Non-Crystalline Solids**, Tucson, v. 385, p. 55-74, Feb. 2014.

MARQUES, G. et al. Evaluation of the chemical composition of different non-woody plant fibres used for pulp and paper manufacturing. **The Open Agriculture Journal**, Sharjah, v. 4, p. 93-101, Mar. 2010.

MIRANDA, C. S. et al. Efeito dos tratamentos superficiais nas propriedades do bagaço da fibra de piaçava *Attalea funifera* Martius. **Química Nova**, São Paulo, v. 38, n. 2, p. 161-165, fev. 2015.

MISSOUM, K.; BELGACEM, M. N.; BRAS, J. nanofibrillated cellulose surface modification: a review. **Materials**, Basel, v. 6, n. 5, p.1745-1766, May 2013.

MISSOUM, K. et al. Antibacterial activity and biodegradability assessment of chemically grafted nanofibrillated cellulose. **Materials Science and Engineering C**, Raleigh, v. 45, p. 477–483, Dec. 2014.

MISSOUM, K. et al. Effect of chemically modified nanofibrillated cellulose addition on the properties of fiber-based materials. **Industrial Crops and Products**, St Martin d'Heres, v. 48, p. 98-105, June 2013.

MOON, R. J. et al. Cellulose nanomaterials review: structure, properties and nanocomposites. **Chemical Society Reviews**, Southampton, v. 40, n. 7, p. 3941–3994, July 2011.

NAKAGAITO, A. N.; YANO, H. The effect of morphological changes from pulp fiber towards nano-scale fibrillated cellulose on the mechanical properties of high-strength plant fiber based composites. **Applied Physics A**, Berlin, v. 78, n. 4, p. 547-552, Mar. 2004.

NGUYEN, H. D. et al. A novel method for preparing microfibrillated cellulose from bamboo fibers. **Advances in Natural Sciences**: nanoscience and nanotechnology, Hanoi, v. 4, n. 015016, p. 1-9, Feb. 2013.

NGUYEN, S. T. et al. Advanced thermal insulation and absorption properties of recycledcellulose aerogels. **Colloids and Surfaces A**: physicochemical and engineering aspects, Paris, v. 445, p. 128-134, Mar. 2014.

NIKOLAJASKI, M. et al. Amino-functionalized cellulose nanoparticles: Preparation, characterization, and interactions with living cells. **Macromolecular Bioscience**, Weinheim, v. 12, n. 7, p. 920-925, July 2012.

OKAHISA, Y. et al. Composites optically transparent wood–cellulose nanocomposite as a base substrate for flexible organic light-emitting diode displays. **Composites Science and Technology**, Barking, v. 69, n. 11-12, p. 1958–1961, Sept. 2009.

OKAHISA, Y. et al. Effects of delignification in the production of plant-based cellulose nanofibers for optically transparent nanocomposites. **Composites Science and Technology**, Barking, v. 71, n. 10, p. 1342–1347, July 2011.

OLIVEIRA, F. R. et al. Photocatalytic properties of sisal fiber coated with nano titanium dioxide. **Materials Today**: proceedings, Kidlington, v. 2, n. 1, p. 41-48, June 2015.

OSHIMA, T. et al. Cellulose aerogel regenerated from ionic liquid solution forimmobilized metal affinity adsorption. **Carbohydrate Polymers**, Barking, v. 103, p. 62-69, Mar. 2014.

PÄÄKKÖ, M. et al. Enzymatic hydrolysis combined with mechanical shearing and high-pressure homogenization for nanoscale cellulose fibrils and strong gels. **Biomacromolecules**, Washington, v. 8, n. 6, p. 1934-941, May 2007.

PANTHAPULAKKAL, S.; SAIN, M. Isolation of nano fibres from hemp and flax and their thermoplastic composites. **Plastic and Polymer Technology**, Terre Haute, v. 2, n. 1, p. 9-16, Mar. 2013.

PANTHAPULAKKAL, S.; SAIN, M. Preparation and characterization of cellulose nanofibril films from wood fibre and their thermoplastic polycarbonate composites. **International Journal of Polymer Science**, Nasr City, v. 2012, Article ID 381342, p. 1-6, 2012.

PARMENTER, K. E.; MILSTEIN, F. Mechanical properties of silica aerogels. **Journal of Non-crystalline Solids**, Tucson, v. 223, n. 3, p. 179–189, Jan. 1998.

PATEL, A. et al. Biodiesel production from non-edible lignocellulosic biomass of *Cassia fistula* L. fruit pulp using oleaginous yeast *Rhodosporidium kratochvilovae* HIMPA1. **Bioresource Technology**, Essex, v. 197, p. 91–98, Dec. 2015.

PELISSARI, F. M.; SOBRAL., P. J. A.; MENEGALLI, F. C. Isolation and characterization of cellulose nanofibers from banana peels. **Cellulose**, Bucharest, v. 21, n. 1, p. 417-432, Feb. 2014.

PIMENTA, M. T. B. et al. Soda-treated sisal/polypropylene composites. **Journal of Polymers and the Environment**, Coventry, v. 16, n. 1, p. 35–39, Feb. 2008.

PINTO, R. J. B. et al. Novel SiO_2/cellulose nanocomposites obtained by in situ synthesis and via polyelectrolytes assembly. **Composites Science and Technology**, Barking, v. 68, n. 3-4, p. 1088-1093, Mar. 2008.

RAABE, J. et al. Biocomposite of cassava starch reinforced with cellulose pulp fibers modified with deposition of Silica (SiO_2) nanoparticles. **Journal of Nanomaterials**, Nasr City, v. 2015, Article ID 493439, p. 1-9, 2015.

RAABE, J. et al. Evaluation of reaction factors for deposition of silica (SiO_2) nanoparticles on cellulose fibers. **Carbohydrate Polymers**, Barking, v. 114, p. 424–431, Dec. 2014.

RAHMAN, M.M.; AFRIN, S.; HAQUE, P. Characterization of crystalline cellulose of jute reinforced poly(vinyl alcohol) (PVA) biocomposite film for potential biomedical applications. **Progress in Biomaterials**, Tehran, v. 3, n. 1, p. 1-9, June 2014.

RAY, D.; SARKAR, B.K. Characterization of alkali-treated jute fibers for physical and mechanical properties. **Journal of Applied Polymer Science**, New York, v. 80, n. 7, p. 1013-1020, May 2001.

REIS, T. H. P. et al. **O silício na nutrição e defesa de plantas**. Belo Horizonte: EPAMIG, 2007. 120 p. (Boletim Técnico, 82, ISSN 0101-062X).

RODIONOVA, G. et al. **Surface modification of microfibrillated cellulose films by Gas-phase Esterification**: improvement of barrier properties. TAPPI Int. Conf. on Nano for the Forest Product Industry. 2010. Disponível em: <http://www.tappi.org/Downloads/Conference-Papers/2010/2010-TAPPI-International-Conference-on-Nanotechnology-for-the-Forest-Product-Industry/10NANO62.aspx>. Acesso em: 02 ago 2013.

ROSA, M. F. et al. Effect of fiber treatments on tensile and thermal properties of starch/ethylene vinyl alcohol copolymers/coir biocomposites. **Bioresource Technology**, Essex, v. 100, n. 21, p. 5196-5202, Nov. 2009.

ROWLAND, S. P.; HOWLEY, P. S. Hydrogen bonding on accessible surfaces of cellulose from various sources and relationship to order within crystalline regions. **Journal of Polymer Science Part A**: polymer chemistry, Weinheim, v. 26, n. 7, p. 1769-1778, July 1988.

SAINI, S. et al. Natural active molecule chemical grafting on the surface ofmicrofibrillated cellulose for fabrication of contact activeantimicrobial surfaces. **Industrial Crops and Products**, St Martin d'Heres, v. 78, p. 82–90, Dec. 2015.

SAITO, T. et al. Homogeneous suspensions of individualized microfibrils from TEMPO-catalyzed oxidation of native cellulose. **Biomacromolecules**, Washington, v. 7, n. 6, p. 1687-1691, May 2006.

SANTOS, N. S. S.; DIAS, C. G. B. T.; MEIRELES, A. C. R. Comportamento da propagação da fratura em compósitos laminados reforçados com fibras vegetais trançadas. In: CONGRESSO BRASILEIRO DE ENGENHARIA E CIÊNCIA DOS MATERIAIS, 17., 2006, Foz do Iguaçu. **Anais**... Foz do Iguaçu: Associação Brasileira de Cerâmica, 2006. p. 2766-2774.

SANTOS, R. P. O. et al. Bio-based materials from the electrospinning of lignocellulosic sisal fibers and recycled PET. **Industrial Crops and Products**, St Martin d'Heres, v. 72, p. 69–76, Oct. 2015.

SANTOS, S. F. et al. Non-conventional cement-based composites reinforced with vegetable fibers: a review of strategies to improve durability. **Materiales de Construcción**, Madrid, v. 65, n. 317, p. 1-20, 2015.

SATYANARAYANA, K. G.; ARIZAGA, G. G. C.; WYPYCH, F. Biodegradable composites based on lignocellulosic fibers – An overview. **Progress in Polymer Science**, Pittsburgh, v. 34, n. 9, p. 982–1021, Sept. 2009.

SATYANARAYANA, K. G.; GUIMARÃES, J. L.; WYPYCH, F. Studies on lignocellulosic fibers of Brazil. **Composites Part A**: Applied Science and Manufacturing, Bristol, n. 38, n. 7, p. 1694-1709, July 2007.

SAVASTANO JÚNIOR, H. **Materiais a base de cimento reforçados com fibra vegetal**: reciclagem de resíduos para a construção de baixo custo. 2000. 152 p. Tese (Livre Docência) - Universidade de São Paulo. Escola Politécnica, São Paulo, 2000.

SCHENZEL, K. et al. NIR FT Raman spectroscopy and micro spectroscopy – new methods for determining objective parameters of hemp and flax fibres. **Pflanzenbauwissenschaften**, v. 11, p. 16–21, Apr. 2007.

SCHUCHARDT, U.; RIBEIRO, M. L. A indústria petroquímica no próximo século: como substituir o petróleo como matéria-prima? **Química Nova**, São Paulo, v. 24, n. 2, p. 247-251, mar./abr. 2001.

SCHURZ, J. Trends in polymer science: a bright future for cellulose. **Progress in Polymer Science**, Oxford, v. 24, n. 4, p. 481–483, 1999.

SEHAQUI, H.; ZHOU, Q.; BERGLUND, L. A. High-porosity aerogels of high specific surface area prepared from nanofibrillated cellulose (NFC). **Composites Science and Technology**, Barking, v. 71, n. 13, p. 1593–1599, Sept. 2011.

SEHAQUI, H.; ZIMMERMANN, T.; TINGAUT, P. Hydrophobic cellulose nanopaper through a mild esterification procedure. **Cellulose**, Bucharest, v. 21, n. 1, p. 367-382, Feb. 2014.

SELIG, M. J. et al. The effect of lignin removal by alkaline peroxide pretreatment on the susceptibility of corn stover to purified cellulolytic and xylanolytic enzymes. **Applied Biochemistry and Biotechnology**, Minneapolis, v. 155, n. 1-3, p. 397–406, May 2009.

SENA NETO, A. R. et al. Comparative study of 12 pineapple leaf fiber varieties for use asmechanical reinforcement in polymer composites. **Industrial Crops and Products**, St Martin d'Heres, v. 64, p. 68–78, Feb. 2015.

SHI, J. et al. Heat insulation performance, mechanics and hydrophobic modification of cellulose–SiO_2 composite aerogels. **Carbohydrate Polymers**, Barking, v. 98, n. 1, p. 282-289, Oct. 2013.

SILVA, A. L. et al. Efeito do tratamento alcalino e branqueamento na morfologia e no índice de cristalinidade da fibra de bucha vegetal (*Luffa cylindrica*). In: CONGRESSO BRASILEIRO DE QUIMICA, 53., 2013, Rio de Janeiro. **Anais**... Rio de Janeiro: ABQ, 2013. 3 p. Disponível em: <http://www.abq.org.br/cbq/2013/trabalhos/12/240516576.html>. Acesso em: 22 jan. 2016.

SILVA, R. et al. Aplicações de fibras lignocelulósicas na química de polímeros e em compósitos. **Química Nova**, São Paulo, v. 32, n. 3, 661-671, abr. 2009.

SIQUEIRA, G.; BRAS, J.; DUFRESNE, A. Cellulosic bionanocomposites: a review of preparation, properties and applications. **Polymers**, Basel, v. 2, n. 4, p. 728-765, Dec. 2010.

SIRÓ, I.; PLACKETT, D. Microfibrillated cellulose and new nanocomposite materials: a review. **Cellulose**, Bucharest, v. 17, n. 3, p. 459–494, June 2010.

SPENCE, K. L. et al. The effect of chemical composition on microfibrillar cellulose films from wood pulps: water interactions and physical properties for packaging applications. **Cellulose**, Bucharest, v. 17, n. 4, p. 835-848, Aug. 2010.

SUN, R. C. et al. Comparative study of hemicelluloses from rice straw by alkali and hydrogen peroxide treatments. **Carbohydrate Polymers**, Barking, v. 42, n. 2, p. 111–122, June 2000.

SUN, R. C. et al. Physicochemical characterization of lignins from rice straw by hydrogen peroxide treatment. **Journal of Applied Polymer Science**, New York, v. 79, n. 4, p. 719-732, Nov. 2001.

SVAGAN, A. **Bio-inspired cellulose nanocomposites and foams based on starch matrix**. 2008. 50 p. Tese (Doctor in KTH Chemical Science and Engineering) - Department of Fibre and Polymer Technology, Stockholm, Swiss, 2008.

SVAGAN, A. J.; HEDENQVIST, M. S.; BERGLUND, L. Reduced water vapour sorption in cellulose nanocomposites with starch matrix. **Composites Science and Technology**, Barking, v. 69, n. 3-4, p. 500-506, Mar. 2009.

SVENSSON, A. et al. Bacterial cellulose as a potential scaffold for tissue engineering of cartilage. **Biomaterials**, New York, v. 26, n. 4, p. 419-431, Feb. 2005.

TAMON, H.; KITAMURA, T.; OKAZAKI, M. Preparation of silica aerogel from TEOS. **Journal of Colloid and Interface Science**, Uppsala, v. 197, n. 2, p. 353–359, Jan. 1998.

TEODORO, K. B. R. et al. Whiskers de fibra de sisal obtidos sob diferentes condições de hidrólise ácida: efeito do tempo e da temperatura de extração. **Polímeros**: ciência e tecnologia, São Carlos, v. 21, n. 4, p. 280-285, set. 2011.

THAPLIYAL, P. C.; SINGH, K. Aerogels as promising thermal insulating materials: an overview. **Journal of Materials**, Nasr City, v. 2014, p. 1-10, Apr. 2014.

TOMLINSON, P. B. **The strutuctural biology of palms**. Oxford: Clarendon, 1990. 465 p.

UMMARTYOTIN, S. et al. Development of transparent bacterial cellulose nanocomposite film as substrate for flexible organic light emitting diode (OLED) display. **Industrial Crops and Products**, St Martin d'Heres, v. 35, n. 1, p. 92-97, Jan. 2012.

URRUZOLA, I. et al. Nanopaper from almond (*Prunus dulcis*) shell. **Cellulose**, Bucharest, v. 21, n. 3, p. 1619-1629, June 2014.

VALO, H. et al. Drug release from nanoparticles embedded in four different nanofibrillar cellulose aerogels. **European Journal of Pharmaceutical Sciences**, Odense, v. 50, n. 1, p. 69-77, Sept. 2013.

VIANA, A. L. et al. Pecíolo de inajá (*Maximiliana maripa* [aubl.] Drud) como fonte de matéria prima para produção de papel na Amazônia. **Revista Eletrônica em Gestão, Educação e Tecnologia Ambiental**, Santa Maria, v. 18, n. 4, p.1512-1520, dez. 2014.

WAGH, P.B. et al. Influence of temperature on the physical properties of citric acid catalyzed TEOS silica aerogels. **Materials Chemistry and Physics**, Sydney, v. 50, n. 1, p. 76-81, Aug. 1997.

WANG, B.; SAIN, M.; OKSMAN, K. Study of structural morphology of hemp fiber from the micro to the nanoscale. **Applied Composite Materials**, Cambridge, v. 14, p. 89-103, Mar. 2007.

WANG, X.; CUI, X.; ZHANG, L. Preparation and characterization of lignin-containing nanofibrillar cellulose. **Procedia Environmental Sciences**, Pequim, v. 16, p. 125 – 130, Dez. 2012.

WISE, L. E.; MARPHY, M.; D'ADIECO, A. Chlorite holocellulose, its fractionation and bearing on summative wood analysis and studies on the hemicelluloses. **Paper Trade Journal**, Cornell, v. 122, n. 2, p. 35–43, 1946.

WONG, J. C. H. et al. Mechanical properties of monolithic silica aerogels made from polyethoxydisiloxanes. **Microporous and Mesoporous Materials**, Mülheim, v. 183, p. 23-29, Jan. 2014.

XIE, Y. et al. Silane coupling agents used for natural fiber/polymer composites: a review. **Composites Part A**: applied science and manufacturing, Bristol, v. 41, n. 7, p. 806-819, July 2010.

XIE, K.; YU, Y.; SHI, Y. Synthesis and characterization of cellulose/silica hybrid materials with chemical crosslinking. **Carbohydrate Polymers**, Barking, v. 78, n. 4, p. 799-805, Nov. 2009.

YAMAUCHI, A. Gels: introduction. In: OSADA, Y.; KAJIWARA, K. (Ed.). **Gels handbook**. the fundamentals. San Diego: Academic, 2001. v. 1, p. 9-12.

YAN, X. Functional inorganic-cellulose hybrid nanocomposites. **Progress in Chemistry**, Beijing, v. 23, n. 11, p. 2183-2199, Nov. 2011.

ZHANG, K.; PEI, Z.; WANG, D. Organic solvent pretreatment of lignocellulosic biomass for biofuels and biochemicals: a review. **Bioresource Technology**, Essex, v. 199, p. 21–33, Jan. 2016.

ZHANG, X. et al. Solid-state flexible polyaniline/silver cellulose nanofibrils aerogel supercapacitors. **Journal of Power Sources**, Ulm, v. 246, p. 283-289, Jan. 2014.

ZHAO, X. et al. Delignification of sugarcane bagasse with alkali and peracetic acid and characterization of the pulp. **BioResources**, Kurashiki, v. 5, n. 3, p. 1565-1580, Aug. 2010.

ZHAO, X.; WU, R.; LIU, D. Production of pulp, ethanol and lignin from sugarcane bagasse by alkali-peracetic acid delignification. **Biomass and bioenergy**, Aberdeen, v. 35, n. 7, p. 2874-2882, July 2011.

ZHU, X. et al. Cationic amphiphilic microfibrillated cellulose (MFC) for potential use for bile acid sorption. **Carbohydrate Polymers**, Barking, v. 132, p. 598–605, Nov. 2015.

ZHUANG, X. et al. Liquid hot water pretreatment of lignocellulosic biomass for bioethanol production accompanying with high valuable products. **Bioresource Technology**, Essex, v. 199, p. 68-75, Jan. 2016.

ZIMMERMANN, T.; PÖHLER, E.; GEIGER, T. Cellulose fibrils for Polymer Reinforcement. **Advanced Engineering Materials**, Weinheim, v. 6, n. 9, p. 754-761, Sept. 2004.

ZULUAGA, R. et al. Cellulose microfibrils from banana rachis: Effect of alkaline treatments on structural and morphological features. **Carbohydrate Polymers**, Barking, v. 76, n. 1, p. 51-59, Mar. 2009.

SEGUNDA PARTE – ARTIGOS

ARTIGO 1 ***New pathways of chemical pretreatments to obtain cellulose nanofibrils from a raw non-wood fiber and comparison with commercial wood cellulose pulp***

Alessandra de Souza Fonsecaa,h, Suhara Panthapulakkalb, Samir Kumar Konarb, Mohini Sainb,c, Lina Bufalinod, Joabel Raabee, Ires Paula de Andrade Mirandaf, Maria Alice Martinsg, Gustavo Henrique Denzin Tonolih.

a CAPES Foundation, Ministry of Education of Brazil, Brasília, Distrito Federal, 70.040-020, Brazil.
b Centre for Biocomposites and Biomaterials Processing, Faculty of Forestry, University of Toronto, Toronto, Ontario M5S 3B3, Canada.
c Adjunct, Centre of Excellence for Advanced Materials Research, King AbdulAziz University, Jeddah 21589, KS.
d Forestry Science Department, State University of Amapá -UEAP, Ave Presidente Vargas 650, P.O. Box 1039, Macapá, AP, Brazil.
eDepartment of Forest Engineering, Faculty of Technology, University of Brasília - UnB, Campus Darcy Ribeiro, Asa Norte, P.O. Box 04357, 70910-900, Brasilia, DF, Brazil.
f Brazilian National Institute for Amazon Research - INPA, Laboratory of Palms, Ave Andre Araujo 2936, 69060-001 Manaus, AM, Brazil
g National Nanotechnology Laboratory for Agrobusiness (LNNA), Embrapa Instrumentation (CNPDIA), Rua XV de Novembro 1452, Centro, 13560-970, São Carlos, SP, Brazil.
h Department of Forest Science, Federal University of Lavras, Ave Doutor Sylvio Menicucci 1001, bairro Kennedy, P.O. Box 3037, 37200-000, Lavras, Minas Gerais, Brazil.
**Corresponding author: gustavotonoli@yahoo.com.br, +553538291426.*

Artigo formatado de acordo com as normas para submissão do periodico Macromolecules

ABSTRACT

This study aimed to investigate potential chemical pretreatments to be performed previously to the production of cellulose nanofibrils of jute fibers. Fibers were submitted either to mild or strong alkaline pretreatments. Mild alkaline pretreatment was combined with bleaching with sodium hydroxide and tetraacetylethylenediamine. Cellulose nanofibrils were produced by mechanical fibrillation and films were obtained by the casting method. In addition, nanofibrillation and analyses were carried out for commercial bleached wood pulps. Starting fibers were analyzed by major chemical composition, attenuated total reflectance Fourier-transform infrared (ATR-FTIR) spectroscopy, light and electron microscopy (SEM), and X-ray diffraction (XRD). Transmission electron microscopy was used to investigate cellulose nanofibrils. Films were compared by their mechanical strength. The most effective nanofibrillation was observed for fibers pretreated under mild alkali pre-treatment followed by both bleaching procedures with average diameters of nearly 20 nm. The crystalline index increased for pre-treated fibers in relation to the raw fibers. Overall, films made from jute pre-treated fibers exhibited compatible mechanical strength in relation to those made from commercial wood pulp. Films produced with jute fibers bleached with tetraacetylethylenediamine stood out. The defibrillation process shows to be highly influenced by the by the chemical pretreatments.

KEYWORDS: Jute, Mechanical shearing actions, Defibrillation, Tensile strength, Plant fiber.

1 INTRODUCTION

Society is increasingly demanding for more environmental-friendly-products and materials made from renewable and sustainable resources. The competitiveness of natural fibers is increasing for different applications [1], especially for composite manufacturing. Jute (*Corchorus sp.*) is a natural fiber successfully used for the development of reinforced composites [2-4]. It is one of the most important temporary crops in Brazil, which is the 7th largest producer. The Brazilian Amazonas state is the major producer of jute fibers, since provides 980 tons of the total 1029 tons produced in the national territory [5-6]. Most of the jute production is used as raw material for cordage and textile industries, which, according to information from local producers, generate around 10% of fibrous wastes with no suitable application. As these fibers are rich in cellulose they are potential raw materials for production of cellulose nanofibrils.

Cellulose nanostructures have been studied for a myriad range of applications such as reinforcements for improvement of mechanical and barrier properties in biocomposites [7-8], additives in paper making [9], paints and coatings [10-11], biomedical and pharmaceutical applications [12-13], and electronic substrates [14-15]. It is well known that cellulose suspensions from mechanical defibrillation of the fiber cell wall yield cellulose nanofibrils with heterogeneous sizes. Several works have been done aiming to improve the defibrillation and homogeneity of the micro/nanofibers by pretreatments of the starting cellulose fibers [7,16-21]. Additionally, several works reported the production of cellulose nanofibrils from wood [22-24] and some non-wood resources such as bagasse and rice straw]20], basts fibers from hemp and flax [7,25-26], banana rachis [27], bamboo [28-30], *Aloe vera* [31], leaves of sisal and abaca [21]. There are

few studies regarding jute fibers and nanofibers in the literature [21] and more drawbacks have to be added to allow future application of this material. The aim of this study was to investigate potential chemical pretreatments of the jute fibers to be carried out previously to the production of micro/nanofibers by mechanical fibrillation. Those structures are called cellulose nanofibrils. They were also obtained from commercial *Eucalyptus* and *Pinus* cellulose pulp, which were considered quality parameters.

2 EXPERIMENTAL

2.1 Materials

Jute fibers used in this study were donated by Brasjuta da Amazonia S.A. company (Manaus/AM, Brazil). Bleached commercial wood kraft pulps from *Eucalyptus* sp. (hardwood short fibers) and *Pinus* sp. (softwood long fibers) were provided by Fibria Celulose S/A (São Paulo, Brazil) and Buckeye Technologies (Florida, USA), respectively.

2.2 Chemical pretreatments of the jute fibers

The long raw jute fibers were cut into lengths of about 1 cm previously to the four different pathways of chemical pretreatments, described as follows:

(i) mild alkaline treatment - fibers were immersed in 5 wt% NaOH aqueous solution at a fiber/solution proportion of 1:20 (w/v) for 60 min at 80°C under constant mechanical stirring (~355 rpm);

(ii) mild alkaline treatment followed by bleaching with hydrogen peroxide - after the alkaline treatment described above, fibers were subjected to bleaching using a 5 wt% NaOH / 16 wt% H_2O_2 aqueous solution. The fiber/solution proportion was 1:40 (w/v).

The fiber suspensions were placed in double locked zip bags and submerged in water bath at 55°C for 90 min. The bags were shook and mixed manually every ~10 min during reaction;

(iii) mild alkaline treatment followed by bleaching with tetraacetylethylenediamine (TAED) - the same mild alkali and bleaching procedures described above were applied, but bleaching was achieved using tetraacetylethylenediamine (TAED) at 0.05% (based on dry mass);

(iv) strong alkaline treatment - reaction was conducted with NaOH 5% at 150°C and pressure around 1 MPa for 30 min. The fiber/solution ratio was 1/20 (w:v).

Eucalyptus and *Pinus* kraft pulps were not pre-treated and followed to next steps as received by suppliers.

2.3 Production of the cellulose nanofibrils

All the pretreated jute fibers, *Eucalyptus* sp. and *Pinus* sp. pulps were immersed in water (1% wt consistency) for at least 24 h, and disintegrated by stirring for 15 min before being submitted to mechanical defibrillation. Each suspension was passed through the grinder (Masuko Sangyo Co., LTD.) at 1500 rpm with stone disks widely opened with the aim to homogenize eventual clumps and fiber agglomerates. About 500 mL of the initial solution was collected before starting the defibrillation process. This aliquot was determined as the 0 (zero) step, meaning no passages through grinder. The remaining suspensions were defibrillated with the grinder at rotation of 1500 rpm [29-30] and with different numbers of final passages until final gel consistence of cellulose nanofibrils consisting of cellulose micro/nanofibers. The final suspensions were kept at 4.0 ± 0.2°C.

Pulp sheets (before defibrillation) and cellulose nanofibrils films were prepared to characterize the strength and crystalline structure by the casting method. The procedure for preparation of the sheets is reported in previous works [22,26,31]. The raw materials, procedures and final materials are schematized in Figure 1.

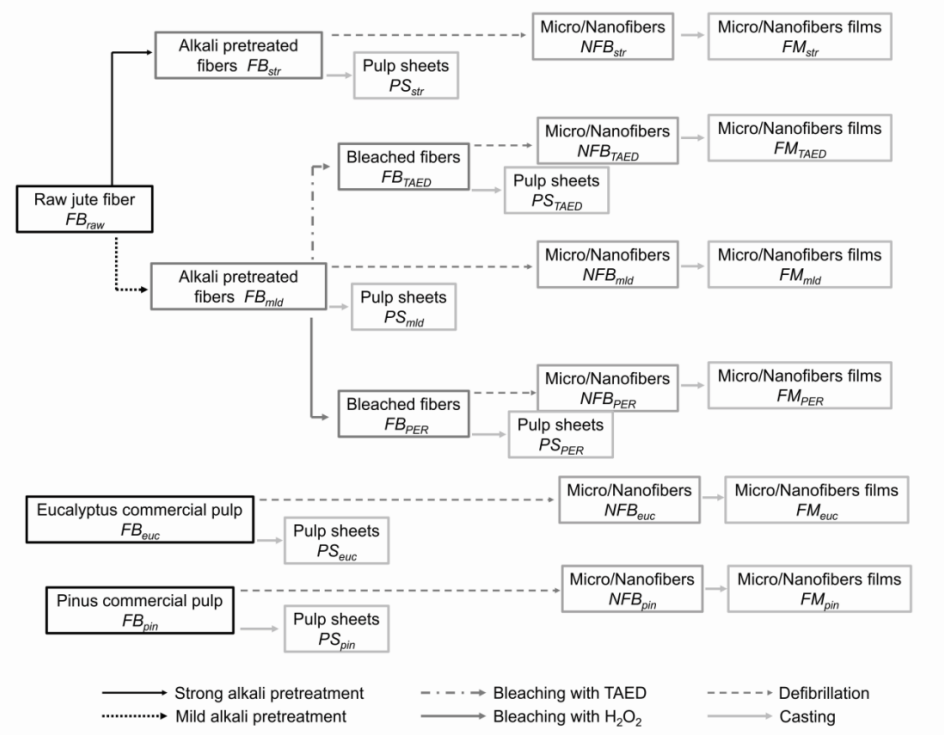

Figure 1 Scheme of the chemical pretreatments and mechanical pathways to obtain cellulose nanofibrils and films from jute fibers and commercial wood pulps

2.4 Characterization of the fibers and cellulose nanofibrils

2.4.1 Chemical composition

The samples were previously milled and the extractives, lignin, holocellulose (cellulose + hemicelluloses) and ashes were determined. The contents of cellulose [32-33], hemicelluloses [33], and lignin [34] were determined in extractive-free samples

according to standardized procedures. Determination of the extractives content [35] and ash content [36] also followed standardized recommendations and were carried out based on the whole mass of the samples. No extractive analysis was carried out to pretreated jute fibers since the alkali treatment removes the secondary cell wall components that occur naturally in small quantities in bast fibers.

2.4.2 Scanning electron microscopy (SEM)

SEM was performed using a JSM-6610LV SEM (JEOL Ltd., Japan) instrument to evaluate the morphology of the pulp fibers. A drop of dilute suspension of the fibers was deposited on a metal stub covered by a carbon-coated tape. The samples were oven dried at 40°C before gold coating (around 2–3 nm thickness layer). Fiber diameters were determined using the ImageJ software [37]. At least 100 individual fiber measurements were performed for each sample.

2.4.3 Attenuated total reflectance Fourier-transform infrared (ATR-FTIR) spectroscopy

ATR-FTIR spectra of the all pulps and nanofiber films were obtained using a Bruker Tensor 27 FTIR spectrometer (Bruker Optic Inc.) with a “Smart Orbit” micro-ATR accessory. The spectra were recorded from 4000 to 600 cm^{-1} wave numbers at a resolution of 4 cm^{-1} with 28 scans.

2.4.4 Light microscopy (LM)

Light microscopic (LM) images were used for estimating the fiber residual fraction after defibrillation (Equation 1, i.e. the content of fibers that was not fully defibrillated), using a Leitz Wetzlar microscope (Ernst Leitz Wetzlar Company, Germany) with transmission

mode and Nikon COOLPIX5400 coupled camera. At least 100 pictures were used for the measurements of each sample.

$$Fiber_{residual}(\%)=(n/N).100 \quad (1)$$

Where: *n* is the number of the pictures with residual fibers and *N* is the total number of pictures captured.

2.4.5 Transmission Electron Microscopy (TEM)

The morphology of the cellulose nanofibrils was investigated using a Hitachi H-7000 TEM (Hitachi Ltda., Japan) instrument and using an accelerated voltage of 75 kV. Sample preparation and TEM configurations followed recommendations described elsewhere [23,31]. Diameter measurements of the nanofibrils were performed for at least 100 individual structures using the ImageJ software.

2.4.6 X-ray diffraction (XRD)

XRD patterns of the micro/nanofiber films were determined on a Philip PW3710 X-ray diffractometer using Cu-K□ radiation. Diffractograms were collected with a voltage of 40 kV and 40 mA current, with a scan angle from 5° to 40° and a scan speed of 2 Θ/s. The crystalline index (CI) was estimated in accordance with the established Segal method [38] as in Equation 2. The amorphous fraction was recorded between $2\theta=18^{o}$ and $2\theta=22^{o}$ because there was essentially no crystalline diffraction peak in this region for cellulose I powders with crystallites having preferred orientation along the fiber axis [39]. All samples were dried at 50°C overnight prior to the analysis.

$$CI = \left(\frac{H_{002} - H_m}{H_{002}} \right) \qquad (2)$$

Where: H_{002} is the height of the 002 peak, and H_m is the height of the minimum intensity in the region of the amorphous fraction that is normally around 2θ=18° for cellulose Iβ and 2θ=16° for cellulose II [40-41].

Crystallite size (CS) was estimated through use of the Scherrer method [42] in Equation 3:

$$CS=(K\lambda)/(\beta \cos\theta) \qquad (3)$$

Where: *CS* is the size (in nm) perpendicular to the lattice plane represented by the peak in question - (002) plane; *K* is a constant that depends on the crystal shape (K=0.89); λ is the wave length of the incident X-ray (1.5425 Å); θ is the Bragg angle corresponding to the (002) plane (i.e. half of the 2θ value in the position of the peak); and β the peak width at half maximum height (pwhm in radians) of the (002) reflection.

2.4.7 Mechanical properties

Tensile properties of pulp sheets and cellulose nanofibrils films were determined according to standard [43] (type V) with the specimens cut from the sheets using a standard die type 5-IMP-2. Tensile strength, Young's modulus, and percentage of elongation of the specimens were determined using an universal testing machine (3367, Instron Corp.). The tests were performed using a crosshead speed of 2.5 mm/min, gauge

length of 25 mm and 1 kN load cell capacity. All the specimens were oven-dried at 50°C at 105°C during 2 h before testing. From 5 to 10 specimens were used for sample.

The parametric F test was applied at 5% of significance. Tukey test (95% probability) was used for multiple comparisons of the averages in the R 2.13.0 software [44].

3 RESULTS AND DISCUSSION

3.1 Chemical composition and morphology of the pre-treated fibers

The data show that extractive content was higher in the jute fiber than in the reference species of *Eucalyptus* sp. and *Pinus* sp. (Table 1). Only strong alkaline pretreatment substantially removed lignin to below 1%; hence delignification was similar to that obtained by industrial kraft pulping.

Table 1. Chemical composition of the samples.

Fiber conditions	Extractives	Lignin	Holocellulose (C+H)*	Ash
	(% by mass)			
FB_{raw}	1.8	11.9	85.4 (C=53.2 + H=32.2)	0.9
FB_{mld}	-	11.8	87.8 (C=77.2 + H=10.6)	0.4
FB_{PER}	-	9.5	89.8 (C=78.6 + H=11.2)	0.7
FB_{TAED}	-	11.2	88.2 (C=78.1 + H=10.1)	0.6
FB_{str}	-	0.9	98.6 (C=92.1 + H=6.5)	0.5
FB_{euc}	0.2	1.0	98.2 (C=86.3 + H=11.9)	0.6
FB_{pin}	0.2	1.6	97.3	0.9

*Holocellulose is the sum of cellulose (C) and hemicelluloses (H) contents. For *Pinus* pulp, the cellulose and hemicelluloses contents were not determined. FB_{raw}: Raw jute fiber; FB_{mld}: Jute mild alkaline; FB_{PER}: Jute mild alkaline + hydrogen peroxide bleached; FB_{TAED}: Jute mild alkaline + TAED bleached; FB_{str}: Jute strong alkaline; FB_{euc}: Commercial *Eucalyptus* pulp; FB_{euc}: Commercial *Pinus* pulp.

Hemicelluloses of the jute fibers remarkably decreased after all pretreatments and became similar to that found for *Eucalyptus* pulp, but contents above 6% can be found for all starting fibers. This result is not expected to hinder nanofiber production since

hemicelluloses act as inhibitors of microfibrils coalescence which may facilitate delamination [7, 45].

Cellulose is considered the major framework component of the fiber structure. It provides strength, stiffness and structural stability of the fiber. Overall, an effective cellulose isolation is desired before cellulose nanofibril production. After mild alkali treatment cellulose raised from 53.2% to 77.2%, while strong alkali treatment raised this value to above 90%. During alkali pretreatment, alkali sensitive hydroxyl groups present among the fiber molecules are broken down and move out from the fiber structure. The superficial mild pretreatment of natural fibers with NaOH results only in partial removal of amorphous materials [46].

Figure 2 depicts the ATR-FTIR spectra of the raw, pretreated and commercial fibers. All the pre-treated fibers showed a peak at 1650 cm^{-1}, which is possibly due to water adhered to the fibers. The remarkably lower peak exhibited by the raw jute fibers support this possibility. The peak at 1735 cm^{-1} corresponds to vibrations of acetyl and uronic ester groups of hemicelluloses or ester linkage of carboxylic groups of the ferulic and p-coumaric acids of lignin [47-49]. The peak at 2850 cm^{-1} related to C-H stretching in lignin and waxes was not completely eliminated after the pretreatments and it is also appeared in the spectra of the wood pulps. Also, peaks at around 1595, 1530-1465, 1512, 1440, 1410 and 1253 cm^{-1} detect the presence of lignin [4,47,50] and their intensities were reduced in the pretreated samples due to partial degradation of this component as confirmed by chemical analyses. The reduction of the peak intensity at 1372 and 1244 cm^{-1} is a consequence of the low hemicelluloses content [50]. Cellulose can be identified [47, 51] by possible assignment of β-glucosidic linkage at 897-890 cm^{-1} and assignments

out-of-plane bending vibration of intermolecular O-H groups at 675-667 cm^{-1} and of antisymmetric C-O-C stretching at 1160 cm^{-1}. The others characteristic bands for cellulose are 4000-2995, 1430, 1375-1373, and 1282-1278 cm^{-1} for crystalline domains; and 2902-2892, 1261-1263, 1337, and 993-900 cm^{-1} for amorphous domains. Cellulose Iβ [52-53] is recognized by a peak at 710 cm^{-1} (as observed for FB_{PER}) and cellulose Iα [52-53] by a peak at 750 cm^{-1}.

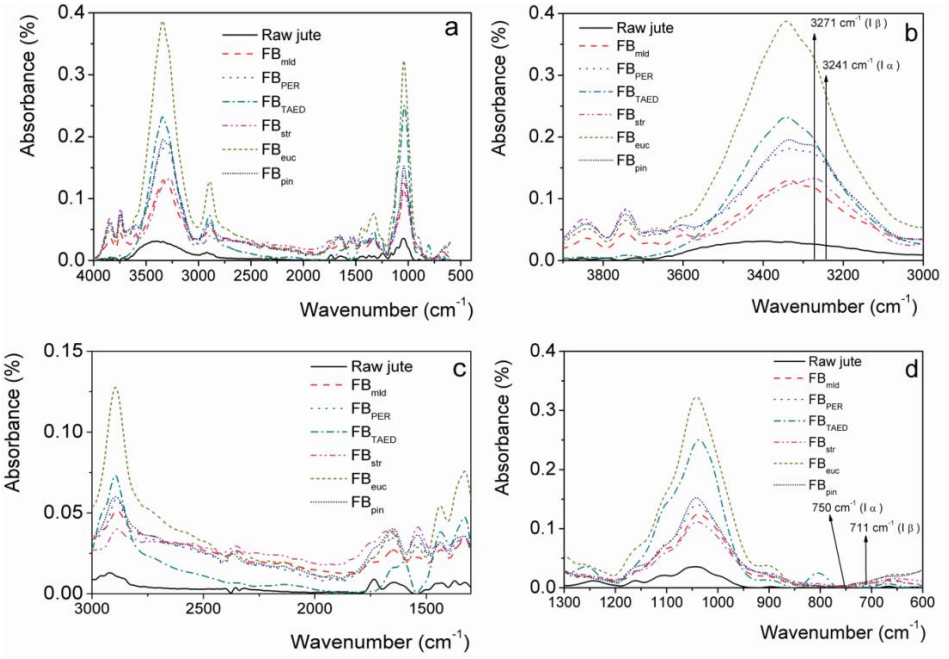

Figure 2 Full spectra with absorption between 4000-600 cm^{-1}; h) detail of absorption bands at 3241 and 3271 cm^{-1} correspondent to Iα and Iβ cellulose, respectively; i) detail of absorption bands at 3000-1300 cm^{-1}; j) detail of absorption bands at 750 and 711 cm^{-1} correspondent to Iα and Iβ cellulose, respectively

The plant fibers degree of individualization into cellular structures is clearly observed by SEM micrographs (Fig. 3a-f). FB_{PER} and FB_{str} had more effective fiber individualization. Their morphology even become similar to those of commercial wood pulps. This effect is directly related to removal of amorphous hemicelluloses and lignin which are binders

that unite adjacent fibers [21, 27, 54] into bundles. From the commercial/technical point of view, the jute fiber bundles correspond to fibers, but from the botanical/anatomical point of view the fiber is necessarily an individualized cell which is released after chemical pretreatments as required for nanofibrillation.

SEM micrographs (Fig. 3a-d) were used for morphological measurements and show that the raw jute is comprised of bundles (Fig. 3 b-c, dashed circle) of individual fibers (Fig. 3 c, arrow) with average diameter of 16 ± 3 μm, with individual values in the range between 6 μm (minimum) and 25 μm (maximum), and an average fiber length of around 2 mm. These values are lower than those reported elsewhere [55-57] probably as a consequence of environmental factors from the growing sites in Brazil. The diameter of all the pre-treated jute fibers was in the range of 1-20 μm as observed in Figure 3g. The difference in diameter between the jute and commercial pulps is related to differences in morphology of the plant groups Gymnosperm and Angiosperm. Jute and *Eucalyptus* are both Angiosperms and show similar fiber aspect after pre-treatment of the former. *Eucalyptus* is classified as very short fiber species [58] with average length lower than 0.9 mm. Jute and *Pinus* are classified as long fibers [58] with average length higher than 1.6 mm.

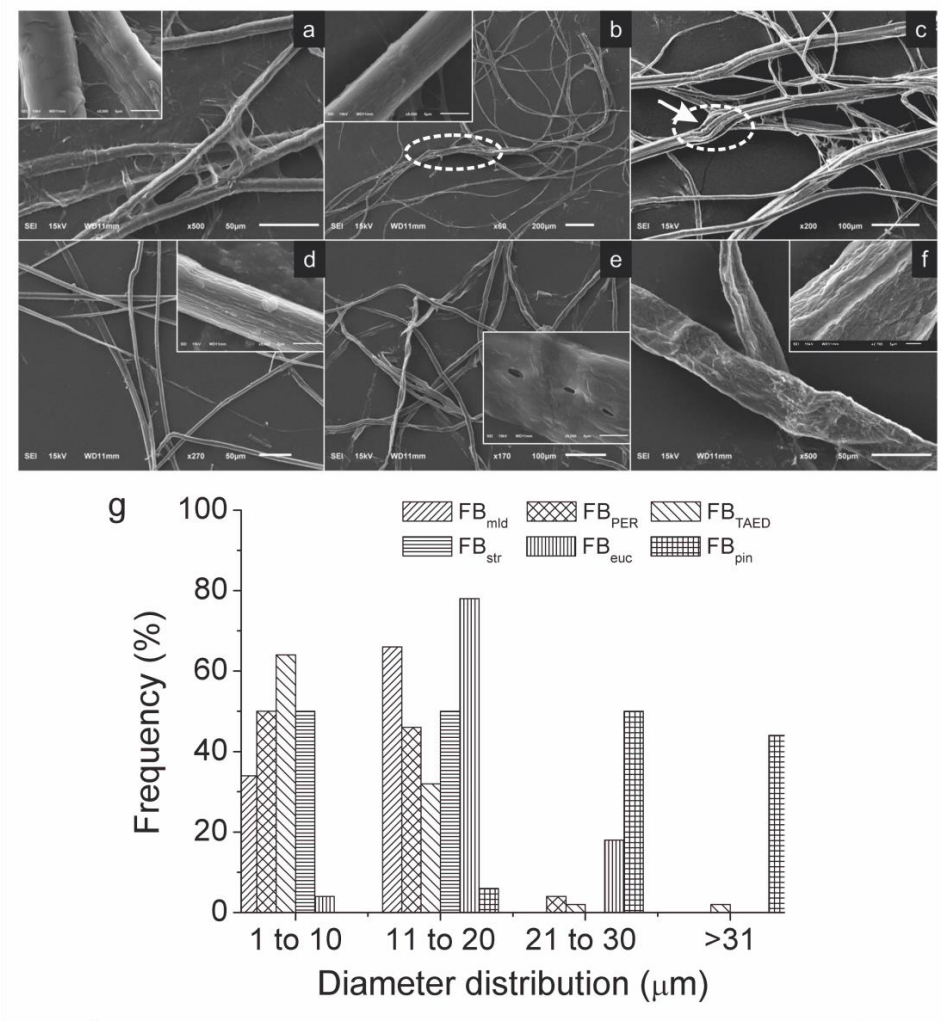

Figure 3 Typical SEM images of the different fiber conditions before defibrillation: a) FB_{mld}; b) FB_{PER}; c) FB_{TAED}; d) FB_{str}; e) FB_{euc}; f) FB_{pin}; and g) diameter distribution. Dashed circle shows regions of the FB_{raw} consisting of bundles of individual fibers (arrow)

3.2 Residual content of fibers after defibrillation

It is important to have substantial evidence about the fraction of cellulose nanofibrils that present diameter lower than 100 mm, and also the morphology of the nanofibers in

those suspensions [16]. Overall, after processing in grinder, the cellulose nanofibrils suspension may contain the following structures: (i) individualized micro/nanofibers; (ii) fibers under incomplete defibrillation; (iii) clusters and bundles of micro/nanofibers; and (iv) non-defibrillated fibers (Fig. 4a-f). The fibers pre-treated by alkaline pulping under pressure showed the most effective defibrillation mainly due to lower lignin content. This condition facilitates swelling of the fibers and improves deconstruction of the fiber cell wall. Only 3% of the samples exhibited non-defibrillated fibers, while 50% are fully defibrillated and 47% are fibers under defibrillation.

Fibers submitted to bleaching with TAED previous to defibrillation had the highest residual fiber fraction. Furthermore, some fibers remained intact into the suspension, while others appeared in advanced defibrillation (Fig. 4g). Mechanical defibrillation can shorten the fibers/micro/nanofibers, because they can be cut by direct shearing forces when passing through the grinder stones [59]. NFB_{pin} also presented lower content of residual fibers than NFB_{euc} (Fig. 4g) probably due to its higher length (FB_{pin}) that increases its defibrillation area.

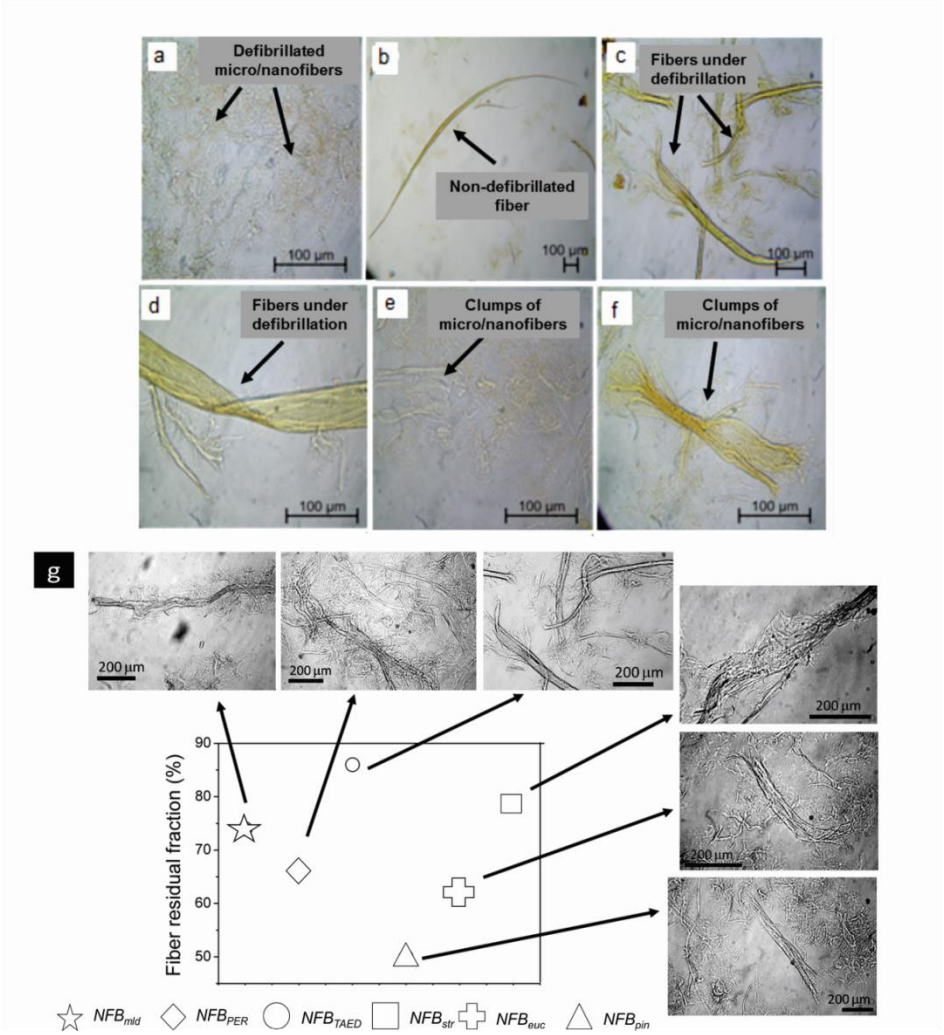

Figure 4 Examples of residual fibers on cellulose nanofibrils: (a) Defibrillated; (b) non-defibrillated; (c-d) under defibrillation; (e-f) clumps of nanofibrils; and (g) Fiber residual fraction after defibrillation and typical light microscopic (LM) images of the fibers under defibrillation for each condition. This fraction is related to sum of non-defibrillated fibers and fibers under defibrillation

3.3. Morphology of the micro/nanofibers

Morphology aspects of the cellulose nanofibrils are depicted in Figure 5. Suspension from defibrillation of the pretreated jute fibers shows deconstruction of the fiber cell wall presenting several entanglements of the long fibrils and nanofibrils (Fig.s 5a-d). FB_{mld} and FB_{TAED} resulted in suspensions with higher degree of nanofibrillation (Fig. 5a and Fig. 5c, respectively). In addition, nanofibrils from FB_{mld} appear less degraded in comparison to the others (Fig. 5a). For the NFB_{str} the aspect of cellulose nanocrystals appears when using higher magnification (Fig. 5d).

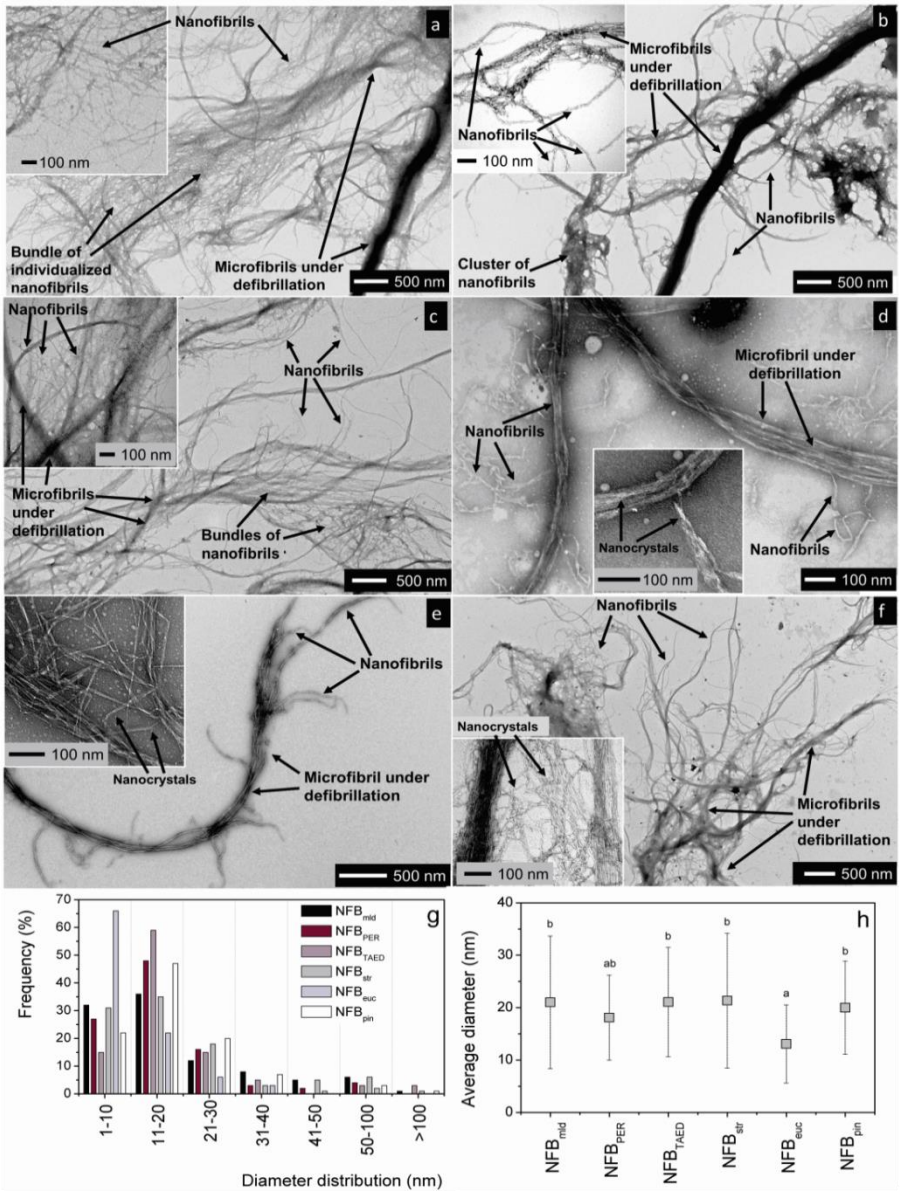

Figure 5 Typical TEM images of the cellulose nanofibrils from the different conditions: a) NFB_{mld}; b) NFB_{PER}; c) NFB_{TAED}; d) NFB_{str}; e) NFB_{euc}; and f) NFB_{pin}. High magnifications turn the nanocrystals more visible in b), d) and e); g) Diameter distribution; h) average diameter of the cellulose nanofibrils (different letters differ at 95% probability by Tukey test); Typical TEM images showing evidences of the crystals in the cellulose nanofibrils from: d) NFB_{PER}; e) NFB_{str}; and f) NFB_{euc}

As discussed above, some pretreatments did not effectively removed lignin from the cell wall; hence defibrillation process was hindered. FB_{mld} required more passages through the grinder (5 more passages than FB_{PER} and FB_{str}) to obtain the final consistence of a gel. Bleached jute fibers required the same amount of passages to isolate cellulose nanofibrils, without causing excessive degradation as alkaline pulped fibers. Each starting fibers reacted differently for the number of passages through the grinder (defibrillator) which varied from 15-20 passages.

The strong alkaline pulping pretreatment easily removed lignin and hemicelluloses, bud caused excessively degradation of starting fibers due to high pH (pH~13) [21]. NFB_{str} showed relatively large diameters probably due to dissolution of smaller nanofibrils.

The removal of hemicelluloses from the jute fibers through alkaline pretreatment may also have contributed to damage [7, 21, 27, 54] since cellulose chains become excessively exposed. Additionally, under higher magnifications the cellulose nanocrystals are more visible in NFB_{PER} (Fig. 5b), NFB_{str} (Fig. 5d) and NFB_{euc} (Fig. 5e) probably as a result of the chemical activities that effectivelly removed the non-cellulosic fractions from the starting fibers. NFB_{euc} (Fig. 5e) is similar to NFB_{str} (Fig. 5d) becoming like-degraded morphology meanwhile NFB_{pin} has a well-fibrillated morphology observed to NFB_{mld} (Fig. 5a) and NFB_{TAED} (Fig. 5c).

The diameter distribution (Fig. 5g) and average diameter of cellulose nanofibrils (Fig. 5h) were determined using the TEM images. Almost 80-95% of nanofiber diameters were lower than 35 nm. The average nanofiber diameters in the NFB_{mld}, NFB_{PER} , NFB_{TAED} and NFB_{str} suspensios are 21 ± 13 nm, 18 ± 8 nm, 21 ± 10 nm, and 21 ± 13 nm, respectively. Average diameter of NFB_{euc} (13 ± 8 nm) was lower than that of NFB_{pin} (20

± 9 nm) and of all jute cellulose nanofibrils. NFB_{mld} has around 67% of well individualized nanofibrils with diameters bellow 20 nm. Around 75% of nanofibrils obtained from FB_{PER}, FB_{TAED} and FB_{str} are lower than 20 nm in diameter. NFB_{euc} and NFB_{pin} also present ~86% and ~67% of their nanofibrils with diameter bellow 20 nm, respectively.

Despite the presence of lignin, cellulose nanofibrils were obtained for from all samples. The largest content of structures in the nanoscale (1 to 100 nm) was observed for NFB_{euc} and NFB_{pin}.

3.4. Crystallinity of the cellulose nanofibrils films

X-ray diffractograms (XRD) of the films show patterns of both crystalline and amorphous peaks as typically occurs for semicrystalline materials (Fig. 6a-c).

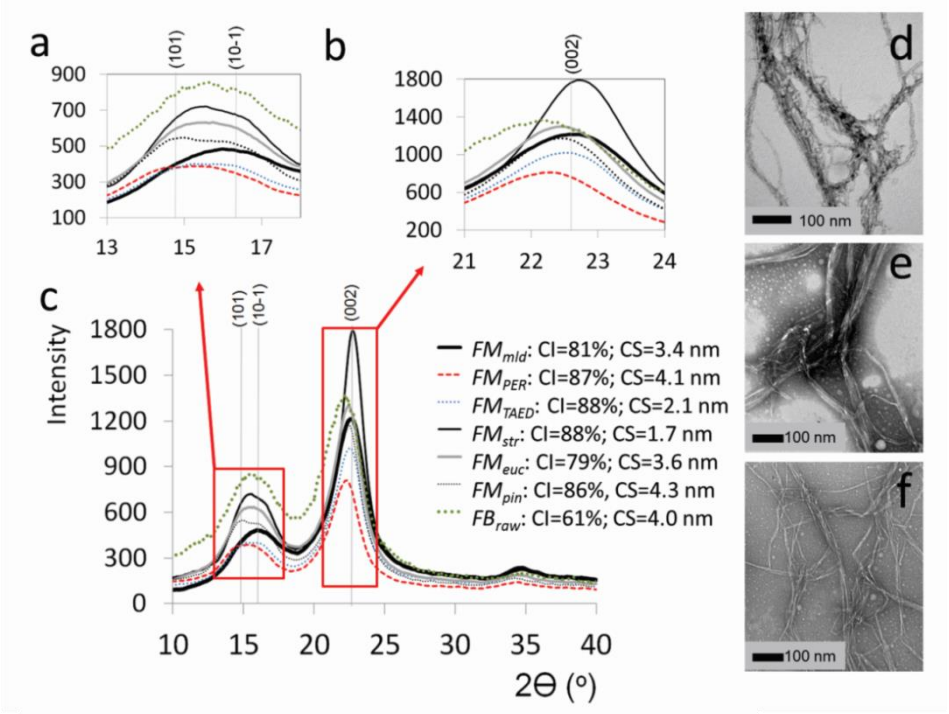

Figure 6 Cellulose nanofibrils XRD patterns: (a-c) raw jute and films of cellulose nanofibrils, average values of crystalline index (CI) and crystallite size (CS) obtained from the XRD patterns; (d-g) examples of individualized nanofibrils morphology

Amorphous domains of cellulose are detected between $2\Theta=18^{o}$ and $2\Theta=20^{o}$, since there is essentially no crystalline diffraction at this region [39]. This also suggests that majority of this cellulose exists as Iβ cellulose polymorph [39, 41].

All fiber samples exhibited a sharp peak at $2\theta=22.6^{o}$, which is assigned to the (002) lattice plane of cellulose I [60]. XRD data showed minor variation in the position of the cellulose I (002) peak (Fig. 6). The peaks became sharper in the diffractograms of pretreated fibers, which is an indicative of increases in crystallinity the (002) plane [42]. The two overlapping weaker diffraction peaks at $2\theta=14.8^{o}$ and $2\theta=16.3^{o}$ are assigned to the (101) and (10-1) lattice planes of cellulose I [61-62]. Those become more eminent

and separated from each other after pretreatments, with a little dislocation of the (101) peak to lower values. Similar changes were observed in the literature [63]. The peak at around $2\theta=35^{o}$ corresponds to the (040) lattice planes and it is comprised of several reflections due to the absence of preferred orientation of the crystals [39].

Overall, removal of amorphous lignin and hemicelluloses from the cellulose wall without alterations of the crystalline structure of the cellulose was achieved. Similarly results were reported in the liteture [23, 29, 64]. Crystalline indexes varied among pretreated fibers and they were all higher in relation to the one determined for raw jute fiber. The amorphous components surround semicrystalline cellulose and result in lower crystalline index [50]. As they are removed along with some amorphous cellulose, peaks related to crystals become more evident.

Alkaline pretreatments aim to selectively attack amorphous domains rather than crystals of the cellulose. The crystallite size (CS) of the cellulose fibers decreased during most of pretreatments with strong alkaline and TAED bleached conditions presenting the lower CS values. Only when amorphous regions are no longer accessible, crystalline domains may be degraded [65]. Figures 6 d-g show some nanostructures with morphologies very close to nanocrystals at high magnications TEM images. Despite the lower CI for NFB_{euc} (CI=79%), it was observed that the nanocrystals seem narrower and more individualized in relation to the other samples.

3.5. Changes in the ATR-FTIR spectroscopy of the cellulose nanofibrils films

Differences in crystal and amorphous domains for the different conditions were also attested by ATR_FTIR spectroscopy (Fig. 7). The decrease in the crystalline organization (and/or content) leads to a significant simplification of the spectra through

reduction in intensity or even disappearance of the bands characteristic of the crystalline domains. The broad band that ranges between 3100-3600 cm^{-1} corresponds to the O-H stretching vibration [60]; hence it is closely related to the hydrogen bonds in the fibers and cellulose nanofibrils. Normally, the characteristic peaks of hydrogen bonds from the spectra of amorphous celluloses become smoother and less prominent, compared to those depicted by crystalline cellulose. This behavior corresponds to the scission of the intra and intermolecular hydrogen bonds of amorphous cellulose. Additionally this, peak is displaced to higher wave number values when the samples have high amount of amorphous components [66], such as raw jute fibers. The presence of amorphous fraction can be further confirmed by the decrease in the intensity of the band at 2900 cm^{-1} which corresponds to the C–H stretching vibration [66, 67].

Finally, the bands at 1430 cm^{-1} and 1370 cm^{-1}, assigned to a symmetric CH_2 bending vibration of the crystalline domains, are lower for raw jute, i.e. for a lower crystalline index. The peaks at around 1155 cm^{-1} (referred to C–O vibration), 1105 cm^{-1} (related to ring asymmetric valence), and 1000 cm^{-1} (related to C–O valence vibration at Carbon (6)) are very low for the raw jute and increased for all pretreated samples. FM_{TAED} shows higher intensity peaks at 2960 cm^{-1}, 1260 cm^{-1} and 800 cm^{-1}, which is due to C-O stretching of acetyl groups in hemicelluloses (Fig. 7c, d).

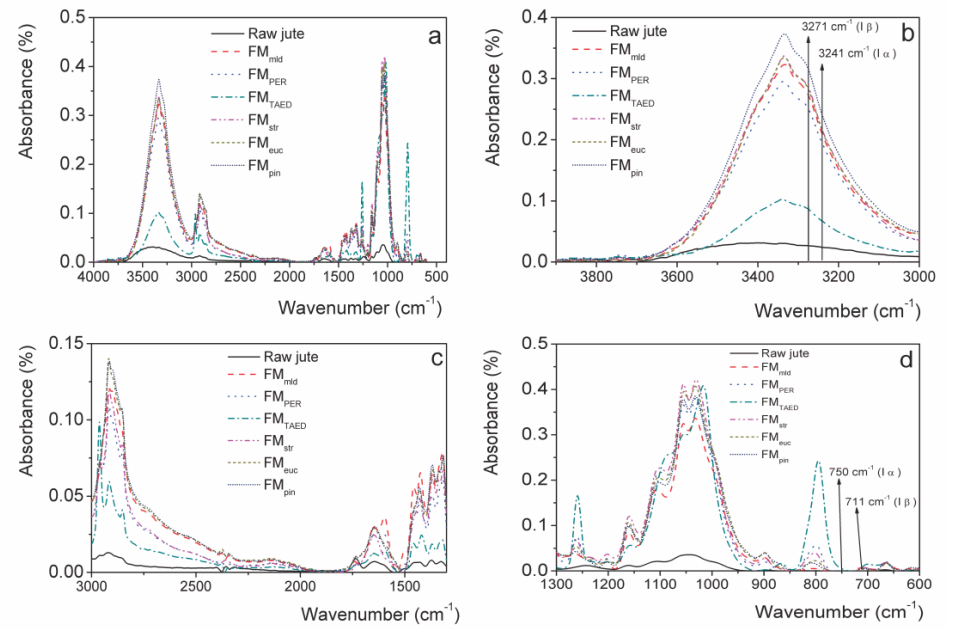

Figure 7 ATR-FTIR spectra of the cellulose nanofibrils films exception to raw jute fibers curve: a) full spectra with absorption between 4000-600 cm^{-1}; b) detail of absorption bands at 3241 and 3271 cm^{-1} correspondent to Iα and Iβ cellulose, respectively; c) detail of absorption bands at 3000-1300 cm^{-1}; and d) detail of absorption bands at 750 and 711 cm^{-1} correspondent to Iα and Iβ, respectively

3.6. Mechanical performance of the films

The mechanical properties of the pulp and micro/nanofiber sheets are shown in Figure 8. All the micro/nanofiber sheets exhibited significantly higher tensile strength than films made from micro-sized fibers (Fig. 8a). This result is mainly attributed to the increase in the surface area of micro/nanofibers, which increases the number of free hydrogen groups available for bonding.

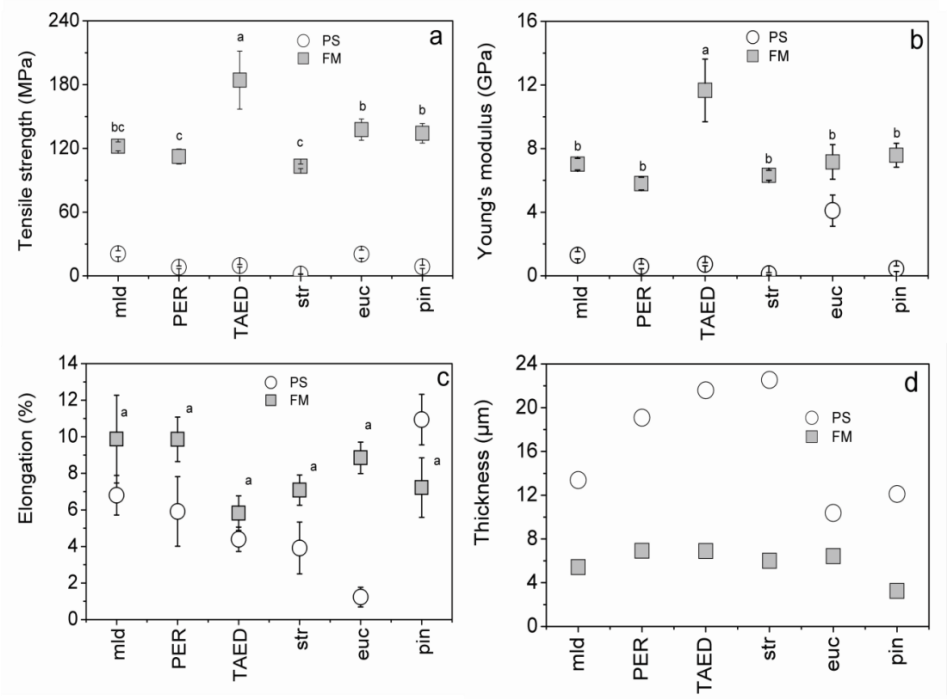

Figure 8 Thickness and mechanical properties of the pulp sheets (PS) and cellulose nanofibrils films (FM): a) tensile strength; b) Young's modulus; c) elongation; and d) thickness. Different letters means statistical differences at 95% probability at Tukey test

Previous studies found that the presence of lignin and hemicelluloses influence the final mechanical properties of the individual fibers [18, 21, 27, 68]. The elongation at break of the films may decrease when they are basically composed of cellulose because this component is not very extensible [69]. The larger number of hydrogen bonds available in cellulose nanofibrils improves film cohesion and leads to lower thickness. FM_{TAED} showed higher tensile strength (~184 MPa) and Young's modulus (~12 GPa). However, it showed lower elongation (~6%) than FM_{mld} (~10%) and FM_{PER} (~10%). Overall, they become alike the commercial wood pulps: FM_{euc} had statistically similar tensile strength to FM_{pin} which was higher than that found to FM_{mild}, FM_{PER} and FM_{str}. The Young's modulus for FM_{euc} and FM_{pin} has no difference with the counterparts cited above.

The mechanical performance of the films was closely related to the chemical composition of the cellulose nanofibrils, since higher residual non-cellulosic fractions provided higher tensile strength.

Hemicelluloses may act as inhibitors of the coalescence of cellulose nanofibrils during drying, and can participate on the enhancement of mechanical properties in composites [68]. The presence of lignin may significantly increase film toughness, tensile index and elastic modulus [18]. However, normally high content of lignin means less fibrillated fibers, which can adversely affect mechanical properties. Higher cellulose contents provide higher Young´s Module to cellulose nanofibrils films because of its natural stiffness [69]. Hemicelluloses can deform greater than crystalline cellulose, and play an important role in adhesion between cellulose nanofibrils, which contribute to mechanical strength [68]. The presence of lignin significantly increased toughness, tensile strength, and elastic modulus of similar microfibril films [18].

The FM_{str}, and FM_{PER} presented the lowest values of tensile strength and Yong's modulus, probably caused by an excessive alkali exposition of cellulose chains during the pretreatments processing. On the other hand, FM_{TAED} showed higher contents of fibers under advanced defibrillation process; hence a larger surface area (Fig. 5a) allowed greater tensile strength. In addition, improved distribution of the nanofibrils led to more efficient packaging and compact structure of the cellulose film. Aggregations of cellulose nanofibrils formed in suspensions and consolidated during film drying, may act as stress concentration points and decrease strength [70].

The values of tensile strength observed in the results are far higher than values found for polyethylene – LLDPE (37 MPa), polycaprolactone – PCL (21–42 MPa), polypropylene

– PP (35 MPa), and poly (lactic acid) – PLA (50-70 MPa); which are polymers frequently used in flexible packages [71-73, 60].

Finally, the results assure that mild pretreatments followed by mechanical deconstruction successfully generate high quality cellulose nanofibrils; hence the concept of using necessarily strong acid hydrolysis or very expensive and specific enzyme treatments may be avoided. The pretreatments used in this study are inexpensive and have the potential to be applied at large scale transformation processes.

4 CONCLUSIONS

Cellulose nanofibrils were obtained from all pre-treated jute fibers. Pretreated jute fibers can generate cellulose nanofibrils with better mechanical properties than commercial bleached wood pulps. TAED bleached and mild alkaline pretreatments were more effective to produce films with better tensile properties. Films from strong alkaline condition showed lowest tensile strength and Young's modulus. The proposed pre-treatment pathways may be useful for partial deconstruction of the jute macrofibers for obtaining cellulose nanofibrils with large surface area and useful for engineering fiber-based materials and polymeric composites for a myriad of applications.

ACKNOWLEDGMENTS

The authors are grateful for the financial support provided by CAPES Foundation (Process n. BEX 14459/13-2 and scholarship PDSE/CAPES, process n. 99999.012163/2013-09), CNPq Foundation (Process n. 484082/2013-2 and 506506/2013-4), FAPEMIG Foundation, Brazil; University of Toronto and Centre for Biocomposites and Biomaterials Processing -CBBP, Canada. Thanks also to Brazilian

Network of Lignocellulosic Composites and Nanocomposites (RELIGAR), BrasJuta da Amazônia S.A. company, Graduate Program in Biomaterials Engineering (UFLA) and Graduate Program in Wood Science and Technology (UFLA), Brazil.

REFERENCES

[1] Food and Agriculture Organization of the United Nation - FAO(2011) Report of the joint meeting of the thirty-sixth session of the intergovernmental group on hard fibres and the thirty-eighth session of the intergovernmental group on jute, kenaf and allied fibres and the seventeenth session of the sub-group of sisal producing countries. FAO website. http://www.fao.org/docrep/meeting/024/md052e.pdf .Accessed 3 June, 2015

[2] Ramesh M,; Palanikumar K, Reddy KH (2013) Comparative evaluation on properties of hybrid glass fiber- sisal/jute reinforced epoxy composites. Procedia Eng 51:745-750

[3] Pantamanatsopa P, Ariyawiriyanan W, Meekeaw T, Suthamyong R, Arrub K, Hamada H (2014) Effect of modified jute fiber on mechanical properties of green rubber composite. Energy Procedia 56:641–647

[4] Rahman MM, Afrin S, Haque P (2014) Characterization of crystalline cellulose of jute reinforced poly(vinyl alcohol) (PVA) biocomposite film for potential biomedical applications. Prog Biomater 3:9 pp.

[5] Food and Agriculture Organization of the United Nation –FAO (2013) FAO Statistical Yearbook 2013 world food and agriculture. FAO Website. http://www.fao.org/docrep/018/i3107e/i3107e.PDF. Accessed 3 June 2015

[6] Instituto Brasileiro de Geografia e estatística - IBGE (2013) Produção Agrícola Municipal Culturas temporárias e permanentes 2013. ftp://ftp.ibge.gov.br/Producao_Agricola/Producao_Agricola_Municipal_[anual]/2013/pam2013.pdf. Accessed 3 June 2015 (in portuguese)

[7] Klemm D, Kramer F, Moritz S, Lindström T, Ankerfors M, Gray D, Dorris A (2011) Cellulose: fascinating biopolymer and sustainable raw material. Angew Chem Int Ed 50:5438–5466

[8] Lavoine N, Desloges I, Dufresne A, Bras J (2012) Microfibrillated cellulose – Its barrier properties and applications in cellulosic materials. Carbohydr Polym 90:735– 764

[9] Arbatan T, Zhang L, Fang X-Y, Shen W (2012) Cellulose nanofibers as binder for fabrication of superhydrophobic paper. Chem Eng J 210: 74–79

[10] Li F, Biagioni P, Bollani M, Maccagnan A, Piergiovanni L (2013) Multi-functional coating of cellulose nanocrystals for flexible packaging applications. Cellulose 20:2491–504

[11] Salas C, Nypelö T, Rodriguez-Abreu C, Carrillo C, Rojas OJ (2014) Nanocellulose properties and applications in colloids and interfaces. Curr Opin Colloid Interface Sci 19:383–396

[12] Svensson A, Nicklasson E, Harrah T, Panilaitis B, Kaplan DL, Brittberg M, Gatenholm P (2005) Bacterial cellulose as a potential scaffold for tissue engineering of cartilage. Biomaterials 26:419–431

[13] Nikolajaski M, Wotschadlo J, Clement J H, Heinze T (2012) Amino-functionalized cellulose nanoparticles: Preparation, characterization, and interactions with living cells. Macromol Biosci12:920–925

[14] Okahisa Y, Yoshida A, Miyaguchi S, Yano H (2009) Composites optically transparent wood–cellulose nanocomposite as a base substrate for flexible organic light-emitting diode displays. Compos Sci Technol 69:1958–1961

[15] Ummartyotin S, Juntaro J, Sain M, Manuspiya H (2012) Development of transparent bacterial cellulose nanocomposite film as substrate for flexible organic light emitting diode (OLED) display. Ind Crops Prod 35:92– 97

[16] Chinga-Carrasco G (2011) Cellulose fibres, nanofibrils and microfibrils: The morphological sequence of MFC componentes from a plant physiology and fibre technology point of view. Nanoscale Res Lett 6:7pp.

[17] Janardhnan S, Sain M (2011) Isolation of cellulose nanofibers: effect of biotreatment on hydrogen bonding network in wood fibers. Int J Polym Sci ID 279610, http://dx.doi.org/10.1155/2011/279610

[18] Spence KL, Venditti RA, Rojas OJ, Habibi Y, Pawlak JJ (2010) The effect of chemical composition on microfibrillar cellulose films from wood pulps: water interactions and physical properties for packaging applications. Cellulose 17:835–848

[19] Isogai A, Saito T, Fukuzumi H (2011) TEMPO-oxidized cellulose nanofibers. Nanoscale 3:71-85

[20] Hassan ML, Mathew AP, Hassan EA, El-Wakil NA, Oksman K (2012) Nanofibers from bagasse and rice straw: process optimization and properties. Wood Sci Technol 46:193–205

[21] Alila S, Besbes I, Vilar MR, Mutjé P, Boufi S (2013) Non-woody plants as raw materials for production of microfibrillated cellulose (MFC): A comparative study. Ind Crops Prod 41:250–259

[22] Panthapulakkal S, Sain M, (2012) Preparation and characterization of cellulose nanofibril films from wood fibre and their thermoplastic polycarbonate composites. Int J Polym Sci ID 381342, http://dx.doi.org/10.1155/2012/381342

[23] Tonoli GHD, Teixeira EM, Correa AC, Marconcini JM, Caixeta LA, Pereira-da-Silva MA, Mattoso LHC (2012) Cellulose micro/nanofibers from Eucaliptus kraft pulp: preparation and properties. Carbohydr Polym 89:80–88

[24] Bufalino L, Mendes LM, Tonoli GHD, Rodrigues A, Fonseca A, Cunha PI, Marconcini JM (2014) New products made with lignocellulosic nanofibers from Brazilian amazon forest. IOP Conf Ser Mater Sci Eng 64, doi:10.1088/1757-899X/64/1/012012

[25] Wang B, Sain M, Oksman K (2007) Study of structural morphology of hemp fiber from the micro to the nanoscale. Appl Compos Mater 14:89–103

[26] Panthapulakkal S, Sain M (2013) Isolation of nanofibres from hemp and flax and their thermoplastic composites. Plastic and Polymer Technology 2:9-16

[27] Zuluaga R, Putaux JL, Cruz J, Vélez J, Mondragon I, Gañán P (2009) Cellulose microfibrils from banana rachis: Effect of alkaline treatments on structural and morphological features. Carbohydr Polym76:51–59

[28] Nguyen HD, Mai TTT, Nguyen NB, Dang TD, Le MLP, Dang TT, Tran VM (2013) A novel method for preparing microfibrillated cellulose from bamboo fibers. Adv Nat Sci Nanosci Nanotechnol 4:015016

[29] Guimarães Jr M, Botaro VR, Novack KM, Teixeira FG, Tonoli GHD (2015a) Starch/PVA-based nanocomposites reinforced with bamboo nanofibrils. Ind Crops Prod 70:72-83

[30] Guimarães Jr M, Botaro VR, Novack KM, Flauzino Neto WP, Mendes LM, Tonoli GHD (2015b) Preparation of cellulose nanofibrils from bamboo pulp by mechanical defibrillation for their applications in biodegradable composites. J Nanosci Nanotechnol 15:1-18

[31] Cheng S, Panthapulakkal S, Sain M, Asiri A (2014) Aloe vera Rind Cellulose Nanofibers-Reinforced Films. J Appl Polym Sci 40592

[32] Browning BL (1967) Methods of wood chemistry. Wiley, New York

[33] Kennedy F, Phillips G O, Williams EPA (1987) Wood and cellulosics: industrial utilization, biotechnology, structure and properties. Ellis horwood, Chichester

[34] American Society for Testing and Materials (2009) Standard test method for acid insoluble residue in biomass ASTM E 1721-01

[35] American Society for Testing and Materials (2008) Standard test method for Determination of ethanol extractives in biomass ASTM E 1690-08

[36] American Society for Testing and Materials (2007) Standard Test Method for Ash in Biomass ASTM E 1755-01

[37] Schneider CA, Rasband WS, Eliceiri KW (2012) Image to ImageJ: 25 years of image analysis. Nat Methods 9:671-675

[38] Segal L, Creely JJ, Martin AE, Conrad CM (1959) An empirical method for estimating the degree of crystallinity of native cellulose using the X-Ray diffractometer. Text Res J 29:786-794

[39] French AD (2014) Idealized powder diffraction patterns for cellulose polymorphs. Cellulose 21:885–896.

[40] Azubuike CP, Okhamafe AO (2012) Physicochemical, spectroscopic and thermal properties of microcrystalline cellulose derived from corn cobs. Int J Recycling Org Waste Agric 1:7 pp.

[41] French AD, Cintrón MS (2013) Cellulose polymorphy, crystallite size, and the Segal Crystallinity Index. Cellulose 20:583-588

[42] Cao Y, Tan H (2005) Study on crystal structures of enzyme-hydrolyzed cellulosic materials by X-ray diffraction. Enzyme Microb Technol 36:314-317

[43] American Society for Testing and Materials (2010) Standard Test Method for Tensile Properties of Plastics ASTM D 638-10

[44] R Core Team (2014). The R Project for Statistical Computing. http://www.R-project.org. Accessed 18 March 2014

[45] Zhang HR, Tong MW (2007) Influence of hemicelluloses on the structure and properties of lyocell fibers. Polymer Engineering Science 47:702–706

[46] Kabir, MM, Wang H, Lau, KT, Cardona F (2012) Chemical treatments on plant-based natural fibre reinforced polymer composites: An overview. Compos Part B Eng 43:2883–2892

[47] Ray D, Sarkar BK (2001) Characterization of alkali-treated jute fibers for physical and mechanical properties. J Appl Polym Sci 80:1013–1020

[48] Sun RC, Sung XF, Liu GQ, Fowler P, Tomkinson J (2002) Structural and physicochemical characterization of hemicelluloses isolated by alkaline peroxide from barley straw. Polym. Int 51:117–124

[49] Sun XF, Xu F, Sun RC, Fowler P, Baird MS (2005) Characteristics of degraded cellulose obtained from steam-exploded wheat straw. Carbohydr Res 340:97–106

[50] Khan GMA, Alam MS (2013) Surface chemical treatments of jute fiber for high value composite uses. Res Rev J Mater Sci 1:39-44

[51] Abidi N, Cabrales L, Haigler CH (2014) Changes in the cell wall and cellulose content of developing cotton fibers investigated by FTIR spectroscopy. Carbohydr Polym 100:9-16

[52] Oh SY, Yoo DI, Shin Y, Seo G (2005) FTIR analysis of cellulose treated with sodium hydroxide and carbon dioxide. Carbohydr Res 340:417–428

[53] Åkerholm M, Hinterstoisser B, Salmén L (2004) Characterization of the crystalline structure of cellulose using static and dynamic FT-IR spectroscopy. Carbohydr Res 339:569–578

[54] Marques G, Rencoret J, Gutiérrez A, Del Río JC (2010) Evaluation of the chemical composition of different non-woody plant fibres used for pulp and paper manufacturing. Open Agric J4:93–101

[55] Lin J, Yu L, Tian F, Zhao N, Li X, Bian F, Wang J (2014) Cellulose nanofibrils aerogels generated from jute fibers. Carbohydr Polym 109:35–43

[56] Alves C, Ferrão PMC, Silva AJ, Reis LG, Freitas M, Rodrigues LB, Alves DE (2010) Ecodesign of automotive components making use of natural jute fiber composites. J Cleaner Prod 18:313–327

[57] Mannan KM, Talukder MAI (1997) Characterization of raw, delignified and bleached jute fibres by study of absorption of moisture and some mechanical properties. Polymer 38:2493-2500

[58] Coradin VTR, Muñiz GIDE (1992) Normas e procedimentos em estudos de anatomia da madeira: Angiospermae II-Gimnospermae IBAMA série técnica 15: 17 pp (in Portuguese)

[59] Gharehkhani S, Sadeghinezhad E, Kazi SN, Yarmand H, Badarudin A, Safaei MR, Zubir MNM (2015) Basic effects of pulp refining on fiber properties—A review. Carbohydr Polym 115:785–803

[60] Liu D, Yuan X, Bhattacharyya D (2012) The effects of cellulose nanowhiskers on electrospun poly (lactic acid) nanofibres. J Mater Sci 47:3159-3165

[61] Klemm D, Heublein B, Fink HP, Bohn A (2005) Cellulose: fascinating biopolymer and sustainable raw material. Angew Chem Int Ed 44:3358-93.

[62] Besbes I, Vilar MR, Boufi S (2011) Nanofibrillated cellulose from TEMPO-oxidized eucalyptus fibres: Effect of the carboxyl content. Carbohydr Polym 84:975-983

[63] Chan CH, Chia CH, Zakaria S, Ahmad I, Dufresne A (2013) Production and characterization of cellulose and nanocrystalline cellulose from kenaf core wood. BioResources 8:447-460

[64] Qing Y, Sabo R, Zhu JY, Agarwal U, Cai Z,Wu Y (2013) A comparative study of cellulose nanofibrils disintegrated via multiple processing approaches. Carbohydr Polym 97:226– 234

[65] Moxley GM, Zhu Z, Zhang YHP (2008) Efficient sugar release by the cellulose solvent based lignocellulose fractionation technology and enzymatic cellulose hydrolysis. J Agric Food Chem 56:7885-7890

[66] Ciolacu D, Ciolacu F, Popa VI (2011) Amorphous cellulose – structure and characterization. Cellul Chem Technol 45:13-21

[67] Siroky J, Blackburn JS, Bechtold T, Taylor J, White P (2010) Attenuated total reflectance Fourier-transform Infrared spectroscopy analysis of crystallinity changes in lyocell following continuous treatment with sodium hydroxide. Cellulose 17:103–115

[68] Iwamoto S, Abe K, Yano H (2008) The effect of hemicelluloses on wood pulp nanofibrillation and nanofiber network characteristics. Biomacromolecules 9:1022–1026

[69] Grüneberger F, Künniger T, Zimmermann T, Arnold M (2014) Nanofibrillated cellulose in wood coatings: mechanical properties of free composite films. J Mater Sci 49:6437-6448

[70] Arjmandi R, Hassan A, Eichhorn SJ, Haafiz MKM, Zakaria Z, Tanjung FA (2015) Enhanced ductility and tensile properties of hybrid montmorillonite/cellulose nanowhiskers reinforced polylactic acid nanocomposites. J Mater Sci 50:3118-3130

[71] Mark HM, Bilakes NM, Overberg CG, Mendes G (1986) Encyclopedia of Polymer Science and Engineering. John-Wiley & Sons, New York

[72] Avérous LJ (2004) Biodegradable multiphase systems based on plasticized starch: a review. Macromol Sci Part C Polym Rev 44:231–274

[73] Auras R, Harte B, Selke S (2004) An overview of polylactides as packaging materials. Macromol Biosci 4:835–864

(VERSÃO PRELIMINAR)

ARTIGO 2 ***Impact of tetraethyl orthosilicate content on the thermal and physical performance of aerogel structures obtained with cellulose nanofibrils***

Alessandra de Souza Fonseca[a,b], Joabel Raabe[c], Maria Alice Martins[d], José Manoel Marconcini[d], Suhara Panthapulakkal[e], Mohini Sain[e,f], Gustavo Henrique Denzin Tonoli[a]*

*a Department of Forest Science, Federal University of Lavras, Doutor Sylvio Menicucci Ave., 1001 - Kennedy, P.O. Box 3037, 37200-000, Lavras, Minas Gerais, Brazil.*Corresponding author: gustavotonoli@yahoo.com.br*
b CAPES Foundation, Ministry of Education of Brazil, Brasília, Brazil; adnax_florestal@hotmail.com
c Department of Forest Engineering, Faculty of Technology, University of Brasília - UnB, Campus Darcy Ribeiro, Asa Norte, P.O. Box 04357, 70910-900, Brasilia, DF, Brazil; joabeljr@hotmail.com
d National Nanotechnology Laboratory for Agrobusiness (LNNA), Embrapa Instrumentation (CNPDIA), Rua XV de Novembro 1452, Centro, 13560-970, São Carlos, SP, Brazil; maria-alice.martins@embrapa.br, marconcini@cnpdia.embrapa.br
e Centre for Biocomposites and Biomaterials Processing, Faculty of Forestry, University of Toronto, Toronto, Ontario M5S 3B3, Canada; s.panthapulakkal@utoronto.ca, m.sain@utoronto.ca
f King Abdulaziz University, Jeddah, KSA.

Artigo formatado de acordo com as normas para submissão do periódico Carbohydrate Polymers.

ABSTRACT

The study aimed to obtain silica particles to produce hybrid aerogels and investigate their morphology and physical properties. The silica+cellulose aerogels (SCA) were produced from microfibrillated cellulose suspension in the sol-gel process with six different concentrations of silica precursor (tetraethyl orthosilicate - TEOS), followed by freeze-drying. Morphological analysis was done from SCA images. Fourier transform infrared spectroscopy (FTIR) was used to evaluate the effectiveness of the surface modification. Thermal and moisture adsorption analysis were done to investigate their physical properties. Increasing TEOS concentration increased the thermal stability of the aerogels. SCA 0.50 and SCA1.00 show less moisture adsorbent hybrid aerogels when compared to their counterparts, besides maintaining a good porous structure and expanded morphology. The present work contributes with important information on surface-modified nanostructured cellulose for the development of new and engineered cellulose-based materials for diverse applications.

KEYWORDS: sol-gel process, hydrid composite, TEOS, thermogravimetry, moisture adsorption.

1. INTRODUCTION

Cellulose has been used as a polymeric matrix to produce hybrid materials for different applications in combination to silica - SiO_2 (Guzun et al., 2014; He, Chao, Gao, He & Li, 2014; Liu, Yu, Hu, Liu & Liu, 2013; Ashori, Sheykhnazari, Tabarsa, Shakeri & Golalipour, 2012; Cai et al., 2012; Hubbe, Rojas, Lucia & Sain, 2008). Silica also has been used for modification of cellulose fiber surface (Raabe et al., 2014; Xie; Yu & Shi, 2009; Pinto, Marques, Barros-Timmons, Trindade & Pascoal Neto, 2008).

Silica particles and nanoparticles can be synthetized on cellulose surface by the sol-gel method using water glass as silica source (Liu, Yu, Hu, Liu & Liu, 2013), coupling and crosslinking agents (Xie, Yu & Shi, 2009) and organosilanes as silica precursors such as polyethoxy disiloxane (Demilecamps, Beauger, Hildenbrand, Rigacci & Budtova, 2015), methyltrimethoxysilane (He, Chao, Gao, He & Li, 2014), tetramethyl orthosilicate (Maleki, Durães & Portugal, 2014) and tetraethyl ortosilicate – TEOS (Pinto, Marques, Barros-Timmons, Trindade & Pascoal Neto, 2008; Xie, Yu & Shi, 2009; Cai et al., 2012; Ashori, Sheykhnazari, Tabarsa, Shakeri & Golalipour, 2012; Guzun et al., 2014; Raabe et al. 2014) using different mechanisms such as (i) Stöber process or in situ synthesis in aqueous medium (Guzun et al., 2014). The Stöber process is well known to produce silica particles using excess of water and some alcohol as a solvent and ammonium hydroxide as catalyzer in a alkaline process; and (ii) in situ synthesis in alcoholic medium (Pinto, Marques, Barros-Timmons, Trindade & Pascoal Neto, 2008; Raabe et al., 2014) in both cases with ammonium hydroxide acting as catalyzer. Tetraethyl orthosilicate (TEOS) is a metal alkoxide commonly used as nanostructured silica or nanostructured silica dioxide (SiO_2) precursor to introduce silica nanoparticles on the surface of different organic-polymers (Yano, Iwata & Kurita, 1998) such as cellulosic-based fibers (Raabe et al., 2014; Ashori, Sheykhnazari, Tabarsa, Shakeri & Golalipour, 2012), nanofibers (Shi, Lu, Guo, Zhang & Cao, 2013; Xie, Yu & Shi, 2009) and bacterial-cellulose (Guzun et al., 2014; Ashori, Sheykhnazari, Tabarsa, Shakeri & Golalipour, 2012).

Immersion, impregnation and impregnation using molecular diffusion and forced flow induced by pressure gradient are some examples of mechanisms to grown silica particles and nanoparticles on organic surfaces (Pinto, Marques, Barros-Timmons, Trindade & Pascoal Neto, 2008; Ashori, Sheykhnazari, Tabarsa, Shakeri & Golalipour, 2012; Cai et al., 2012; Liu, Yu, Hu, Liu & Liu,

2013; Guzun et al., 2014; Raabe et al., 2014; Maleki, Durães & Portugal, 2014; Demilecamps, Beauger, Hildenbrand, Rigacci & Budtova, 2015). Acetic acid can work well as catalyzer to grown silica particles (De, Karmakar & Ganguli, 2000; Ashori, Sheykhnazari, Tabarsa,\ Shakeri & Golalipour, 2012) under aqueous medium using TEOS as silica precursor.

Typical gel-synthesis procedures have been used to produce bulk gel, films, fibers and powders (Brinker & Scherer, 1990). The sol-gel method was already used to produce hybrid nanocomposite mainly the cellulose-silica aerogels, a strongly reinforced and light hybrid aerogel with high ductility characteristic of the cellulose aerogel and the lowest thermal properties related to silica-aerogels. The synthesized cellulose-silica composite can be useful as thermal insulator material with high mechanical strength and stability, with the ability to form sheets, fibers or beads (Maleki, Durães & Portugal, 2014) as well as like-foam porous materials or aerogels. Previous studies had successfully made cellulose-silica aerogels focusing their hydrophobic behavior, superficial area also their thermal insulation and mechanical properties (Demilecamps, Beauger, Hildenbrand, Rigacci & Budtova, 2015; He, Chao, Gao, He & Li, 2014; Liu, Yu, Hu, Liu & Liu, 2013; Cai et al., 2012).

Therefore, the present study aimed to evaluate the impact of the TEOS content on the thermal properties and physical performance of silica+cellulose aerogels (SCA).

2. EXPERIMENTAL

2.1. Obtention of the nanofibrils

Cellulose nanofibrils were obtained from a mix of softwood and hardwood commercial bleached pulp fibers donated by Domtar Corporation of Canada, using mechanical defibrillation in a grinder (Masuko Corp., Japan) at 1500 rpm, with 2.4% of pulp concentration and around 10 passages through the

defibrillator, similar to procedures described in previous works (Fonseca et al., 2016; Bufalino et al., 2015; Guimarães Jr., Botaro, Novack, Teixeira & Tonoli, 2015a).

2.2. Production of the aerogels

Suspensions with around 0.5 g (dry basis) of cellulose nanofibrils (1% of solids) and 1 mL of acetic acid 0.1 M were used for preparation of the aerogels. The silica precursor Tetraethyl orthosilicate (TEOS) with six different concentrations from 0.00 to 3.00% in relation to the total mass of water (200 g), and in combination with the cellulose nanofibrils lead to the silica+cellulose aerogels (SCA) with different TEOS contents. The procedure adapted from Ashori, Sheykhnazari, Tabarsa, Shakeri & Golalipour (2012) using acetic acid as catalyzer is detailed in Figure 1. The frozen samples were freeze-dried. The aerogels with no silica precursor were called control aerogel (CA).

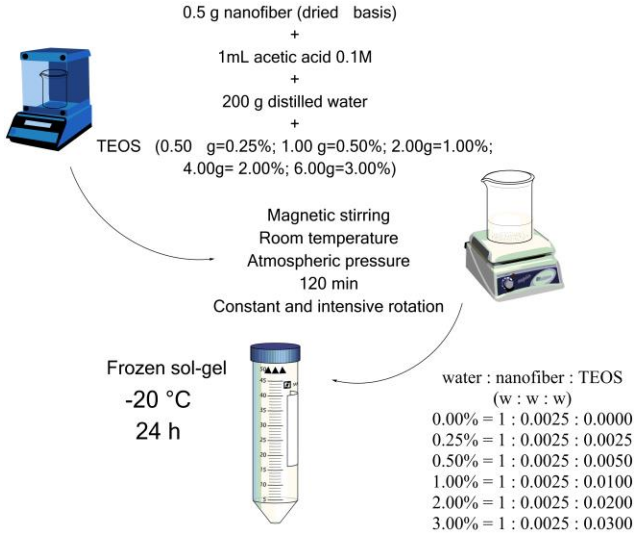

Figure 1. Illustrated description of the procedure and the proportions applied to produce the control aerogel (CA) and the cellulose+silica aerogels (SCA).

The TEOS ratios are summarized on Table 1 Water and nanofibers proportions had a fixed amount of 1 and 0.25, respectively.

Table 1. Scheme of the chemical proportions used to prepare the aerogels.

Aerogels	TEOS (%)	Proportion of TEOS (weight)*	Mass TEOS (g)**
Control (CA)	-	0	0
SCA0.25	0.25%	0.0025	0.5
SCA0.50	0.50%	0.0050	1.0
SCA1.00	1.00%	0.0100	2.0
SCA2.00	2.00%	0.0200	4.0
SCA.3.00	3.00%	0.0300	6.0

* Proportion of the weight of the TEOS related to total water content used to prepare the SCA.
** Mass of the TEOS used to prepare the SCA, in grams.

2.3 Characterization of the aerogels

2.3.1. Fourier transform infrared spectroscopy (FTIR)

Fourier transform infrared spectroscopy (FTIR) was performed to evaluate the effectiveness of the silica deposition. FTIR spectrum of the sample obtained was examined in a KBr pellet in the proportion of 1:100 (w:w) on a Bruker Tensor 27 FTIR spectrometer (Bruker Optics Inc., USA) between 4000 and 400 cm-1 region.

2.3.2. Light microscopy (LM)

Microscopic images using light microscopy (LM) were captured in the Nikon digital sight DS-Ri1 camera coupled to a Nikon SMZ1500 (Nikon, Japan)

microscope stereoscope with the NIS-Elements D 3.21.00 (Nikon, Japan) imaging software.

2.3.3. Environmental scanning electron microscopy (SEM/STEM)

High-resolution images of the microstructure of the CA and SCA were obtained in an scanning electron microscope (SEM) microscope LEO Evo40 XVP (Carl Zeiss AG, Germany) and an environmental scanning electron microscope (SEM/STEM) microscope FEI QUANTA FEG 250 ESEM (FEI Company, USA). Samples were carbon coated before SEM/STEM analyses and gold coated before SEM analyses. Aerogel samples were fractured in liquid nitrogen, and then covered with a thin carbon layer when using the energy-dispersive X-ray spectrometry (EDX) system for identification of silicon (Si) atoms.

2.3.4. Transmission electron microscopy (TEM)

Aerogel samples were fixed in epoxy resin and thin slices (lower than 100 nm) were obtained in an ultramicrotome. A Hitachi S-5200 transmission electron microscope (TEM) equipped with an Oxford Inca EDX system was used in order to localize the presence of silicon (Si) and oxygen (O) atoms on the surface of the samples.

2.3.5. Thermogravimetry

CA and SCA were subject to thermogravimetric analysis (TGA) in a TGA-Q500 (TA Instruments, USA). Samples with around 4 mg were heated in a Pt crucible from 25 to 600°C in synthetic air flowing at 60 mL.min-1, and heating rate of 10°C.min-1.

2.3.6. Moisture adsorption

Specimens with around 2.0 cm × 1.0 cm × 0.5 cm were dried for 24 h at 103 ± 2°C, weighted, and kept in a hermetically sealed container with 97 ± 2% of relative humidity (RH) and 20 ± 2°C, using a saturated potassium sulfate solution, as prescribed by the ASTM E104 (ASTM, 2012) standard. The moisture adsorbed by the samples was determined measuring the mass of the CA and SCA at successive intervals until they reached a constant weight. The amount of moisture adsorbed (MA) by the samples was calculated using Eq (1):

$$MA_{(\%)} = \left[\frac{(M_t - M_0)}{M_0}\right] \times 100 \quad (1)$$

Where, M0 and Mt are the initial mass of the sample (prior to exposure to moisture) and the sample mass after t hours of exposure to moisture (97 ± 2 % RH), respectively. Each data point represents an average of three samples for each CA and SCA.

3. RESULTS AND DISCUSSION

3.1 Structure of the aerogels, FTIR results and silica nanostructures

High mechanical defibrillation applied to fibers through the commercial defibrillator (Masuko Corp.) was effective in disintegrating the pulp fibers into individual micro/nanofibrils in some extent (Tonoli et al., 2016). The final morphology of the SCA was influenced by the TEOS addition. In absence of TEOS, the silica precursor, pure cellulose aerogel was not able to be formed (Figure 2a). It was found some internal voids (Ø=19.30±15.01 μm) as a result of an inefficient formation of the nanostructured web of nanofibrils, causing the collapse of the network and nanofibrils agglomeration during the freeze-drying process. The hybrid aerogel (SCA) with the most expanded volume was

obtained with SCA 0.25 (Figure 2b) followed by SCA 0.50 (Figure 2c) and SCA 1.00.

The FTIR spectra are also presented in Figure 2 (bellow). The peak at 1160 cm-1 is correspondent to C-O-C bonds (Ashori, Sheykhnazari, Tabarsa, Shakeri & Golalipour, 2012) in the covalent chemical connections between cellulose molecules. The peaks related to Si-bonding functions are in the regions A and B shown in the detail of Figure 2. Region A presents peaks at 1250-1150 cm-1 correspondents to Si-O-Si and Si-O bonds (Nagai & Hashimoto, 2001) with the exception for TEOS concentration of 0.25%. Region B is related to Si-O-Si bonds at 1120-1080 cm-1 (Zhou, Cui, Zhang, Zhang & Yin, 2008; Li, Chen & Zhang, 2008; Hsieh, Wu & Yang, 2008; Yin, Wang & Wang, 2012), Si-O-C at 1100-1048 cm-1 (Yeh, Chen & Huang, 2007; Liu, Yu, Hu, Liu & Liu, 2013) and Si-O at 1090 cm-1 (Guzun et al., 2014). Region B also presents peaks related to Si-O-Si bonds at 1150-1050 cm-1 (Nagai & Hashimoto, 2001) for TEOS concentrations lower than 1%. Changes in the spectra of the SCA can also be found at 450 cm-1 and 800 cm-1 (Hsieh, Wu & Yang, 2008; Yin, Wang & Wang, 2012; Liu, Yu, Hu, Liu & Liu, 2013) as well assigned to Si-O-Si bonds.

Ashori, Sheykhnazari, Tabarsa, Shakeri & Golalipour (2012) assigned the peak at 460 cm-1 as correspondent to Si-O-Si bending in bacterial cellulose+silica composites. The assignment to Si-O-Si symmetric stretching was identified by Ashori, Sheykhnazari, Tabarsa, Shakeri & Golalipour (2012) at 804 cm-1 as chemical structure of pure silica gel. De, Karmakar & Ganguli (2000) referee Si-O-Si symmetric stretching to formations of Si-O4 network of SiO_2 at 805 cm-1. According to those authors, the increase of the peak at 805 cm-1 is a result of the condensation of Si-O-Si monomers, and they relate Si-OH silanol groups formation to the 950 cm-1 band, as also observed in region C for all SCA samples. The water molecule peak at 1630 cm-1 (Hsieh, Wu & Yang, 2008) has no decreasing when the concentration of silica precursor increased, despite

TEOS being associated with hydrophobizing process. It may indicate that no chemical reaction was happened to the cellulose and the silica source as presented by Liu, Yu, Hu, Liu & Liu (2013) and Demilecamps, Beauger, Hildenbrand, Rigacci & Budtova (2015).

Higher bands at around 3460cm-1 may be related to moisture and silanol stretching, while the band at ~3300 cm-1 correspond to OH stretching (Ashori, Sheykhnazari, Tabarsa, Shakeri & Golalipour, 2012) that decrease with the increase of TEOS concentration (with the exception of 0.50% and 1.00% TEOS). It can be the consequence of the direct increase of silanol groups when the TEOS concentration increases to above 1.00%, as well as by the increase of OH bonds due to hydrolysis of TEOS and condensation of hydroxylated monomers in the cellulose free radicals.

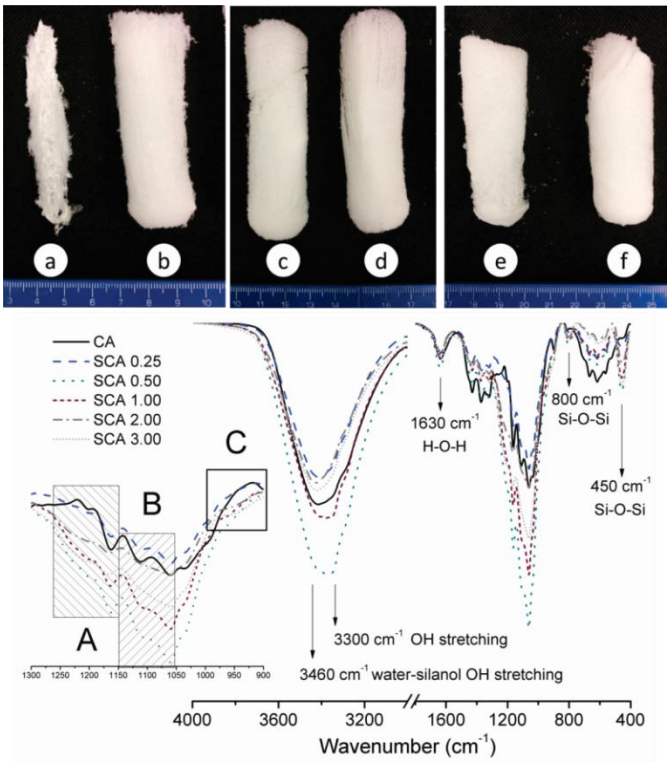

Figure 2. Above: general view of the different aerogels: - (a) with no TEOS (control aerogel- CA); (b) with 0.25% TEOS (SCA 0.25); (c) with 0.50% TEOS (SCA 0.50); (d) with 1.00% TEOS (SCA 1.00); (e) with 2.00% TEOS (SCA 2.00); (f) with 3.00% TEOS (SCA 3.00). Scale in cm. Bellow: FTIR spectra of the different aerogel treatments with tree different regions A, B and C that confirm the assignments for Si-bonds.

The Si-O-Si bonds are called siloxane bridges as a result of hydrolysis and condensation process of the silica precursor molecules, which in the present case is TEOS, a kind of silicon alkoxide Si(OCH2CH3)4 with common chemical formula of Si(OR), tetrahedral structure and non-polar molecules, considered the first pure silica sols produced from tetraethoxysilane (Lacourse, 1988) and often referred as tetraethyl orthosilicate (Brinker & Scherer, 1990). Silicate gel is most often synthesized by hydrolyzing monomeric tetra functional alkoxide

precursors employing acid or base as a catalyst. At the functional group level, three reactions are generally used to describe the sol-gel process (Brinker & Scherer, 1990): hydrolysis-esterification, alcohol condensation-alcoholysis and water condensation-hydrolysis.

In the theoretical hydrolysis of the siloxane bond under neutral and acid conditions, the factors more important to reduce the energy of reaction barrier are the protonation of oxygen siloxane (acid catalysis) accomplished by a basic assistance to nucleophile, removing the proton from nucleophile. The enhanced reactivity of the terminal siloxane bond in siloxanols is connected partly with the ability of the Si-OH group to participate in hydrogen bond structures facilitating the intramolecular proton transfer to the siloxane oxygen (Cypryk & Apeloig, 2002). Added to it, Marques, Trindade & Pascoal Neto (2006) affirm that the surface of cellulose fibers can satisfactory act as hydrophilic substrat for nucleation and to grow inorganic particles in excess of water.

In the present study, probably the Si-O-Si monomers may be produced via water condensation because of the excess of water in the ternary system water:acid:TEOS. Then, it forms rings that are basic frameworks to discrete colloidal particles formation, commonly observed in aqueous systems by the maximization of the number of Si-O-Si bonds and minimization the number of terminal hydroxyl groups through internal condensation (Iler, 1979), as showed in Figure 3c and Figure 3f. Aqueous silicate polymerization and smooth colloidal particles should occur when the sol-gel system occur under sufficient high water:Si ratio (Brinker & Scherer, 1990), what agree to the statement above and to the showed in Figure 3c.

Coalesced silica particles present similar structure to the silica structures obtained in the present study (Figure 3), such as close rings (Figure 3e, 3f) or spherical structures (Figure 3a, 3b, 3c). It may be the result of particle-particle interactions after collision and local condensations reactions, forming a neck

between particles like has been cited by Lacourse (1988) using alkoxide as silica precursor at somewhat lower pH between 4 and 8. According to Iler (1979), the silica sols has tendency to form closed rings and spherical particles rather than crosslinked chains. More detailed information about the sol-gel chemistry and schematic representation of the silica structures in silica aerogels are presented in Maleki, Durães & Portugal (2014). Arenas et al. (2007) present similar TEM images to those obtained in the present study (Figure 3f and Figure 3i). Those authors obtained silica xerogels by sol-gel method with water:acid:TEOS system with 4:4:1 molar ratio under room temperature.

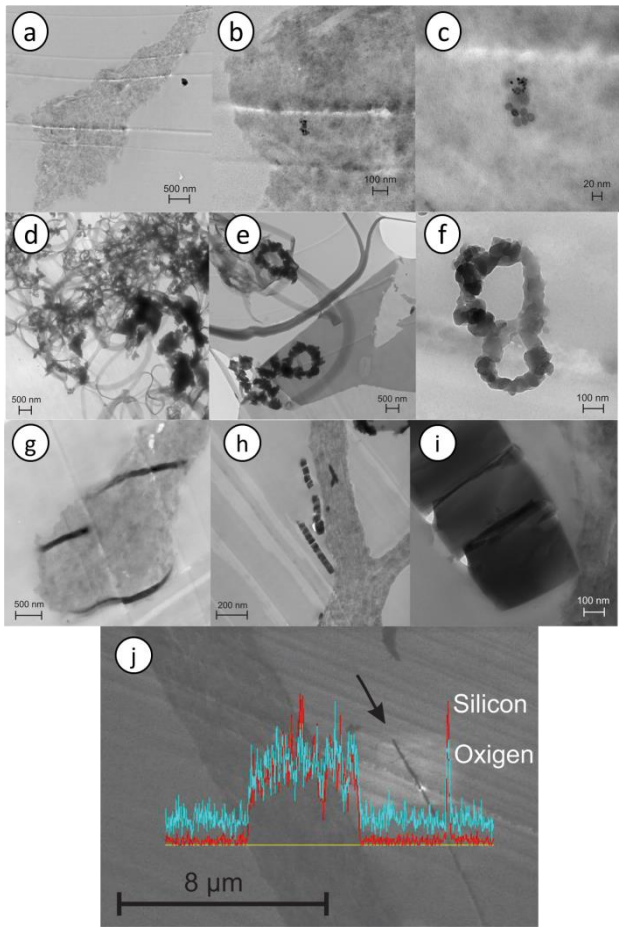

Figure 3. Transmission electron microscope (TEM) images of epoxy-fixed samples of the SCA 1.00 aerogel: (a) dark agglomerate beside cellulose nanofibrils; (b) dark agglomeration into the nano structured aerogel; (c) detail of the silica dark agglomerates in the nano structured aerogel, showing well-defined spherical particles of different sizes; (d) cellulose network with entanglements of silica micro/nanostructures; (e) detail of the silica structures entangled into the network of cellulose nanofibrils; (f) detail of the silica nano structures; (g,h) dark filaments are longitudinal cross-section of the silica nano structures into and out of the network of cellulose nanofibrils; (i) detail of large dark structures probably related to silica; (j) micrograph with energy-dispersive X-ray spectrometry confirming the presence of silica in the nano structured aerogel.

Water and TEOS are immiscible, and it is why alcohol is generally added as a co-solvent (Lacourse, 1988). Brinker & Scherer (1990) also explain that the alcohol produced as the by-product of the hydrolysis reaction is enough to homogenize the system, working as a solvent and as participant in the reverse reactions of esterification or alcoholysis. As also observed in Maleki, Durães & Portugal (2014), the primary and secondary silica particles were shown in Figure 3c, presenting smaller particles (~5 nm).

The kinetics of the sol-gel reactions is slow at room temperature and often requires several days to complete reaction. For this reason, in the present work, an acid catalyst was added to the system. Specially to catalyze the hydrolysis and condensation of silicon that are slower than observed in transition metals system due to silicon lower electropositivity, which provide less susceptibility to nucleophilic attack (Brinker & Scherer, 1990). The amount and type of catalyst play a key-role in the microstructural, physical and optical properties of the final hybrid composite. Any protic acid can be an acid catalyst (Abdul Khalil et al., 2014). The acetic acid, one of the polar protic solvents similar to water and ethanol, is a very suitable addition in silicon alkoxide solutions for the synthesis of spherical silica microspheres with a large range of size variation (De, Karmakar & Ganguli, 2000) as observed in Figures 6a-c. Acetic acid attacks TEOS readily, specially when in absence of water, whereas in the presence of water, the hydrolysis reaction can be faster with acetic acid (Dood, Berkhout, Kats, Polman & Blaaderen, 2002).

Silica particles produced by Raabe et al. (2014) and Pinto, Marques, Barros-Timmons, Trindade & Pascoal Neto (2008) also using TEOS as silica precursor and base catalyst, presented diameters similar to the present study (10.9±6.4 nm), corroborating the statements of Lacourse (1988) and Iler (1979) for synthesis of silica particles at lower pH (4-8) using acid sols.

The EDX results were summarized in Figure 3j and corroborate the FTIR results, showing the presence of silica coalesced (Figures 3g, 3h and 3i) into the nano structured aerogels (Figures 3h, 3i). The EDX line map through the cross section of the SCA 1.00 shows clearly the presence of silicon in the aerogel structure. Oxygen:silicon ratio can be estimated by the proportions: of the peaks, whose higher peaks of silicon are followed by relatively lower peaks of oxygen (Figure 3j), as supported by the different assignments for Si-O-Si in the FTIR analysis (Figure 2).

Brinker (1988) state that condensation may result in structures ranging from molecular networks to colloidal particles, when reverse reactions occur in the sol-gel systems. Then, probably reverse reactions occurred in the present sol-gel system, since all acid catalyzed process led to polysiloxanes, whose the reactions of the SiO bond cleavage by acid or water, as well as their reverse reactions, significantly affect the polycondensation course, causing depolymerization and resulting in low molecular weight products (Cypryk & Apeloig, 2002).

As found by Wilczek & Chojnowski (1983), the equilibrium of condensation/siloxane bond cleavage is very sensitive to the proton donor-acceptor properties of the medium as well as to the presence of water or other sources that form strong hydrogen bonds. According to that, the excess of water from the ternary system in this study is probably causing unbalance of the condensation/depolymerization reactions in the sol-gel process, and increasing depolymerization reactions. Because water is produced as by-product of the condensation reaction, the water:Si ratio value of 2 is theoretically sufficient to complete hydrolysis and condensation to anhydrous silica. However, even in excess of water, with water:Si ratios values higher than 2, the reaction does not go to completion. Instead, a spectrum of intermediate species is generated (Brinker & Scherer, 1990). According to these former authors, the structure of

sol-gel silicate evolves sequentially as product of successive hydrolysis and condensation reactions.

Ashori, Sheykhnazari, Tabarsa, Shakeri & Golalipour (2012) stated that silanol condenses forming silica, which reacts by hydrogen bonds or condensation reactions with cellulose and after 48 h of immersion they found large amount of silica nanoparticles confined in the voids in the cellulose network. Homogeneous spherical silica can be obtained using acetic acid at lower concentration ratio to TEOS (Elsagh, 2012). Higher acetic acid ratios resulted in high rate of agglomerations and particles with lower diameter, while increasing TEOS ratio increases the diameter of the silica particles.

The results agree with the statements of Brinker & Scherer (1990) about variation in the synthesis conditions of silica in the sol-gel process causing modifications in the structure and properties of the polysilicate products. According to De, Karmakar & Ganguli (2000), controlling water: acid: TEOS molar ratios has been showed suitable to obtain spherical monodisperse and dense silica powders, and they suggest the best proportion of 1:4:4. Brinker & Scherer (1990) suggest that intermediate values of pH (3-8) represent conditions in which a spectrum of transitional structures might be expected, with the dissolution and condensation rates increasing smoothly with increase of pH, whereas the hydrolysis rate goes through a minimum at a neutral pH. Also, increased water: Si ratios increase the dissolution and hydrolysis rate at any particular pH value. However, also in the range of pH 7-8, the dissolution and hydrolysis rates increased. For instance, the sol-gel system in the present study occurred under the water: TEOS ratio range from 400 (TEOS 0.25%=0.5g) to 33 (TEOS 3%=6.0g).

Larger-length scales silicate particles formed at intermediate pH (3-8) can be rapidly aggregated by reaction-limited colloid aggregation (RLCA) kinetic growth model as presented in Figure 3d-e. Cluster-cluster growth or reduced

functionality results in weakly branched mass or fractal surfaces (Brinker & Scherer, 1990). According to De, Karmakar & Ganguli (2000), the generation of silica particles occurs by the transient formation of large silicate polymeric units that grow to dense micro/nanometric spherical silica particles at the end of the reaction. Then, lower time reaction (2 h) as used in the present work probably is too short to grow large silica particles, but was effective to influence the morphology of the aerogels.

3.2 Micro/nanostructure of the aerogel

Figure 4 shows the microstructure of the different aerogels by light microscopy (LM). Aerogels without TEOS presented agglomerated nanofibrils of cellulose (as previously of observed in Figure 2a), with limited micro/nanostructured porosity between the network of nanofibrils (Figures 4a-c). The presence of TEOS influences the microstructure of the aerogels, leading to a like-foam appearance (Figures 2b-f) and maintaining the high degree of fibrillation of the cellulose structure, probably as consequence of the organic-inorganic interactions promoted by the sol-gel process (Figures 4d-r).

SCA 0.25 and SCA 0.50 showed like-foam porous morphology with homogeneous distribution of the micro/nanostructured voids (Figures 4d-i). High TEOS concentration (from 1.00% to 3.00%) led also to the micro/nanostructured porosity, but apparently presenting voids with larger sizes (Figures 4j-r). He, Chao, Gao, He & Li (2014) and Liu, Yu, Hu, Liu & Liu (2013) found similar microstructure for freeze-dried hydrogels from regenerated cellulose and silica precursor in several concentrations.

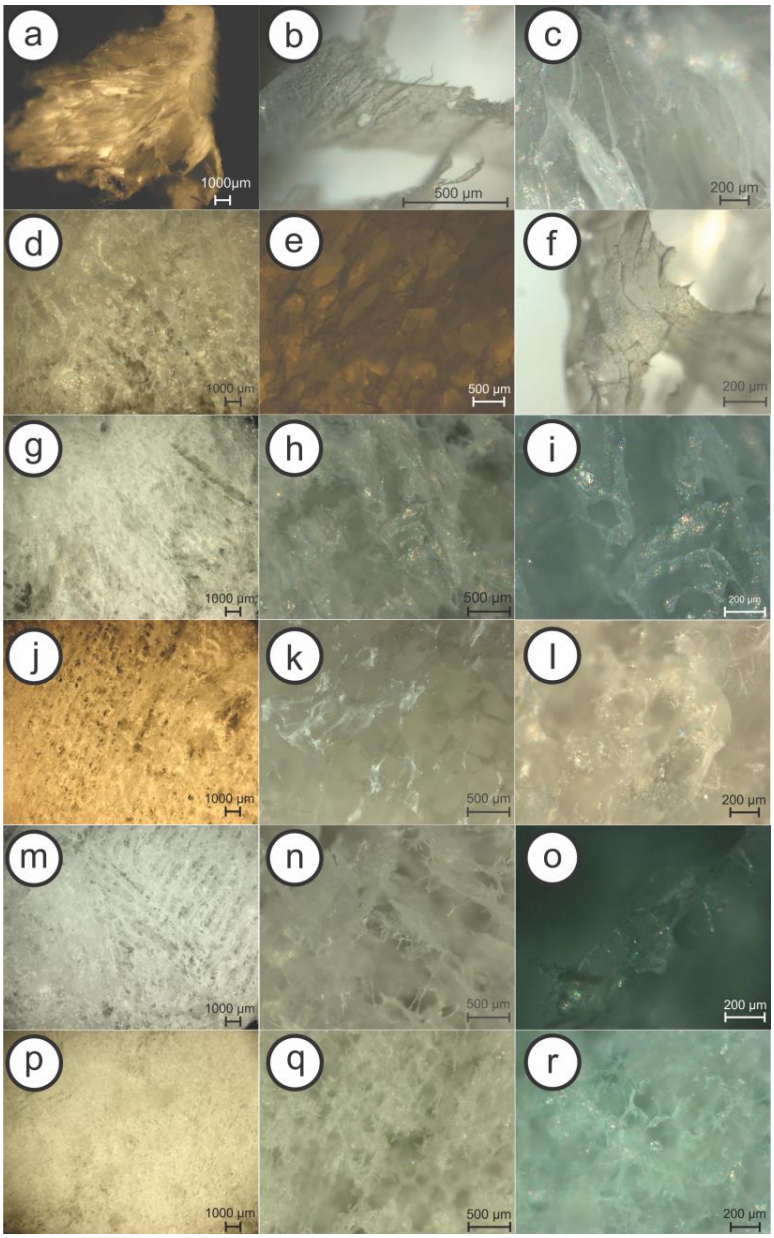

Figure 4. Light microscope images of the aerogels with different concentrations of TEOS under stereoscope: (a-c) with no TEOS (CA); (d-f) with 0.25% TEOS (SCA 0.25); (g-i) with 0.50% TEOS (SCA 0.50); (j-l) with 1.00% TEOS (SCA 1.00); (m-o) with 2.00% TEOS (SCA 2.00); and (p-r) with 3.00% TEOS (SCA 3.00).

Micro/nanostructure of the aerogels can also be seen in Figure 5 through scanning electron microscopy (SEM). The aerogel obtained without TEOS presents more agglomerated microstructures (Figures 5a-c) and probably with large possibilities for bonding between hydroxyl groups of the nanofibril network. The freeze-drying of the cellulose nanofibrils without TEOS led to tubular structures (Figure 5a, dashed rectangle) as a result of the agglomeration of the cellulose nanofibrils in the absence of the silica precursor, while in the aerogels obtained with TEOS, the silica particles formed seems to act prejudicing those continued bonds during freeze-drying.

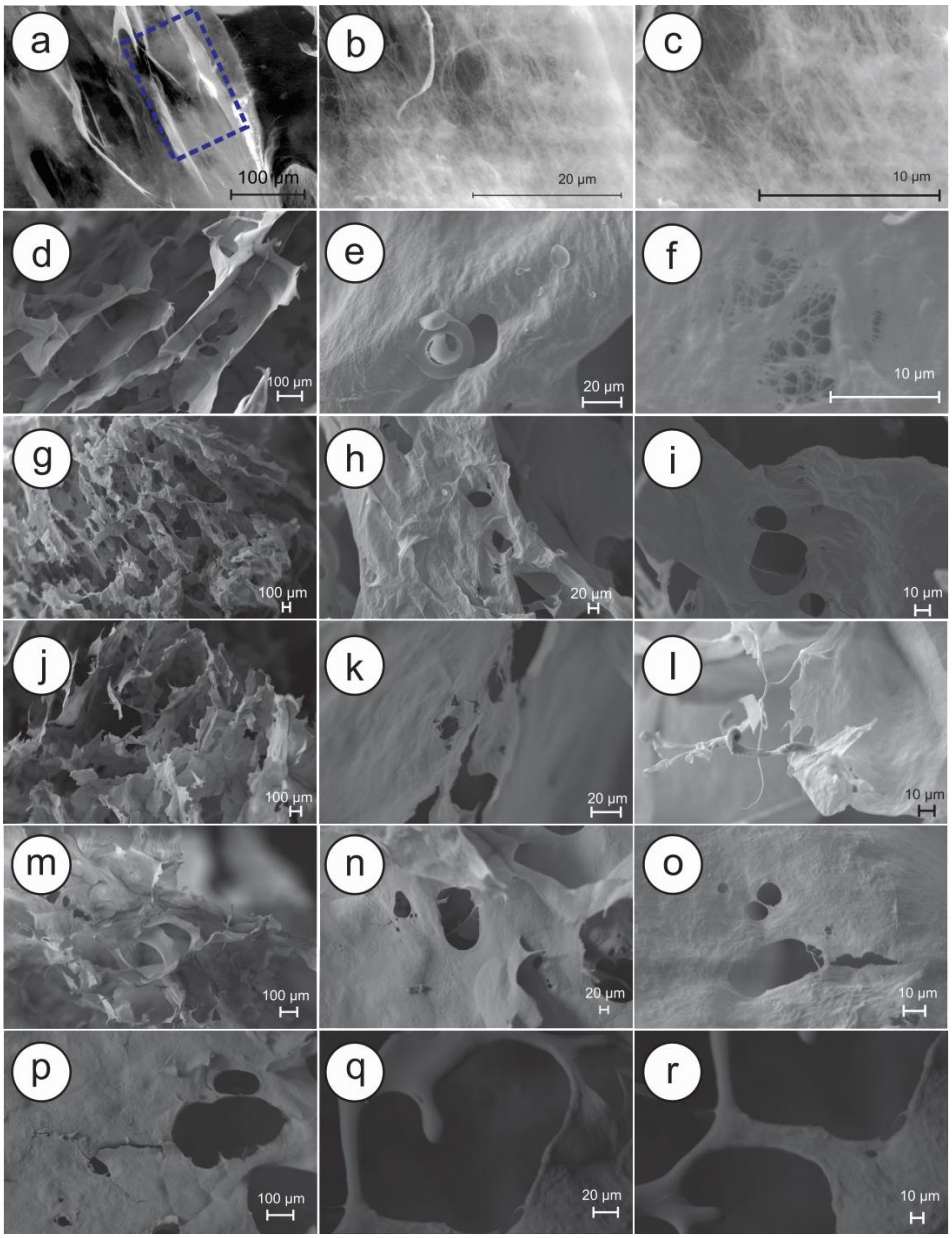

Figure 5. Scanning electron microscopy (SEM) images of the aerogels made from freeze-dried nanofibrils: (a-c) with no TEOS (CA - control); (d-e) with 0.25% TEOS (SCA 0.25); (g-i) with 0.50% TEOS (SCA 0.50); (j-l) with 1.00% TEOS (SCA 1.00); (m-o) with 2.00% TEOS (SCA 2.00); and (p-r) with 3.00% TEOS (SCA 3.00).

Figures 5d-f show the wall structures of the aerogel SCA 0.25 with voids diameter in the range from 140 nm to 150 µm (average 4.91±16.71 µm); SCA 0.50 (Figure 5g-i) has voids diameter ranging from 190 nm to 77.89 µm (average 5.81 ± 13.41µm); For SCA 1.00 (Figure 5j-l) the voids diameter range from 350 nm to 252.16 µm (average 25.28 ± 45.90 µm); the voids diameter range from 260 nm to 150.70 µm (average 19.40 ± 34.79) for SCA 2.00 (Figure 5m-o) and a range from 1.30 µm to 280.11 µm (average 41.12 ± 58.72 µm) for SCA 3.00 (Figure 5p-r).

Some spherical structures were observed probably as consequence of agglomeration of the silica structures (Figure 5e). Increasing the TEOS concentration, it was observed smooth structures in the aerogels (Figure 5g-i), which is probably due to formation of a network of Si–O–H. . .O–C hydrogen bonds once hydrolysed silanes (silanol groups) adsorb on the cellulose nanofibrils surface (Castellano et al., 2004). Aerogels obtained with 2.00% of TEOS (SCA 2.00) showed cells with reduced dimensions (Figure 5m-o) compared to aerogels with lower TEOS concentration. As previously discussed, the Si-O-Si symmetric stretching was identified by Ashori, Sheykhnazari, Tabarsa, Shakeri & Golalipour (2012) at 804 cm-1 as the chemical structure of pure silica gel and De, Karmakar & Ganguli (2000) stated that Si-O-Si symmetric stretching to formations of Si-O4 network of SiO_2 at 805 cm-1. According to them, the increase of the peak at 805 cm-1 is a result of the condensation of Si-O-Si monomers that can generate spherical particles.

3.3 Themogravimetric analysis of the aerogel

Three characteristic regions of decomposition of the cellulosic materials was observed, as presented by Raabe et al. (2014): (1) from room temperature to around 150°C, as consequence of volatiles and dehydration (Yildiz & Gumuskaya, 2007); (2) around 350°C, related to decomposition of cellulose

(Órfão, Antunes & Figueiredo, 1999), where a large amount of weight loss occurs; and near to 500°C, as consequence of the oxidation reactions of the remaining organic materials (Corradini, Imam, Agnalli & Mattoso, 2009) as observed in Figure 6.

In general, higher contents of TEOS led to higher Tonset values and higher residual mass (Figure 6a), as a clue that silica has improved the thermal stability of the aerogels (Raabe et al., 2014). The highest mass loss occurs at around 325°C (Figure 6b) for all conditions. DTG curves (Figure 6c) also show that decomposition of the aerogels occurred in different stages, indicating the presence of different components that decompose at different temperatures. The dominant thermogravimetric (DTG) peak observed in the control sample occurred at around 325-330°C. This is in the temperature range corresponding to the weight loss of hemicelluloses (225-325°C), residual lignin (250-500°C) and cellulose (305-375°C) as reported by Prins et al. (2006). The stability of the aerogels at higher temperatures (350oC to 500oC) was also greatly improved due to the presence of silica. The thermal properties of the aerogels are an important parameter for identifying the different applications for these nanostructured cellulose materials.

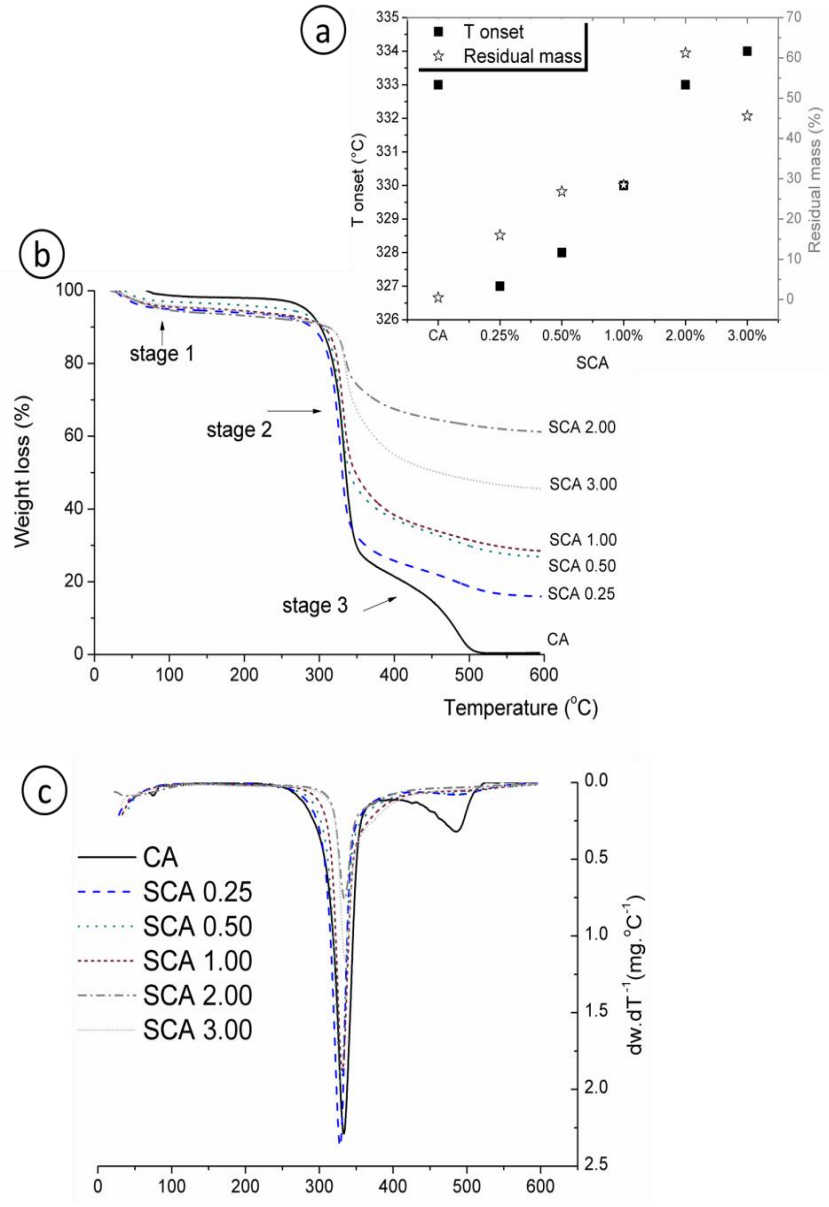

Figure 6. Thermogravimetry results: (a) onset decomposition temperature (Tonset) and residual mass; (b) TG curves; and (c) DTG curves.

For the control sample (CA), the TGA curves have been observed three distinct weight losses (Fig. 6 b) similar results presented by Rani, Rudhziah, Ahmad & Mohamed (2014). The first distinct weight loss is about 2% in the temperature range of 70-150°C, related to moisture in the sample. Similar results are found by Raabe et al. (2014). The SCA showed a weight loss range from 4.0% (SCA 3.00) to 7.0% (SCA 0.25). The second weigth loss of the control – CA (~69%) was observed in the range of 250-350°C and represents the thermal decomposition of the polysaccharide (Biswal & Singh, 2009). At this temperature range the SCA showed a weight loss range from 33.0% (SCA 2.00) to 77.0% (SCA 0.25). The thermal degradation of the remaining materials (the third weight loss) at temperature range of 360-550°C for the control (CA) is about 25%. At temperature higher than 550°C, only carbon residues and inorganic component can be found. All the SCA have not showed the third weight loss region as presented in Figure 6 b-c. It may caused by the presence of the silica called residual mass (Fig. 6 a) that has been showed values in the range from 16% (SCA 0.25) to 60% (SCA 2.00).

3.4 Moisture adsorption of the aerogels

Moisture adsorption in function of time is presented in Figure 7. Even after ~450 h exposition to the high humidity environment (98%), there was no stabilization of the aerogels mass, for all conditions. All the aerogels show moisture adsorption lower than 12%. Statistical analysis shows SCA 0.50 and SCA 1.00 with lower adsorbed moisture values agreeing to FTIR spectra that shows intense shoulders on regions A and B in the Figure 2, related to presence of different types of silica bonds. The increased moisture adsorption for SCA 2.00 could be a consequence of hydrogen bonds of water vapor with the unreacted silanol groups as corroborated by the FTIR analysis at 950 cm-1 (Figure 2, region C) and elsewhere (De, Karmakar & Ganguli, 2000). The aerogels

synthesized by the lower and higher concentrations of TEOS (SCA 0.25 and SCA 3.00) are statically equal to control samples may as a consequence of inefficient reactions by the lack and excess of precursor mass compare to cellulose nanofibrils mass, respectively.

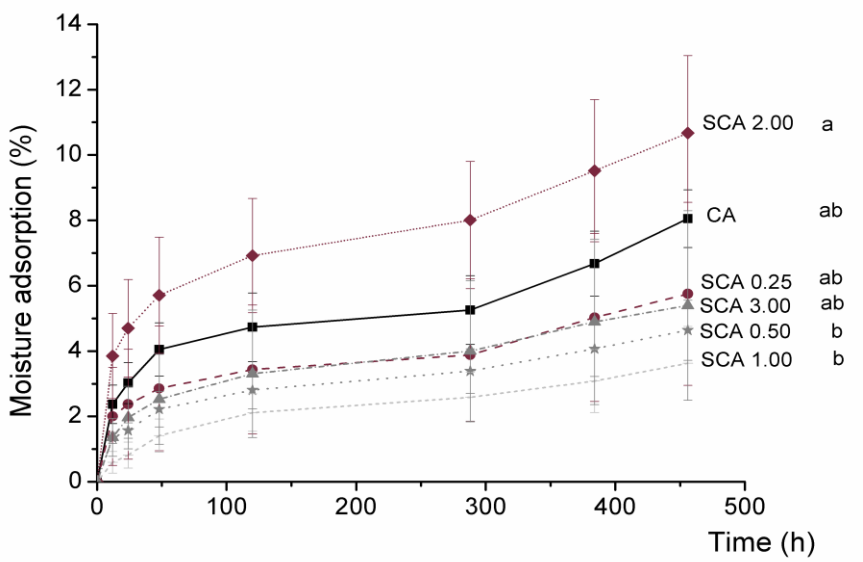

Figure 7. Average and standard deviation values of moisture adsorption in function of time, for aerogels with different contents of TEOS. Means with different letters are significantly different by Tukey test at 95% of probability.

4. CONCLUSIONS

Cellulose nanofibrils were successfully obtained through mechanical defibrillation of cellulose pulp. The silica precursor (TEOS) favored the formation of a micro/nanostructured aerogels. Silica structures appears as agglomerates of micro/nanoparticles or a network of silanol groups. Cellulose+silica aerogels were produced and 0.25% of TEOS (SCA 0.25) was found to provide an improved network of cellulose nanofibrils, leading to a homogeneous like-foam porous structure. Increasing TEOS concentration

increased the thermal stability of the aerogels. In general, the presence of TEOS decreased moisture adsorption, mainly under concentrations of 0.50 and 1.00% studied. The present work contributes with information about cellulose nanofibrils, and further development of this approach could improve the performance of these aerogels for a myriad of applications, and for development of new and engineered cellulose+silica hybrids.

5. ACKNOWLEDGMENTS

The authors acknowledge the financial support of the Brazilian Government through Coordenação de Aperfeiçoamento de Pessoal de Nível Superior – CAPES (CAPES-Embrapa Edital 01/2011, and scholarship PDSE/CAPES, process n. 99999.012163/2013-09), Conselho Nacional de Desenvolvimento Científico e Tecnológico (CNPq), Fundação de Amparo à Pesquisa do Estado de Minas Gerais (FAPEMIG), Rede Brasileira de Compósitos e Nanocompósitos Lignocelulósicos (RELIGAR) and Laboratory of Electron Microscopy and Ultra-Structural Analysis (LME) in the Department of Plant Pathology at Federal University of Lavras (UFLA), Brazil. Thanks also to the Centre for Biocomposite and Biomaterial Processing - CBBP/University of Toronto, Canada.

6. REFERENCES

Abdul Khalil, H.P.S., Davoudpour, Y., Islam, Md.N., Mustapha, A., Sudesh, K., Dungani, R. & Jawaid, M. (2014). Production and modification of nanofibrillated cellulose using various mechanical processes: A review. Carbohydrate Polymers, 99, 649– 665.

Arenas, L.T., Simm, C.W., Gushikem, Y., Dias, S.L.P., Moro, C.C., Costa, T.M.H. & Benvenutti, E.V. (2007). Synthesis of Silica Xerogels with High

Surface Area using Acetic Acid as Catalyst. Journal of Brazilian Chemistry Society, 18, 886-890.

Ashori, A., Sheykhnazari, S., Tabarsa, T., Shakeri, A. & Golalipour, M. (2012). Bacterial cellulose/silica nanocomposites: Preparation and characterization. Carbohydrate Polymers, 90, 413– 418.

ASTM. (2012). American Society for Testing and Materials (ASTM). Standard Practice for Maintaining Constant Relative Humidity by Means of Aqueous Solutions, E104 - 02. ASTM, Philadelphia (2012).

Brinker, C. J. & Scherer, G.W. (1990). Sol–gel science: The physics and chemistry of sol–gel processing. Academic Press, San Diego, 881p.

Brinker, C.J. (1988). Hydrolysis and condensation of silicates: effects on structure. Journal of Non- crystalline Solids, 100, 31-50.

Biswal, D.R. & Singh, R.P. (2009). Characterisation of carboxymethyl cellulose and polyacrylamide graft copolymer. Carbohydrate Polymers, 57, 379–387.

Bufalino, L., Sena Neto, A.R., Tonoli, G.H.D., Fonseca, A.S., Costa, T.G., Marconcini, J.M., Colodette, J.L., Labory, C.R.G., Mendes, L.M. (2015). How the chemical nature of Brazilian hardwoods affects nanofibrillation of cellulose fibers and film optical quality. Cellulose, 22, 3657-3672.

Cai, J., Liu, S., Feng, J., Kimura, S., Wada, M., Kuga, S. & Zhang, L. (2012). Cellulose–Silica Nanocomposite Aerogels by In Situ Formation of Silica in Cellulose Gel. Angew. Chem. 124, 2118 –2121.

Castellano, M., Gandini, A., Fabbri, P. & Belgacem, M.N. (2004). Modification of cellulose fibres with organosilanes: under what conditions does coupling occur? Journal of Colloid and Interface Science, 273, 505–511.

Cordeiro, N., Gouveia, C. & John, M.J. (2011). Investigation of surface properties of physico- chemically modified natural fibres using inverse gas chromatography. Industrial Crops and Products, 33, 108–115.

Corradini, E., Imam, S. H., Agnalli, J. A. M. & Mattoso, L. H. C. (2009). Effect of coconut, sisal and jute fibers on the properties of starch/gluten/glycerol matrix. Journal of Polymers and Environment, 17, 1–9.

Cypryk, M. & Apeloig, Y. (2002). Mechanism of the Acid-Catalyzed Si-O Bond Cleavage in Siloxanes and Siloxanols. A Theoretical Study. Organometallics, 21, 2165-2175.

De, G., Karmakar, B. & Ganguli, D. (2000). Hydrolysis±condensation reactions of TEOS in the presence of acetic acid leading to the generation of glass-like silica microspheres in solution at room temperature. Journal of Materials Chemistry, 10, 2289-2293.

Demilecamps, A., Beauger, C., Hildenbrand, C., Rigacci, A. & Budtova, T. (2015). Cellulose–silica aerogels. Carbohydrate Polymers, 122, 293–300.

Dood, M.J.A., Berkhout, B., Kats, C.M., Polman, A. & Blaaderen, A. (2002). Acid-Based Synthesis of Monodisperse Rare-Earth-Doped Colloidal SiO_2 Spheres. Chem. Mater., 14, 2849- 2853.

Elsagh, A. (2012). Synthesis of Silica Nanostructures and Optimization of their Size and Morphology by Use of Changing in Synthesis Conditions. E-Journal of Chemistry, 9, 659-668.

Fonseca, C.S., Silva, T.F., Silva, M.F., Oliveira, I.R.C., Mendes, R.F., Hein, P.R.G., Mendes, L.M. & Tonoli, G.H.D. (2016). Eucalyptus cellulose micro/nanofibers in extruded fiber-cement composites. Cerne, 22,1–9 (in press).

Guzun, A. S., Stroescu, M., Jinga, S.I., Voicu, G., Grumezescu, A.M. & Holban, A.M. (2014). Plackett–Burman experimental design for bacterial cellulose–silica composites synthesis. Materials Science and Engineering C, 42, 280–288.

Guimarães Junior, M. Botaro, V.R., Novack, K.M., Teixeira, F.G. &Tonoli, G.H.D. (2015a). Starch/PVA-based nanocomposites reinforced with bamboo nanofibrils. Industrial Crops and Products, 70, 72– 83.

He, F., Chao, S., Gao, Y., He, X. & Li, M. (2014). Fabrication of hydrophobic silica–cellulose aerogels by using dimethylsulfoxide(DMSO) as solvent. Materials Letters, 137, 167–169.

Hsieh, C., Wu, F. & Yang, S. (2008). Superhydrophobicity from composite nano/microstructures: Carbon fabrics coated with silica nanoparticles. Surface ; Coatings Technology, 202, 6103–6108.

Hubbe, M. A., Rojas, O. J., Lucia, L. A. & Sain, M. (2008). Cellulosic nanocomposites: A review. Bioresources, 3, 929–980.

Iler, R. K. (1979). The Chemistry of Silica: solubility, polymerization, colloid and surface properties and biochemistry; Wiley, New York, 896p.

Kabir, M.M., Wang, H., Lau, K.T. & Cardona, F. (2012). Chemical treatments on plant-based natural fibre reinforced polymer composites: An overview. Composites Part B: Engineering, 43, 2883–2892.

Kalia, S., Thakur, K., Celli, A., Kiechel, M.A. & Schauer, C.L. (2013). Surface modification of plant fibers using environmentfriendly methods for their application in polymer composites, textile industry and antimicrobial activities: A review. Journal of Environmental Chemical Engineering, 1, 97–112.

Lacourse, W.C. (1988). Continuous filament fibers by the Sol-Gel Process. In: Sol-Gel Technology for Thin Films, Fibers, Preforms, Electronics and Specialty Shapes. Lisa C. Klein (Eds.). Noyes Publications, New Jersey, 407p.

Li, F.; Chen, W.; Zhang, S.S. (2008). Development of DNA electrochemical biosensor based on covalent immobilization of probe DNA by direct

coupling of sol–gel and self-assembly technologies. Biosens. Bioelectron., 24, 781–786.

Liu, S., Yu, T., Hu, N., Liu, R. & Liu, X. (2013). High strength cellulose aerogels prepared by spatially confined synthesis of silica in bioscaffolds. Colloids and Surfaces A: Physicochem. Eng. Aspects, 439, 159– 166.

Love, K.T., Nicholson, B.K., Lloyd, J.A., Franich, R.A., Kibblewhite, R.P. & Mansfield, S.D. (2008). Modification of Kraft wood pulp fibre with silica for surface functionalisation. Composites: Part A, 39, 1815–1821.

Maleki, H., Durães, L. & Portugal, A. (2014). An overview on silica aerogels synthesis and different mechanical reinforcing strategies. Journal of Non-Crystalline Solids, 385, 55–74.

Marques, P.A.A.P., Trindade, T. & Pascoal Neto, C. Titanium dioxide/cellulose nanocomposites prepared by a controlled hydrolysis method. Composite Science & Technology,66, 1038–44, 2006.

Nagai, N. & Hashimoto, H. (2001). FT-IR-ATR study of depth profile of SiO_2 ultra-thin films. Applied Surface Science, 172, 307-311.

Órfão, J. J. M., Antunes, F. J. A. & Figueiredo, J. L. (1999). Pyrolysis kinetics of lignocellulosic materials-three independent reaction models. Fuel, 78, 349–358.

Pinto, R.J.B., Marques, P.A.A.P., Barros-Timmons, A.M., Trindade, T. & Pascoal Neto, C. (2008). Novel SiO_2/cellulose nanocomposites obtained by in situ synthesis and via polyelectrolytes assembly. Composites Science and Technology, 68, 1088–1093.

Prins, M.J., Ptasinski, K.J., Janssen, F.J.J.G. (2006). Torrefaction of wood. Part 1. Weight loss kinetics. Journal of Analytical and Applied Pyrolysis, 77, 28–34.

Raabe, J., Fonseca, A.S., Bufalino, L., Ribeiro, C., Martins, M.A., Marconcini, J.M., Mendes, L.M. & Tonoli, G.H.D. (2015). Biocomposite of Cassava

Starch Reinforced with Cellulose Pulp Fibers Modified with Deposition of Silica (SiO_2). Nanoparticles. Journal of Nanomaterials, Article ID 493439, 9 pp.

Raabe, J., Fonseca, A.S., Bufalino, L., Ribeiro, C., Martins, M.A., Marconcini, J.M. & Tonoli, G.H.D. (2014). Evaluation of reaction factors for deposition of silica (SiO_2) nanoparticles on cellulose fibers. Carbohydrate Polymers, 114, 424–431.

Shi, J., Lu, L., Guo, W., Zhang, J. & Cao, Y. (2013). Heat insulation performance, mechanics and hydrophobic modification of cellulose–SiO_2 composite aerogels. Carbohydrate Polymers, 98, 282– 289.

Siró, I. & Plackett, D. (2010). Microfibrillated cellulose and new nanocomposite materials: a review. Cellulose, 17, 459–494.

Tonoli, G.H.D., Holtman, K.M., Glenn, G., Fonseca, A.S., Wood, D., Williams, T., Sa, V.A., Torres, L., Klamczynski, A. & Orts, W.J. (2016) Properties of cellulose micro/nanofibers obtained from eucalyptus pulp fiber treated with anaerobic digestate and high shear mixing. Cellulose, 1-18 (in press).

Wilczek, L. & Chojnowski, J. (1983). Studies of siloxane-acid model system: hexamethyldisiloxane- trifluoroacetic acid. Die Makromolekulare Chemie, 184, 77–90.

Xie, K., Yu, Y. & Shi, Y. (2009). Synthesis and characterization of cellulose/silica hybrid materials with chemical crosslinking. Carbohydrate Polymers, 78, 799–805.

Xie, Y., Hill, C.A.S., Xiao, Z., Militz, H. & Mai, C. (2010). Silane coupling agents used for natural fiber/polymer composites: a review. Compos Part A – Appl S, 41, 806–819.

Yano, S.; Iwata, K. & Kurita, K. (1998). Physical properties and structure of organic-inorganic hybrid materials produced by sol-gel process. Materials Science and Engineering C, 6, 75-90.

Yeh, J., Chen, C. & Huang, K. (2007). Synthesis and properties of chitosan/SiO_2 hybrid materials. Materials Letters, 61, 1292–1295.

Yildiz, S. & Gumuskaya, E. (2007). The effect of thermal modification on crystalline structure of cellulose in soft and hardwood. Building and Environmental, 42, 62–67.

Yin, Y., Wang, C. & Wang, Y. (2012). Fabrication and characterization of self-assembled multifunctional coating deposition on a cellulose substrate. Colloids and Surfaces A: Physicochem. Eng. Aspects, 399, 92– 99.

Zhou, Z., Cui, L., Zhang, Y., Zhang, Y. & Yin, N. (2008). Preparation and properties of POSS grafted polypropylene by reactive blending. European Polymer Journal, 44, 3057-3066.

ARTIGO 3 ***Hybrid aerogels of nanocellulose-silica***

Alessandra de Souza Fonseca[a,b], Joabel Raabe[c], Jenaina Ribeiro Soares[d], Suhara Panthapulakkal[e], Mohini Sain[e,f], Gustavo Henrique Denzin Tonoli[a]*

a Department of Forest Science, Federal University of Lavras, Ave Doutor Sylvio Menicucci 1001, bairro Kennedy, P.O. Box 3037, 37200-000, Lavras, Minas Gerais, Brazi; gustavotonoli@yahoo.com.br
b CAPES Foundation, Ministry of Education of Brazil, Brasília, Brazil; adnax_florestal@hotmail.com
c Department of Forest Engineering, Faculty of Technology, University of Brasília - UnB, Campus Darcy Ribeiro, Asa Norte, P.O. Box 04357, 70910-900, Brasilia, DF, Brazil; joabeljr@hotmail.com
d Department of Physics, Federal University of Lavras, Ave Doutor Sylvio Menicucci 1001, bairro Kennedy, P.O. Box 3037, 37200-000, Lavras, Minas Gerais, Brazil; jenaina.soares@dfi.ufla.br
e Centre for Biocomposites and Biomaterials Processing, Faculty of Forestry, University of Toronto, Toronto, Ontario M5S 3B3, Canada; s.panthapulakkal@utoronto.ca, m.sain@utoronto.ca
f King AbdulAziz University, Jeddah, KSA.

**Corresponding author: gustavotonoli@yahoo.com.br*

Artigo formatado de acordo com as normas para submissão do periódico Industrial Crops and Products.

ABSTRACT

The study aimed to analyze physical and mechanical properties of hybrid aerogels of nanocelulose-silica (HANS). The HANS were produced from cellulose nanofibrils (1%) in the sol-gel process with four different concentrations of tetraethyl orthosilicate (TEOS). Fourier Transform Infrared Spectroscopy (FTIR) spectra evaluated the effectiveness of the silica deposition. Thermal and moisture adsorption analysis were done to investigate their physical properties. Compressive test was performed for determination of Young's modulus (E), maximum stress and maximum strain of the HANS. The HANS 0.50% have mechanical properties comparable to the highest tested concentration (1.00%) with more thermal stable behavior. HANS 0.25% was moisture resistant when compared to their counterparts. The mechanical behavior of the HANS was similar to hybrid composite reported in the literature. The present work contributes with important information of the silica deposition on nanostructured cellulose for the development of new and engineered cellulose-based materials by a short synthesis method.

KEYWORDS: silica deposition, hybrid composite, tetraethyl orthosilicate, Eucalyptus cellulose nanofibrils, properties.

1. INTRODUCTION

Aerogels are resulting gels from supercritical drying or freeze-drying methods (efficient but rather expensive and difficult to handle) that has a volume similar to that of the original sol which use air as the medium (Brinker and Scherer, 1990; Job et al., 2005; Cai et al., 2012; Yamauchi, 2001; Sehaqui et al., 2011; Lin et al., 2014). These materials are characterized by their light-weight porous structure, like found as foams with very high specific surface area and low refractive index (Brinker and Scherer, 1990; Kocon et al., 1998; Aegerter et al.,

2011; Wagh et al., 1997). When comparing aerogels with xerogels, the prior has shown superior properties in electrical applications such as batteries, piezoelectric materials, as well as in catalysis reactions while the latter shows better performance when applied to membrane filtration purposes (Pierre and Pajonk, 2002).

Xerogels or dried gel are also new materials that can be used as powder or monolith (Hüsing and Schubert, 1998) made by evaporation of the pore liquid of the wet gels under subcritical conditions such as the formation of a liquid/vapor boundary phase (Jansen and Zimmermann, 1997). This boundary is characterized by its solid network structure which is drastically altered by the large stresses exerted by capillary pressure during evaporation that also use air as the medium (Yamauchi, 2001; Pekala and Alviso, 1992) and due to their dense porous structure collapsed with high porous network, which is promising for many applications as a result of their high specific surface, low thermal conductivities, adsorption and catalysts efforts whereas their long and very difficult process to apply at large scale (Job et al., 2005; Yamauchi, 2001; Pekala and Alviso, 1992).

Cellulose aerogels may play a role as a potential new class of cellulose products (Sehaqui et al., 2011; Thapliyal and Singh, 2014) enriching the demand of the forest research for different purposes, called as biomass-based aerogels or bio-aerogels with plastically mechanical behavior (Demilecamps et al., 2015) while they are strong-lightweight polymeric materials made from aqueous foams stabilized by cellulose nanofibers (Cervin et al., 2013). These materials have a myriad of uses such as supercapacitors (Zhang et al., 2014), adsorption and absorption materials (Oshima et al. 2014; Chin et al., 2014; Jin et al., 2015), thermal insulators (Shi et al., 2013; Nguyen et al., 2014), drug releaser (Valo et al., 2013) and functionalized materials (He et al., 2014; Cai et al., 2015).

A traditional type of aerogels called silica aerogels have high porosity and specific surface area, with extremely low solid density and a low refractive index (Ehrburger-Dolle et al., 1994; Pajonk, 1998). These materials are composed by interconnected silica particles that form an open nanostructure and can exhibit brittle, elastic, or compressible behavior depending on their densities (Parmenter and Milstein, 1998; Wong et al., 2014).

Hybrid aerogels such as cellulose-silica aerogels are also a new generation of bio-aerogels developed to be strongly reinforced and light hybrid aerogel with the high ductility characteristic of aerogels from cellulose (Demilecamps et al., 2015; Jin et al., 2015; Jin et al., 2004; Shi et al., 2013; Lin et al., 2014; Cervin et al., 2013) and the thermal properties as related to silica-aerogels.

Cellulose-silica aerogels are strongly reinforced and light hybrid aerogel with high ductility characteristic of the cellulose aerogel and the lowest thermal conductivity related to silica-aerogels: they can deform about 40% strain and partially recover their original shape under free-stress condition (Demilecamps et al., 2015).

Fiber-reinforced silica aerogels generally exhibit lower compressive strengths and decreased elastic moduli with typical behavior of brittle materials (Parmenter and Milstein, 1998). These materials have high production cost and poor mechanical properties, but advantageous low density and thermal insulation properties (Wong et al., 2014).

Tetraethyl orthosilicate (TEOS) is a alkoxide commonly used as nanostructured silica precursor to introduce silica nanoparticles on the surface of different organic-polymers (Yano et al., 1998). Some studies had successfully synthesized cellulose-silica aerogels using different methods, such as the immersion of tetraethoxysilane (TEOS) in an aqueous solution followed by thermal-press (Ashori et al., 2012), sol–gel synthesis with TEOS as nanostructured Silica precursor followed by supercritical CO_2 drying (Cai et al., 2012) and

impregnating with silica phase the wetting coagulated cellulose with polyethoxydisiloxane, using molecular diffusion and forced flow induced by pressure difference (Demilecamps et al., 2015).

Therefore, the present study aimed to present the morphology, physical and mechanical properties of hybrid aerogels synthesized from Eucalyptus cellulose nanofibrils and different concentrations of silica precursor.

2. EXPERIMENTAL

2.1 Material

Commercial bleached Eucalyptus kraft pulp (hardwood short fibers) was used as raw material. Cellulose nanofibrils 1% concentration was obtained by mechanical defibrillation on a grinder (Masuko Corp., Japan) at 1500 rpm and around 8 passages through the defibrillator, similar to procedures described in previous works (Fonseca et al., 2016; Bufalino et al., 2015; Guimarães Jr., et al, 2015)

2.2 Production of the hybrid aerogels of nanofibrils-silica (HANS).

The sol-gel solutions with a fixed amount of 0.5 g (dried basis) of cellulose nanofibrils and four different concentrations of the silica precursor Tetraethyl orthosilicate (TEOS) were prepared ranging from 0.00 to 1.00% in proportion of the total water mass of 200 g that represent the better concentrations according to previous results. A fixed amount of 1 mL of acetic acid 0.1 N was added. The sol-gel solutions were constant magnetic stirred for 2 h. The HANS were made by freeze drying the sol-gel solutions in Falcon tubes with 50 mL capacity during five days, with the subsequent freeze drying procedure performed -20°C for 24 h.

2.3 Morphological analysis

The Transmission electron microscope Hitachi H-7000 TEM (Hitachi Ltda., Japan) was used under an accelerated voltage of 75 kV to obtain images of the Eucalyptus cellulose nanofibrils in nanoscale. The Leitz Wetzlar light microscope (Ernst Leitz Wetzlar Company, Germany) with transmission mode and Nikon COOLPIX5400 coupled camera were also used to observe the Eucalyptus cellulose nanofibrils in microscopic resolution.

Microscopic images of the hybrid aerogels were also captured by using a Nikon digital sight DS-Ri1 camera coupled to the Microscope Stereoscope Nikon SMZ1500 (Nikon, Japan) using the Imaging software NIS-Elements D 3.21.00 (Nikon, Japan).

High resolution microstructure images of HANS were observed by using a LEO Evo40 XVP scanning electron microscope (SEM, from Carl Zeiss AG, Germany). The samples were coated with gold before SEM analyses, in which longitudinal and cross-section view of the HANS were obtained to analyze the influence of the silica in their morphology. Furthermore, images of the specimens after mechanical test were captured to help in the understanding of the influence of different concentrations of the nanostructured silica precursor on mechanical behavior.

2.4 Silica deposition effectiveness

Fourier transform infrared spectroscopy (FTIR) was performed to evaluate the effectiveness of the surface modification. FTIR spectrum of the sample obtained was examined in a KBr pellet in the proportion of 1:100 (w:w) on a Bruker Tensor 27 FTIR spectrometer (Bruker Optics Inc., USA) between 4000 and 400 cm-1.

2.5 Themogravimetry

Control and hybrid composites were subject to thermogravimetric analysis (TGA) in a thermal gravimetric analyzer (TGA-Q500, TA Instruments, USA). The samples with around 4 mg were heated in a Pt crucible from 25 to 600°C in synthetic air flowing at 60 mL min-1, and heating rate of 10°C min-1. The silica content was determined as the residual mass at 600°C.

2.6 Moisture adsorption analysis

Specimens with 2.0 cm × 1.0 cm × 0.5 cm were dried for 24 h at 103 ± 2°C, weighted, and kept in a hermetically sealed container with 97 ± 2 % of relative humidity (RH) and 20 ± 2°C, using a saturated potassium sulfate solution, as prescribed by the ASTM E104 standard (ASTM, 2012). The moisture adsorbed by the samples by time was determined measuring the mass of the HANS on an analytical balance with 0.0001 g precision at successive intervals until they reached a constant weight. The amount of moisture adsorbed (MA) by the samples was calculated as below (Eq. 01):

$$MA_{(\%)} = \left[\frac{\left(M_t - M_0\right)}{M_0} \right] \times 100 \quad (1)$$

Whereas M0 and Mt are the initial mass of the sample (prior to exposure to moisture) and the sample mass after t hours of moisture exposure (97 ± 2 % RH), respectively.

To perform statistical analysis, an average of three samples for each HANS synthesized the parametric F test was used at the 5% level of significance. When necessary, the Tukey test (95% probability) was applied for multiple comparisons of the averages. All the statistical analyses were performed in the R 2.13.0 software (R CORE TEAM, 2012).

2.7 Compressive properties

Compressive test was performed on cylindrical specimens of 20 mm of diameter and length of 10 mm using an Instron mod. 3367 Universal testing machine (Instron Corp., USA) with 2 kN load cell at 1 mm.min-1 of strain rate and a gauge length of 10 mm. The original and cylindrical aerogels were divided in five pieces cutting them in their cross sections. The compressive strength and compressive modulus (E, Eq.2) were determined. The compressive strength was defined as the maximum stress carried by the specimens during a test (Parmenter and Milstein, 1998):

$$E_{(GPa)} = \frac{\sigma}{\varepsilon} \quad (2)$$

Where σ is the stress and ε is the strain in the elastic (initial, linear) portion of the stress–strain curve.

The samples were oven-dried at 60°C overnight before testing. At least three specimens were produced for each sample. The parametric F test was used at the 5% level of significance, and the Tukey test (95% probability) was used for multiple comparisons of the averages in the R 2.13.0 software (R CORE TEAM, 2012).

After the first compression test, all the specimens partially recovered their original depth. Because of that, the compressive strength values were determined again (maximum compression stress carried by the specimens during a second compression test). The second compression test on the HANS was performed for the previously compressed specimens and the statistical analyses were reapplied.

3. RESULTS AND DISCUSSION

3.1 HANS morphology and silica deposition effectiveness

The Eucalyptus fiber and its cellulose nanofibrils used as raw material to produce the HANS shown on Figure 1. The original fiber from the Eucalyptus Kraft pulp (Figure 1a) was mechanically defibrillated, and its cellulose nanosuspension (Figure 1b) showed cellulose microfibrils and cellulose fibers with high defibrillation levels confirming the heterogeneous feature of microfibrillated cellulose previously mentioned in literature (Zuluaga et al., 2009; Siró and Plackett, 2010; Chinga-Carrasco, 2011; Hassan et al., 2012; Alila et al., 2013).

Usually, the resultant suspension of defibrillated fibers contains: (i) individualized micro/nanofibers; (ii) fibers under defibrillation; (iii) clusters and bundles of micro/nanofibers; and (iv) non-defibrillated fibers (i.e. entire fibers).

We also found in those previous analysis that the synthesized Eucalyptus nanosuspension showed around 60% of residual fraction of fibers, while the large content of fibrils in nanoscale were successfully obtained from Eucalyptus, showing around 86% of their nanofibrils with diameter lower than 20 nm, with average diameter of 13 ± 8 nm. The observed Crystal index was 79%, with narrow and more individualized nanocrystals (like showed in Figure 1c).

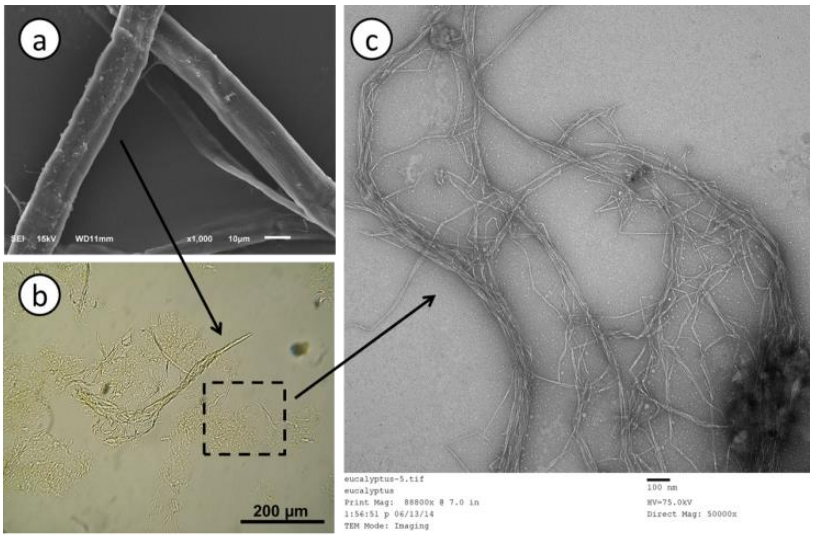

Figure 1. General morphology of Eucalyptus nanofibrils: (a) scanning electron microscope (SEM) images of the fiber; (b) light microscope (LM) images of nanosuspension; (c) transmission electron microscope (TEM) images of nanofibrils.

The final morphology and structural behavior of the cellulose aerogels were influenced by the surface modification. Without the nanostructured silica precursor, the cellulose aerogel was not able to be formed (Figure 2). Some internal faults were observed, probably due to an inefficient nanofibers network formation caused by agglomeration while the freeze drying process, or during the sol-gel reactions.

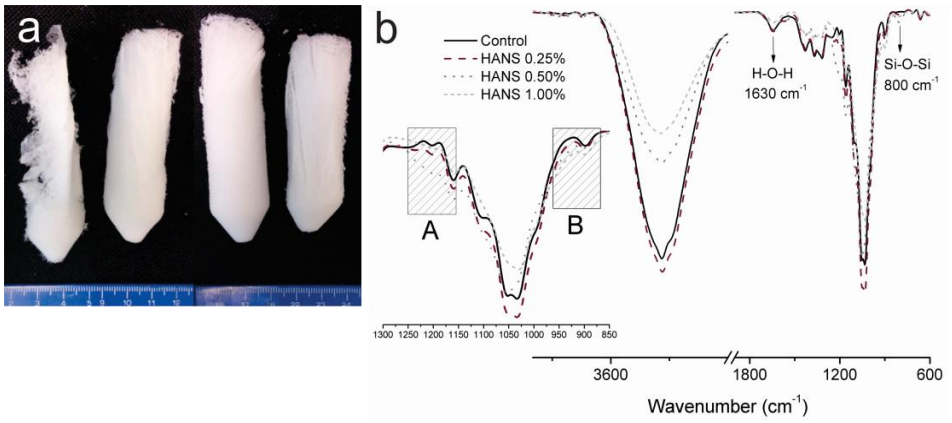

Figure 2. General view of Eucalyptus cellulose aerogels (a) produced by four concentrations of the nanostructured silica precursor tested and (b) FTIR spectra.

The presence of residual hemicellulose and lignin was confirmed with intense peaks at 1735 cm-1 which represents vibrations of acetyl and uronic ester groups of hemicelluloses or ester linkage of carboxylic groups of the ferulic and p-coumaric acids of lignin (Ray and Sarkar, 2001; Sun et al., 2002; Sun et al., 2005).

The effectiveness of the surface modification also can be observed in the FTIR spectra (Figure 2b). The Si-O-Si peaks at 450 cm-1 and 800 cm-1 (Hsieh et al., 2008; Yin et al., 2012; Liu et al., 2013) were found in the nanofibers modified with silica precursor, indicating that no chemical reaction happened to the cellulose and the silica source (Liu et al., 2013). Other regions related to Si-bonding were found in regions A and B in the Figure 2b.

Region A shows Si-O-Si and Si-O peaks in the 1265-1165 cm-1 region (Nagai and Hashimoto, 2001), and region B shows Si-O-Si peaks in the 1120-1080 cm-1 region (Zhou et al., 2008; Hsieh et al., 2008; Yin et al., 2012), Si-O-C at 1100-1048 cm-1 (Yeh et al., 2007; Liu et al., 2013) and Si-O at 1090 cm-1 (Guzun et al., 2014). As stated by Demilecamps et al. (2015) and Liu et al.

(2013), still showing no chemical interactions between cellulose and silica. The water molecule peak at 1630 cm-1 (Hsieh et al., 2008) has a slight increase when the concentration of nanostructured silica precursor increased, despite TEOS being associated with hydrophobizing process. It may be a consequence of the unsatisfactory surface coverage for the purposes of hydrophobization, although showing an influence on the physical structure of the aerogels. The influence of the addition of silica precursor on nanofibers suspension on the cellulose aerogel microstructure can be observed in Figure 2a and 3.

The large difference on the synthesized HANS morphology is clearly showed and detailed on their microscopic view (Figure 3). The presence of TEOS influences the final morphology of the hybrid composite, whereas control shows highly agglomerated cellulose network with lower foam-like appearance when compared with their counterparts.

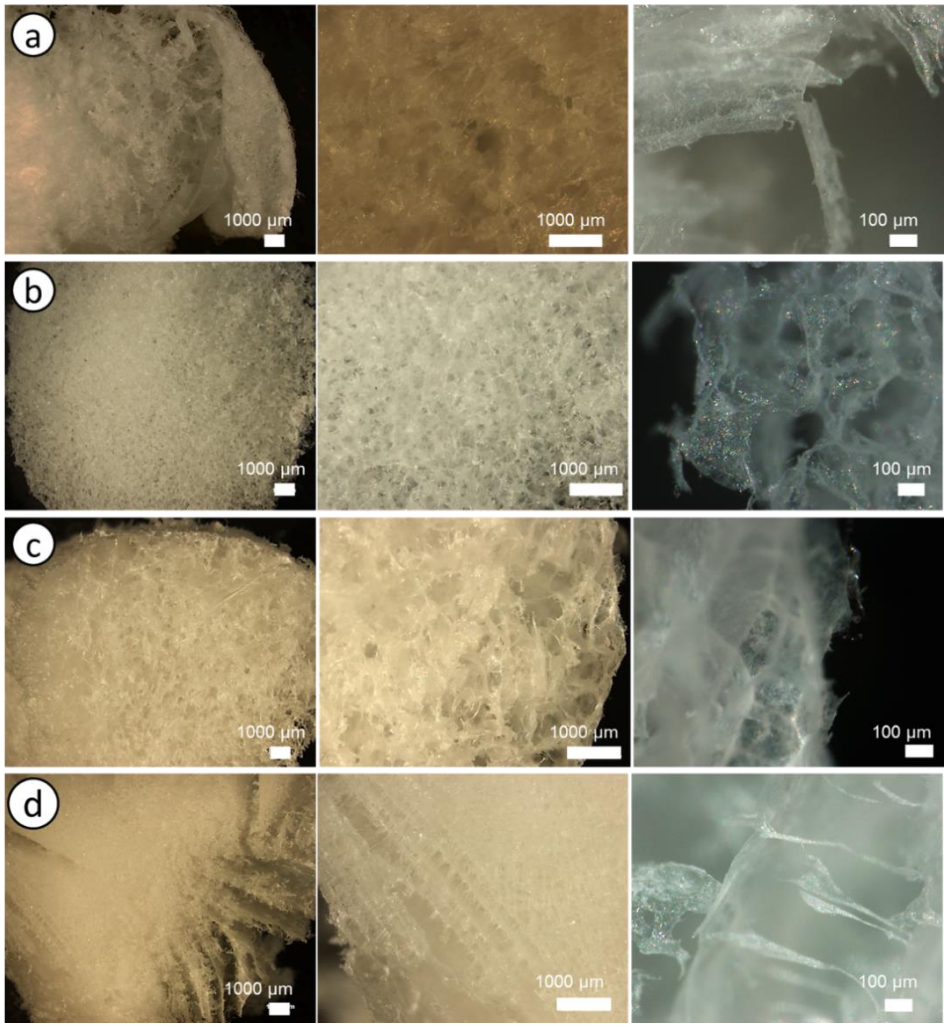

Figure 3. Light microscopic view of hybrid aerogels of nanocelulose-silica – HANS by four concentrations of the nanostructured silica precursor tested: (a) control; (b) HANS 0.25%; (c) HANS 0.50% and (d) HANS 1.00%.

The HANS 0.25% showed the best foam-like appearance, maintaining the high cellulose matrix defibrillation degree which is probably a consequence of a satisfactory organic-inorganic synergy interaction obtained in this procedure. (Figure 3b). HANS 0.50% had foam-like appearance, but some agglomerations

can be observed, mainly on the outer area (Figure 3c), whose cellulosic matrix began to rearrange and form a cellulosic-like membrane, almost mimicking the primary cell wall structure and its random distribution. Its rearrange can be also found in the control most likely as a result of the stronger bondings of the hydroxyl groups on the cellulose matrix. For HANS 0.50%, the synergy of organic-inorganic interaction was not fulfilled, since it showed microscopic morphology similar to control (Figure 3a and 3c) with the double of the TEOS proportion when compared to the control.

The highest concentration of silica precursor made samples more internal-layered (Figure 3d) with lengths smaller than the observed for the concentrations of 0.25% and 0.50% of nanostructured silica precursor (Figure 2a). Also HANS 1.00% is more brittle, with high degree of agglomeration, and make its layered structure (typos) may be a consequence of the excess of silica precursor content in proportion to nanofibrils mass.

According to morphological results, concentration of 0.25% of TEOS has showed more stable and foam-like structure, with the most homogeneous porous appearance.

On the cross-section view is possible to observe the homogeneous morphology generated by 0.25% of nanostructured silica precursor, and the unstable morphologies made by the others concentrations evaluated (Figure 3). For the specimens with 0.50%, the cross-section diameter was reduced. Specimens with 1.00% lost their cross-section circumferential diameter shapes when compared to 0.25% and 0.50% nanostructured silica precursor specimens, adopting a new quasi-triangular cross-sectional shape.

The morphological structure of HANS can be seen in Figure 4. As observed on Figure 4 under cross section view, the microstructure of the control was more agglomerated and collapsed structure with lowest like foam-porous formation. It is may attributed to the stronger hydroxyl bondings into and between cellulose

network surfaces in the absence of TEOS influences (Figure 4a). The aerogel wall shows no porous but some porosity caused by the gaps into cellulosic network (Figure 4b).

Concentrations of TEOS up to 0.25% started to produce foam-like porous structures (Figure 4c), showing well-defined spherical pores with different sizes (Figure 4d) when compared to control, even when the organic-inorganic interaction synergy was not well done, as mentioned previously. However, the some physical coating may be worked enough since the TEOS weight was higher than nanofiber. HANS 0.25% presented foam-like structure with expanded volume.

HANS 50% shows cross-section view foam-like structure with lower total volume when compared to HANS 0.25%, with porous formed by somewhat agglomerated cellulosic networks under TEOS influences (Figure 4e). Single and large perforations were often observed on the aerogel wall, but small ones still occur (Figure 4f).

However, TEOS concentration of 1% made hybrid aerogels with laminated structure (Figure 3d) and brittle behavior even under touch of hands. Cellulosic sheets can be observed in HANS 1.00%, building its internal structure (Figure 4g), with often large complex perforations produced by porous with different sizes, coalesced or not (Figure 4h), mimicking the porous structure found in some wood on cross section view.

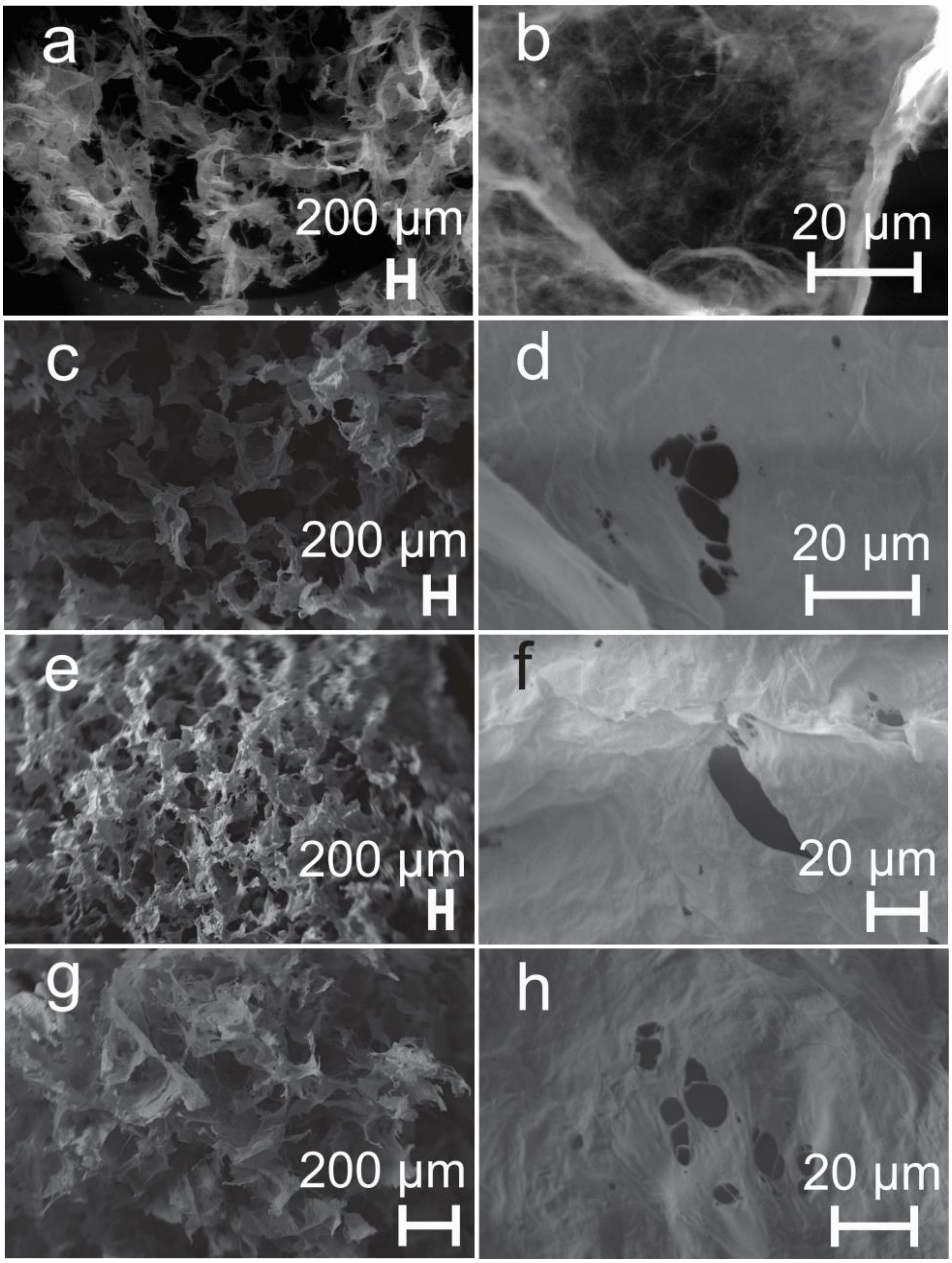

Figure 4. Electron micrographic images of hybrid aerogels of nanocelulose-silica – HANS: (a-b) control; (c-d) HANS 0.25%; (e-f) HANS 0.50% and (g-h) HANS 1.00%.

3.2 Themogravimetry

Some differences on the HANS thermogravimetric behavior when compared to pure cellulose aerogel (control) were found at three characteristics regions of decomposition of cellulosic materials, like showed by Raabe et al. (2014): (1) from room temperature to around 150°C, as a consequence of dehydration and release of volatile (Yildiz and Gumuskaya, 2007); (2) around 350°C, related to cellulose decomposition (Órfão et al., 1999), where a large amount of weight loss occurs; and (3) near to 500°C, as a consequence of oxidation reactions of the remaining organic materials (Corradini et al., 2009) as showed on Figure 5.

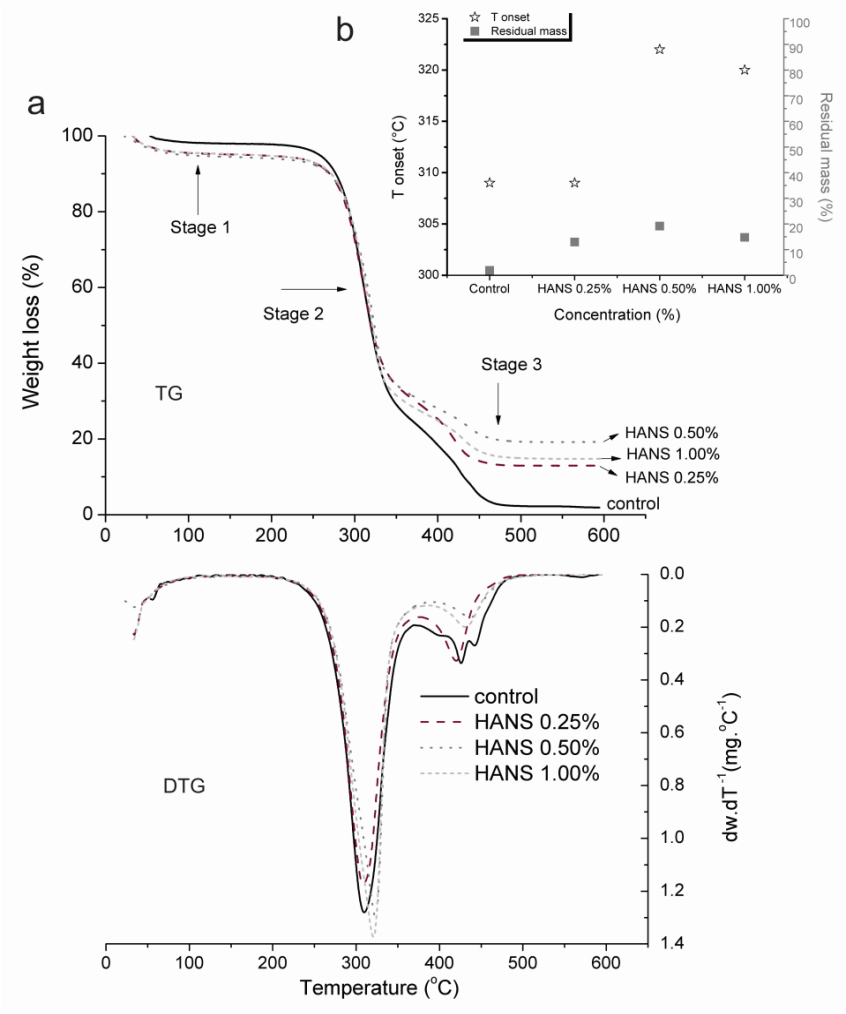

Figure 5. Thermal results: (a) TG and DTG curves and thermal decomposition stages of the hybrid aerogels of nanocelulose-silica (HANS) made by different concentrations of nanostructured silica precursor; (b) The onset decomposition temperature (Tonset) and residual mass of them.

Raabe et al. (2014) found that the highest mass loss occurred on the second stage which temperature of decomposition ranged from 200 to 340°C influenced by the condition of the modification. In this study the second stage has a similar peak range: from 200 to 350°C (Figure 5a) for all the studied conditions, even

control aerogel. Raabe et al. (2014) have modified Eucalyptus cellulose kraft pulp with cellulosic fibers in microscale using the same silica precursor used in the present study, tetraethyl orthosilicate, but using different catalyzer, concentrations of precursor, and reaction factors.

Otherwise, similar results can be found even when the onset degradation temperature has improved, maybe influenced for both, the nanoscale nature of the starting cellulosic material and the presence of silica on the cellulose network, whereas the T onset of the pure cellulose (control) shows similar value to HANS 0.25% (Figure 5b). Hybrid aerogels from TEOS 1.00% concentration show average thermal behavior between that found for the 0.25% and 0.50% concentrations as well as the onset decomposition and residual mass.

The higher thermal stability of HANS synthesized by interaction of nanofibers with TEOS 0.50% showed on stages 2 and 3 may be a result of a satisfactory sol:gel proportion achieved for these modification conditions, as a consequence of the higher residual mass at 600°C, which was 19.15%, also showing more stable thermal behavior compare to modified (12.92 %, for HANS 0.25%; 14.74%, for HANS 1.00%) and unmodified aerogels (1.90%, for control). Therefore, in this study 1% of TEOS was not able to make satisfactory and morphological stable hybrid aerogels and it can be seen on their layered internal structure also showing a brittle aspect (Figure 2a and 3).

Thermal properties can be a helpful tool to analyze the organic-inorganic interaction, expecting changes in thermal events when strong bondings between them occur. Based on that observation, it can be suggested that the Eucalyptus nanofiber-silica interaction are not effective for HANS 0.25% since the thermal events for it were very similar to the pure cellulose aerogel. The changes that can be found (Figure 5a, see stages 2 and 3) may a result of a physical coating of the cellulose networks on the cellulose aerogel matrix, confirming the results discussed on item 2.4, silica deposition effectiveness. The physical interaction

made some influence on the mechanical properties (see Table 1) and the final morphology of the HANS produced (see Figure 2a and 3).

3.3 Moisture adsorption of the aerogels

The moisture adsorption behavior can be seen on Figure 6. All the HANS samples even the control, show lower moisture adsorption (<5%) confirming that the simple change on scale (from micro to nanoscale) of the cellulose matrix may influences the final properties of the synthesized aerogels. The HANS that have TEOS in their composition showed general lower moisture adsorption values when compared to the control aerogel.

After ~450 h of exposition to high humidity environment (98%), the tendency of their mass showed no stabilization. It may be influenced by their internal porous and heterogeneous structure that could store moisture inside producing like "burbles of moisture" insulated in it.

Probably the physical-layered coating was not well distributed on their surface as supposed by their thermal results (Figure 5a) as well by their percentage of residual mass (Figure 5b). The averages were statistically different (Figure 6): The result shows HANS 0.25% with lower moisture adsorption capacity. Control and HANS show the higher values which were statistically similar. HANS 1.00% was between the highest and lowest values of moisture adsorption.

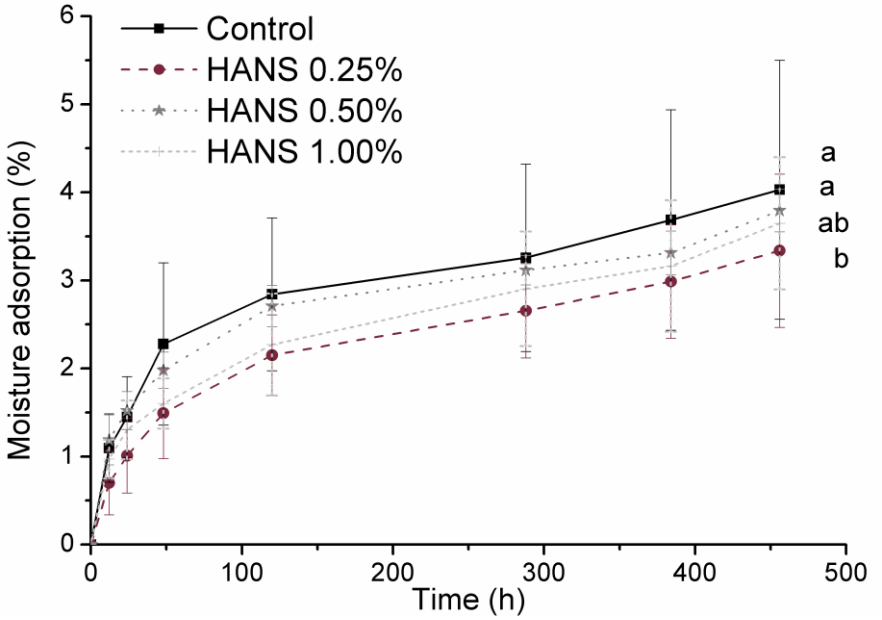

Figure 6. Average and standard deviation values of moisture adsorption in function of time of exposition to moisture (98 % RH) of the HANS.

3.4 Compressive properties and recovery capacity behaviour

The mechanical properties have no statistical difference between the HANS specimens with different concentrations of TEOS as well with different numbers of compression. Although the reductions to stress and strain values, the HANS show no statistical difference on their mechanical properties E modulus, stress and strain at maximum load, compared to their counterparts, for all factors analyzed (Table 1). No mechanical properties were determined for control because they were not effective for obtaining the aerogel structure (see on Figure 2) and no valid E modulus values were found to HANS 0.25%. Even with more stable and homogeneous foam-like structure, HANS 0.25% shows heterogeneous and variable mechanical behavior.

Table 1. Compressive properties of the surface-modified cellulose aerogels once and twice compressed

Fator A	Fator B	Mechanical Properties		
Concentration of TEOS (%)	Compression test	E (kPa)	Stress at Max. Load (kPa)	Strain at Max. Load (%)
0.25	1	-	10.00 ± 4.58	38 ± 23
	2	-	-	39 ± 19
0.50	1	62.48 ± 29.59	9.00 ± 1.00	28 ± 12
	2	24.15 ± 15.67	3.00 ± 2.00	38 ± 21
1.00	1	54.62 ± 14.55	8.67 ± 0.58	20 ± 5
	2	35.44 ± 19.97	4.33 ± 2.52	40 ± 18

All Average values (from three specimens) show no statistical difference between them by Tukey test at 95% of probability. The numerical values following the "± signs" are standard deviations.

All the morphology of the samples compressed once and twice is represented in the Figure 7a-e. The deformation of the HANS 0.25% and 0.50% showed partial deformation while HANS 1% exhibited much more reduction on their dimensions with clear compacted structure after the second compression. The HANS 0.25% and HANS 0.50% samples show lateral folds as the major general deformations obtained (see Figure 7d, 7e).

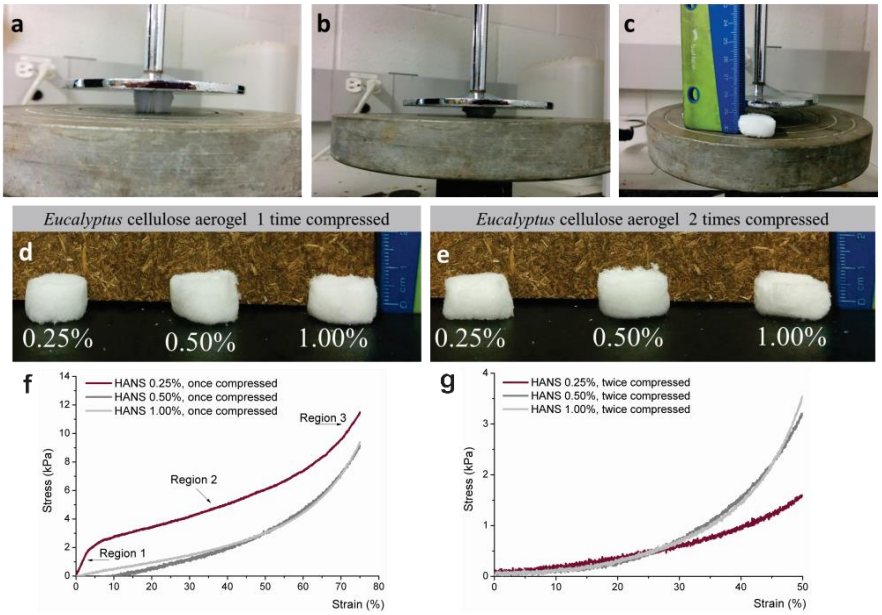

Figure 7. The mechanical compression test of HANS. Specimens before (a), during (b) and after (c) compression test. Representative images of the specimens compressed once (d) and twice (e). After the second compression, the specimens show partial deformation. Stress-strain curves for the once (f) and twice (g) compressed HANS.

The literature related that cellulose-silica aerogels show plastically mechanical behavior: they can be deformed until a strain of 60–80% before complete pore collapse (Demilecamps et al., 2015). They are also often characterized by their wide distribution of pore sizes, from a few tens of nanometers to a few microns, and their large specific surface area ranging from 200 to 500 m2.g-1 (Sescousse et al., 2011; Kobayashi et al., 2014).

All HANS produced samples show up to 70% of strain maximum obtained from the first compression procedure: 71±4% for HANS 0.25%; 75 % for HANS 0.50% and 75 % for HANS 1.00%. The HANS can be compressed until the maximum strain programmed but their mechanical response was expected to be higher, around values found by Demilecamps et al. (2015). However, all hybrid

aerogels shows lower stress maximum after first compression time compare to composite aerogel via diffusion impregnation by them (σ=6.30 MPa): around 0.1428% (HANS 0.50%) and 0.1376% (HANS 1.00%). The reduction after second time compressed were around 0.0476% (HANS 0.50%) and 0.0687% (HANS 1.00%). The same behavior was observed to E modulus obtained by them (E=11.5 MPa): The reduction after first time compressed was around 0.5433% (HANS 0.50%) and 0.4749% (HANS 1.00%); after second compression time was around 0.2100% (HANS 0.50%) and 0.3081% (HANS 1.00%). Nanofibrillated cellulose aerogels and nanofibrilatted cellulose foams (Sehaqui et al., 2011; Cervin et al., 2013) produced elsewhere presented similar behavior of their stress-strain curves to HANS 0.25% samples in the first compression cicle tested in this study. As found by Demilecamps et al (2015), three regions can be distinguished for the stress-strain curves for HANS 0.25% in the first compression: (1) a linear regime at low strains, (2) long plastic deformation region (3) end of compression test with a densification of the specimens (Figure 7f). Those authors state the second region as a consequence of the bending of the pore walls and the last region as collapse of the pore walls. The stress-strain curves of the HANS compressed for the second time were plotted and compared to the first compression (Figure 7g). The average stress values found between the first and second compressed time50% lower for HANS 0.25%, 67% for HANS 0.50% and 50% for HANS 1.00%. The average strain values show 4 % of increasing for HANS 0.25%, 36% to the HANS 0.50% and 95% for HANS 1.00% that characterize them as plastic deformations that may have collapsed their internal structure.

The stress-strain curves show the representative characteristics of the HANS for each concentration of silica precursor for the first (Figure 7f) and second compression cicles (Figure 7g). The behavior of the specimens compressed twice can be considered similar to that compressed once into their own silica

precursor concentration evaluated for HANS 0.50% and 1.00% (Figure 7g). The representative curve for HANS 0.25% showed more heterogeneity and higher values on their mechanical behavior, which can be a consequence of their morphology, but as said before, no statistical difference was found for all mechanical properties evaluated.

The presence of silica shows no influence on the mechanical properties of the aerogels, but the synergy of cellulose–silica compounds provided stiff and ductile aerogel materials as found previously to similar hybrid composite (Demilecamps et al., 2015). The preparation method applied here and the potential properties of the HANS produced in this study may be considered as an interesting way for engineering and development of advanced materials from cellulose-based materials. The morphology of the aerogels was influenced by the presence of silica, although to the different concentrations used here it has no influence on their mechanical properties. The HANS 0.50% was thermally stable and has mechanical properties comparable to the highest tested concentration (HANS 1.00%). Otherwise HANS 0.25% shows more stable water adsorption results.

4. CONCLUSIONS

The method adopted to produce hybrid composite was successfully performed. The final morphology of the cellulose aerogels were influenced by the physical coating surface using TEOS as a silica precursor. The absence of silica precursor damaged the formation of the hybrid composite aerogels. TEOS 0.25% was found to provide an improved network of cellulose nanofibers with a foam-like porous structure in homogeneous and soft-flexible hybrid composite aerogels. Hybrid aerogel with 0.50% of TEOS shows higher thermal stability and TEOS 0.25% made moisture stable hybrid composite, with morphology more porous. Despite no influence of the different silica precursor concentrations on the

compressive strength, all the aerogels obtained presented interesting capacity to recover their original dimensions after the first compression. The present work provided information on hybrid and nanostructured cellulose materials for development of new and engineered cellulose-based materials for diverse applications made by a short synthesis method.

5. ACKNOWLEDGMENTS

The authors acknowledge the financial support of the Brazilian Government through Coordenação de Aperfeiçoamento de Pessoal de Nível Superior – CAPES (CAPES-Embrapa Edital 01/2011, and scholarship PDSE/CAPES, process n. 99999.012163/2013-09), Conselho Nacional de Desenvolvimento Científico e Tecnológico (CNPq), Fundação de Amparo à Pesquisa do Estado de Minas Gerais (FAPEMIG), Rede Brasileira de Compósitos e Nanocompósitos Lignocelulósicos (RELIGAR), Laboratory of Electron Microscopy and Ultra-Structural Analysis (LME) in the Department of Plant Pathology at Federal University of Lavras (UFLA), in Brazil. Thanks also to technical and logistical endorse offer by The Centre for Biocomposite and Biomaterial Processing - CBBP/University of Toronto, in Canada.

6. REFERENCES

Aegerter, M. A.; Leventis, N.; Koebel, M. Aerogels handbook. Springer New York, New York, 2011.

Alila, S.; Besbes, I.; Vilar, M.R.; Mutjé, P.; Boufi, S. Non-woody plants as raw materials for production of microfibrillated cellulose (MFC): A comparative study. Ind. Crop. Prod., 41, 250– 259, 2013.

Ashori, A.; Sheykhnazari, S.; Tabarsa, T.; Shakeri, A.; Masood Golalipour, M. Bacterial cellulose/silica nanocomposites: Preparation and characterization. Carbohyd. Polym., 90, 413– 418, 2012.

ASTM. (2012). American Society for Testing and Materials (ASTM). Standard Practice for Maintaining Constant Relative Humidity by Means of Aqueous Solutions, E104 - 02. ASTM, Philadelphia, 2012.

Brinker, C. J.; Scherer, G.W. Sol–gel science: The physics and chemistry of sol–gel processing. Academic Press, San Diego, 1990.

Bufalino, L., Sena Neto, A.R., Tonoli, G.H.D., Fonseca, A.S., Costa, T.G., Marconcini, J.M., Colodette, J.L., Labory, C.R.G., Mendes, L.M. (2015). How the chemical nature of Brazilian hardwoods affects nanofibrillation of cellulose fibers and film optical quality. Cellulose, 22, 3657-3672.

Cai, H.; Mu, W.; Liu, W.; Zhang, X.; Deng, Y. Sol–Gel Synthesis Highly Porous Titanium Dioxide Microspheres With Cellulose Nanofibrils-Based Aerogel Templates. Inorg. Chem. Commun., 51, 71–74, 2015.

Cai, J.; Liu, S.; Feng, J.; Kimura, S.; Wada, M.; Kuga, S.; Zhang, L. Cellulose–Silica Nanocomposite Aerogels by In Situ Formation of Silica in Cellulose Gel. Angew. Chem. 124, 2118 –2121, 2012.

Cervin, N. T. ; Andersson, L.; Ng, J.B.S.; Olin, P.; BergströM, L.; WåGberg, L. Lightweight and Strong Cellulose Materials Made from Aqueous Foams Stabilized by Nanofibrillated Cellulose. Biomacromolecules, 14, 503−511, 2013.

Chin, S.F.; Romainor, A.N.B.; Pang, S.C. Fabrication of hydrophobicand magnetic cellulose aerogel with high oil absorption capacity. Mater. Lett., v. 115, p. 241–243, 2014.

Chinga-Carrasco, G. Cellulose fibres, nanofibrils and microfibrils: The morphological sequence of MFC components from a plant physiology and fibre technology point of view. Nanoscale Res. Lett., 6, 417, 2011.

Coelho Junior, L. M.; Rezende, J. L. P.; Ávila, E. S.; Oliveira, A. D.; Borges, L. A. C. Analysis of the Brazilian cellulose industry concentration (1998 – 2007). Cerne,16, 209-216, 2010.

Corradini, E.; Imam, S. H.; Agnalli, J. A. M.; Mattoso, L. H. C. Effect of coconut, sisal and jute fibers on the properties of starch/gluten/glycerol matrix. J. Polym. Environ., 17, 1–9, 2009.

Demilecamps, A.; Beauger, C.; Hildenbrand, C.; Rigacci, A.; Budtova, T. Cellulose–silica aerogels. Carbohyd. Polym., 122, 293–300, 2015.

Ehrburger-Dolle, F.; Lavanchy, A.; Stoeckli, F. Determination of the Surface Fractal Dimension of Active Carbons by Mercury Porosimetry. J. Colloid Interf. Sci., 166, 451–461, 1994.

Fonseca, C.S., Silva, T.F., Silva, M.F., Oliveira, I.R.C., Mendes, R.F., Hein, P.R.G., Mendes, L.M.; Tonoli, G.H.D. Eucalyptus cellulose micro/nanofibers in extruded fiber-cement composites. Cerne, 22,1–9, 2016 (in press).

Guimarães Junior, M. Botaro, V.R., Novack, K.M., Teixeira, F.G.;Tonoli, G.H.D. (2015). Starch/PVA-based nanocomposites reinforced with bamboo nanofibrils. Industrial Crops and Products, 70, 72– 83.

Guzun, A. S.; Stroescu, M.; Jinga, S.I.; Voicu, G.; Grumezescu, A.M.; Holban, A.M. Plackett–Burman experimental design for bacterial cellulose–silica composites synthesis. Mater. Sci. Eng. C 42, 280–288, 2014.

Hassan, M.L.; Mathew, A.P.; Hassan, E.A.; El-Wakil, N.A.; Oksman, K. Nanofibers from bagasse and rice straw: process optimization and properties. Wood Sci. Technol., 46, 193–205, 2012.

He, X.; Cheng, L.; Wang, Y.; Zhao, J.; Zhang, W.; Lu, C. Aerogels from quaternary ammonium-functionalized cellulose nanofibers for rapid removal of Cr(vi) from water. Carbohyd. Polym., 111, 683–687, 2014.

Hsieh, C.; Wu, F.; Yang, S. Superhydrophobicity from composite nano/microstructures: Carbon fabrics coated with silica nanoparticles. Surf. Coat Tech., 202, 6103–6108, 2008.

Hüsing, N.; Schubert, U. Aerogels-Airy Materials: Chemistry, Structure, and Properties. Angew. Chem. Int. Ed., 37, 22-45, 1998.

Jansen, R.M.; Zimmermann, A. Process for the Preparation of Xerogels, United States Patent Number 5647962, 1997.

Jin, C.; Han, S.; Li, J.; Sun, Q. Fabrication of cellulose-based aerogels from waste newspaper without any pretreatment and their use for absorbents. Carbohyd. Polym., 123, 150–156, 2015.

Jin, H.; Nishiyama, Y.; Wada, M.; Kuga, S. Nanofibrillar cellulose aerogels. Colloid Surface A, 240, 63–67, 2004.

Job, N.; Théry, A.; Pirard, R.; Marien, J.; Laurent Kocon, L.; Rouzaud, J.N.; Béguin, F.; Pirard, J.P. Carbon aerogels, cryogels and xerogels: Influence of the drying method on the textural properties of porous carbon materials. Carbon, 43, 2481–2494, 2005.

Kobayashi, Y.; Saito, T.; Isogai, A. Aerogels with 3D ordered nanofiber skeletons of liquid-crystalline nanocellulose derivatives as tough and transparentinsulators. Angew. Chem. Int. Ed., 53, 10394–10397, 2014.

Kocon, L.; Despetis, F.; Phalippou, J. Ultralow density silica aerogels byalcohol supercritical drying. J. Non-Cryst. Solids, 225, 96–100, 1998.

Lin, J.; Yu, L.; Tian, F.; Zhao, N.; Li, X.; Bian, F.; Wang, J. Cellulose nanofibrils aerogels generated from jute fibers. Carbohyd. Polym., 109, 35–43, 2014.

Liu, S.; Yu, T.; Hu, N.; Liu, R.; Liu, X. High strength cellulose aerogels prepared by spatially confined synthesis of silica in bioscaffolds. Colloid Surface A, 439, 159– 166, 2013.

Nagai, N.; Hashimoto, H. FT-IR-ATR study of depth profile of SiO_2 ultra-thin films. Appl. Surf. Sci., 172, 307-311, 2001.

Nguyen, S.T.; Feng, J.; Ng, S.K.; Wong, J.P.W.; Tan, V.B.C.; Duong, H.M. Advanced thermal insulation and absorption properties of recycled cellulose aerogels. Colloid Surface A, 445, 128– 134, 2014.

Órfão, J. J. M.; Antunes, F. J. A.; Figueiredo, J. L. Pyrolysis kinetics of lignocellulosic materials-three independent reaction models. Fuel, 78, 349–358, 1999.

Oshima, T.; Sakamoto, T.; Ohe, K.; Baba, Y. Cellulose aerogel regenerated from ionic liquid solution for immobilized metal affinity adsorption. Carbohyd. Polym., 103, 62–69, 2014.

Pajonk, G.M. Transparent silica aerogels. J. Non-Cryst. Solids, 225, 307-314, 1998.

Parmenter, K.E.; Milstein, F. Mechanical properties of silica aerogels. J. Non-Cryst. Solids, 223, 179–189, 1998.

Pekala, R.W.; Alviso, C.T. Carbon aerogels and xerogels. Mat. Res. Soc. Symp. Proc., 270, 3–14, 1992.

Pierre, A.C.; Pajonk, G.M. Chemistry of Aerogels and Their Applications. Chem. Rev., 102, 4243-4265, 2002.

R Core Team. (2012). R: A language and environment for statistical computing. R Foundation for Statistical Computing, Vienna, Austria. ISBN 3-900051-07-0, URL: http://www.R-project.org

Raabe, J.; Fonseca, A.S.; Bufalino, L.; Ribeiro, C.; Martins, M.A.; Marconcini, J.M.; Tonoli, G.H.D. Evaluation of reaction factors for deposition of silica (SiO_2) nanoparticles on cellulose fibers. Carbohyd. Polym., 114, 424–431, 2014.

Ray, D.; Sarkar, B.K. Characterization of Alkali-Treated Jute Fibers for Physical and Mechanical Properties. J. Appl. Polym. Sci., 80, 1013–1020, 2001.

Sehaqui, H.; Zhou, Q.; Berglund, L.A. High-porosity aerogels of high specific surface area prepared from nanofibrillated cellulose (NFC). Compos. Sci. Technol., 71, 1593–1599, 2011.

Sescousse, R.; Gavillon, R.; Budtova, T. Aerocellulose from cellulose–ionic liquid solutions: Preparation, properties and comparison with cellulose–

NaOHand cellulose–NMMO routes. Carbohyd. Polym., 83, 1766–1774, 2011.

Shi, J.; Lingbin, L.; Guo, W.; Zhang, J.; Cao, Y. Heat insulation performance, mechanics and hydrophobic modification of cellulose–SiO_2 composite aerogels. Carbohyd. Polym., 98, 282– 289, 2013.

Siró, I.; Plackett, D. Microfibrillated cellulose and new nanocomposite materials: a review. Cellulose, 17, 459–494, 2010.

Sun, R. C.; Sung, X. F.; Liu, G. Q.; Fowler, P.; Tomkinson, J. Structural and physicochemical characterization of hemicelluloses isolated by alkaline peroxide from barley straw. Polym. Int., 51, 117–124, 2002.

Sun, X. F.; Xu, F.; Sun, R. C.; Fowler, P.; Baird, M. S. Characteristics of degraded cellulose obtained from steam-exploded wheat straw. Carbohyd. Res., 340, 97–106, 2005.

Thapliyal, P.C.; Singh, K. Aerogels as Promising Thermal Insulating Materials: An Overview. Journal of Materials, 2014, 1-10, 2014.

Valo, H.; Arola, S.; Laaksonen, P.; Torkkeli, M.; Peltonen, L.; Linder, M.B.; Serima, R.; Kuga, S.; Hirvonen, J.; Laaksonen, T. Drug release from nanoparticles embedded in four different nanofibrillar cellulose aerogels. Eur. J. Pharm. Sci., 50, 69–77, 2013.

Wagh, P.B.; Pajonk, G.M.; Haranath, D.; Rao, A.V. Influence of temperature on the physical properties of citric acid catalyzed TEOS silica aerogels. Mater. Chem. Phys., 50, 76-81, 1997.

Wong, J. C. H.; Kaymak, H.; Brunner, S.; Koebel, M. Mechanical properties of monolithic silica aerogels made from polyethoxydisiloxanes. Micropor. Mesopor. Mat., 183, 23–29, 2014.

Yamauchi, A. Gels: Introduction. In Osada, Y.; Kajiwara, K. (eds). Gels Handbook. Vol 1: The fundamentals. Academic Press, p. 9-12., 2001.

Yano, S.; Iwata, K.; Kurita, K. Physical properties and structure of organic-inorganic hybrid materials produced by sol-gel process. Mater. Sci. Eng. C, 6, 75-90, 1998.

Yeh, J.; Chen, C.; Huang, K. Synthesis and properties of chitosan/SiO_2 hybrid materials. Mater. Lett., 61, 1292–1295, 2007.

Yildiz, S.; Gumuskaya, E. The effect of thermal modification on crystalline structure of cellulose in soft and hardwood. Build. Environ., 42, 62–67, 2007.

Yin, Y.; Wang, C.; Wang, Y. Fabrication and characterization of self-assembled multifunctional coating deposition on a cellulose substrate. Colloid Surface A, 399, 92– 99, 2012.

Zhang, X.; Lin, Z.; Chen, B.; Zhang, W.; Sharma, S.; Gu, W.; Deng, Y. Solid-State Flexible Polyaniline/Silver Cellulose Nanofibrils Aerogel Supercapacitors. J. Power Sources, 246, 283-289, 2014.

Zhou, Z.; Cui, L.; Zhang, Y.; Zhang, Y.; Yin, N. Preparation and properties of POSS grafted polypropylene by reactive blending. Eur. Polym. J., 44, 3057-3066, 2008.

Zuluaga, R.; Putaux, J.L.; Javier Cruz, J.; Vélez, J.; Mondragon, I.; Gañán, P. Cellulose microfibrils from banana rachis: Effect of alkaline treatments on structural and morphological features. Carbohyd. Polym., 76, 51–59, 2009.